AECOM

APPENDIX CC

Offshore Electric and Magnetic Field Assessment

Photo credit: Matt Goldsmith, Equinor

June 2023

Prepared for

Beacon Wind LLC

Offshore Electric and Magnetic Field Assessment

Beacon Wind Project

Prepared for

Beacon Wind LLC

1600 Washington Boulevard, Suite 800

Stamford, CT 06901

Prepared by

4D Bay Street

Berlin, MD 21811

June 17, 2022

CONTENTS

LIST OF FIGURES

LIST OF TABLES

ACRONYMS AND ABBREVIATIONS

AC	alternating current
Beacon Wind	Beacon Wind LLC
BW1	Beacon Wind 1
BW2	Beacon Wind 2
BOEM	Bureau of Ocean Energy Management
COP	Construction and Operations Plan
DC	direct current
EMF	electric and magnetic field
ERV	effect reference value
ESA	Endangered Species Act
GPS	global positioning system
HDD	horizontal directional drilling
HVAC	high-voltage alternating current
HVDC	high-voltage direct current
Hz	Hertz
Integral	Integral Consulting Inc.
Lease Area	Renewable Energy Lease Area OCS-A 0520
mG	milliGauss
mV	millivolt
MW	megawatt
NEUS	Northeast U.S.
NYSERDA	New York State Energy Research and Development Authority
POI	Point of Interconnection
THC	total haemocyte count
WNC	winter normal conductor

LIMITATIONS

At the request of Beacon Wind LLC (Beacon Wind), Integral Consulting Inc. (Integral) assessed the electric and magnetic field (EMF) levels associated with the offshore electrical transmission system of Beacon Wind 1 (BW1) and Beacon Wind 2 (BW2) (collectively referred to hereafter as the Project). This report is focused on the offshore portion of the BW1 and BW2 Project. The cables assessed include the submarine export cables, the interarray cables, and the section of these cables installed on the exterior of the wind turbines and offshore substation facilities.

In performing the EMF assessment, Integral relied on data provided by Beacon Wind including information on the design, specifications, and usage of the offshore cables associated with BW1 and BW2. All details on the rating, location of routing, and burial depth of the cables were provided by Beacon Wind. Integral cannot verify the correctness of the data provided by Beacon Wind.

A range of Project designs are being considered to allow for assessments of proposed activities and the flexibility to make development decisions prior to construction. The Project design envelope involves several scenarios with potential EMF effects that are associated with Project infrastructure. This EMF assessment considers the information available at this time; the precise locations and schedule of the construction and operation scenarios may be subject to change as the engineering design progresses.

Although Integral has exercised usual and customary care in the conduct of this analysis, the responsibility for the design and operation of the Project remains fully with Beacon Wind. Beacon Wind has confirmed to Integral that the data contained herein are not subject to Critical Energy Infrastructure Information restrictions.

Integral reserves the right to supplement this report and to expand or modify opinions based on review of additional material as it becomes available, through any additional work, or review of additional work performed by others. The opinions and comments formulated during this assessment are based on observations and information available at the time of the investigation. No guarantee or warranty as to future life or performance of any reviewed condition is expressed or implied.

EXECUTIVE SUMMARY

Beacon Wind LLC (Beacon Wind) proposes to construct and operate the Beacon Wind 1 (BW1) and Beacon Wind 2 (BW2) (collectively referred to hereafter as the Project) as two separate developments within the Bureau of Ocean Energy Management (BOEM) designated Renewable Energy Lease Area OCS-A 0520 (Lease Area).

The purpose of the Project is to generate renewable electricity from an offshore wind farm(s) located in the Lease Area. The Project addresses the need identified by northeastern states to achieve offshore renewable energy targets: New York (9,000 megawatts [MW]), Connecticut (2,000 MW), Rhode Island (up to 1,000 MW), and Massachusetts (5,600 MW). Beacon Wind has entered into a purchase and sales agreement for an offshore wind renewable energy certificate for at least 1,230 MW for BW1 as a result of New York State's solicitation for offshore renewable energy certificates, with BW2 being developed to addresses the need for renewable energy identified by states across the region, including New York, Massachusetts, Rhode Island, and Connecticut.

The assessment of electric and magnetic fields (EMFs) presented in this report was performed by Integral Consulting Inc. (Integral) in support of the Construction and Operations Plan (COP). The assessment was performed to evaluate EMFs associated with representative configurations of the proposed BW1 and BW2 offshore electric transmission systems. These systems consist of high-voltage direct current (HVDC) submarine export cables and high-voltage alternating current (HVAC) interarray cables, both of which will be buried under the seafloor or covered by rock, rock bags, or concrete mattresses. Also included was an EMF evaluation of the portions of the HVDC and HVAC cables on the wind turbines and offshore substation facilities. The EMF assessment was based on the maximum capacity limits of the cables corresponding to the winter normal conductor rating.

The approach for assessing Project-related EMF impacts to the marine environment was guided by the internationally accepted environmental risk assessment approach, as well as other standard methods for EMF assessment accepted within the scientific, engineering, and health communities. Effect reference values (ERVs) were used for the risk assessment as representative field strength levels associated with EMF impacts to species within each of the demersal invertebrate, elasmobranch, and finfish groups. The ERVs were selected based on established ecological risk assessment procedures for selection of toxicity reference values and ecological screening benchmarks used in chemical risk assessment. A separate, comprehensive risk assessment has been additionally performed to address potential Project-related EMF impacts to human health in the onshore EMF assessment (Integral 2022) prepared in support of the COP.

The EMF assessment included quantitative modeling of EMF for the BW1 and BW2 offshore components of the electric transmission system, which includes the wind turbines, the offshore

substation facilities, the HVAC interarray cables, and the HVDC submarine export cables. The modeled results were compared to the ERVs to assess the potential for Project-related risk to marine life from EMF. The predicted direct current (DC) and alternating current (AC) EMF values are summarized below.

- The maximum magnetic field strengths and induced electric fields calculated for the BW1 and BW2 HVDC submarine export cables have a *de minimis*[1] risk to all demersal marine species for the majority of the cable route where the cable will be buried and either bundled or separated.
  - In areas where the cable is surface laid and covered with rock, rock bags, or concrete mattresses, the maximum magnetic fields and induced electric fields are elevated though the modeled cover depth is conservatively shallow and the ERVs are based on behavioral changes, which is considered a conservative estimate of potential population level effects. In summary, population level risks to demersal invertebrates are *de minimis*, even under the maximum magnetic field strengths.
- The maximum compass deflection for the BW1 and BW2 HVDC submarine export cables is *de minimis* for a majority of the cable route. In the limited shallow areas where the cable may be surface laid, there is a possibility of impacting surface vessel compasses, though the impact would be minimal and likely not be noticeable by mariners.
  - Modern navigational instruments (e.g., LORAN-C, global positioning system [GPS]) will not be impacted by the altered magnetic field along the cable, or any other Project cables.
- The maximum magnetic field strengths and induced electric fields calculated for the BW1 and BW2 HVAC interarray cables are 3 to 1,000 times lower than ERVs for demersal invertebrates and finfish. Elasmobranchs are not capable of detecting frequencies applicable to all Project cable AC magnetic fields and electric fields. Risks associated with potential exposures to AC magnetic fields and induced electric fields associated with the HVAC interarray cables are *de minimis*.
- The maximum magnetic field strength calculated for the HVAC interarray cables installed along the lower portion of the wind turbine monopiles is 1,200 times lower and the maximum induced AC electric field is 4,600 times lower than the reference value for demersal finish. Risks associated with potential exposures to AC magnetic fields and induced electric fields associated with the wind turbine HVAC interarray cables are *de minimis*.
- The maximum magnetic field strength calculated for the HVAC interarray cables installed along the lower portion of the offshore substation facilities support structure is

[1] In risk assessment, the term *de minimis* is used to refer to risks that are too minor to merit consideration.

1,200 times lower and the maximum induced AC electric field is multiple orders of magnitude times lower than the ERV for demersal finish. Risks associated with potential exposures to AC magnetic fields associated with the offshore substation facility HVAC interarray cables are *de minimis*.

- The maximum magnetic field strength calculated for the HVDC submarine cables installed along the lower portion of the offshore substation facility support structure exceeds the elasmobranch ERV by a factor of 4.6 and is 6.7 times below the ERV for finfish. However, the cable area on the offshore substation facility support structures represent an infinitely small area relative to the broader ecosystem, thus the potential population level risks to elasmobranchs and finfish associated with the DC magnetic fields from the HVDC submarine export cables on the offshore substation facility support structures are *de minimis*.
- The maximum induced DC electric field calculated for the HVDC submarine cables installed along the lower portion of the offshore substation facility support structure is 400 times lower than the ERV for elasmobranchs and finfish. Risks associated with potential exposures to induced DC electric fields associated with the offshore substation facility HVDC submarine export cables are *de minimis*.

Background EMF levels will be dominant everywhere except within close proximity to the cable because of the proportional relationship between the strength of an induced electro-magnetic field and distance. At a distance of 10 ft (3 m) from the cables, the effects of EMF are expected to be negligible whether the submerged cable is buried or exposed. Overall exposure of the study area to the EMF produced will be minimal (<1% of total habitat).

Collectively, the EMF assessment indicates that navigation impacts and potential marine life risks associated with exposure to Project-related EMF from the BW1 and BW2 offshore electric transmission systems are *de minimis*.

1 INTRODUCTION

The purpose of this report is to present the comprehensive assessment performed on potential impacts of electric and magnetic fields (EMFs) associated with the Beacon Wind 1 (BW1) and Beacon Wind 2 (BW2) offshore electric transmission system on the marine environment. The assessment involves a description of the marine environment where the Project's electric transmission system is proposed to be located, the calculation of EMF associated with the proposed system, and an evaluation of the potential for marine life to be exposed to EMF and the degree to which that exposure may cause unintended risk.

1.1 PROJECT DESCRIPTION

Beacon Wind LLC (Beacon Wind) proposes to construct and operate BW1 and BW2 (collectively referred to hereafter as the Project), as two separate offshore wind developments to be located within the Bureau of Ocean Energy Management (BOEM) designated Renewable Energy Lease Area OCS-A 0520 (Lease Area). The Lease Area covers approximately 128,811 ac (521 km^2) and is located approximately 20 mi (32 km) south of Nantucket, Massachusetts, and 60 mi (97 km) east of Montauk, New York (**Figure 1**). The Lease Area was awarded through the BOEM competitive renewable energy lease auction of the Wind Energy Area offshore of Massachusetts.

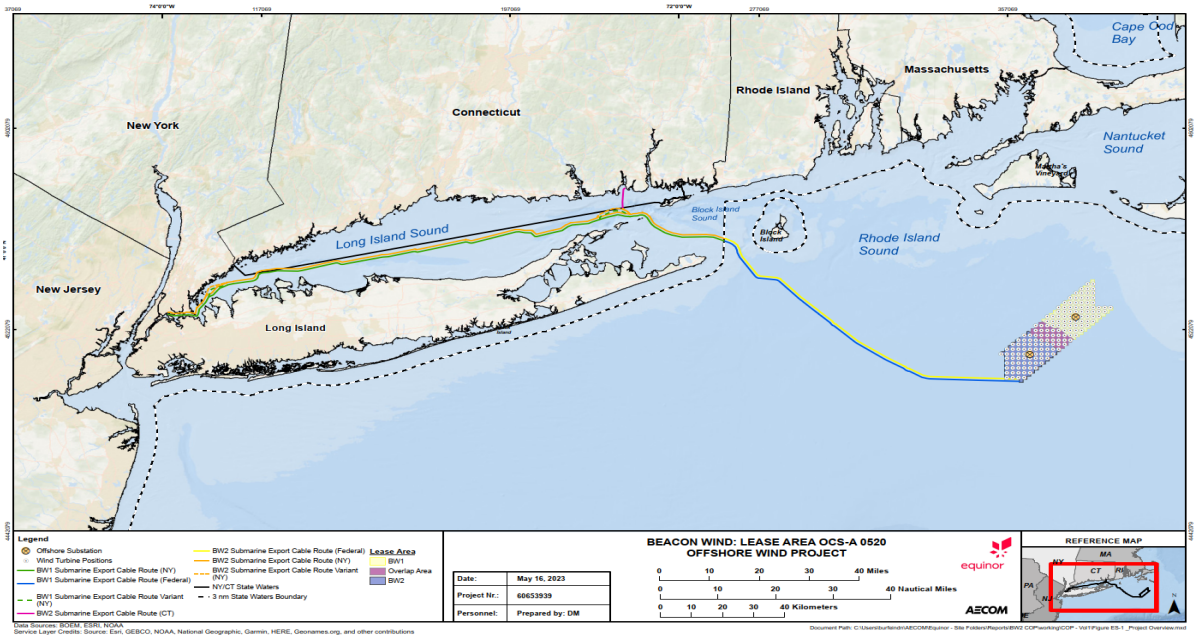

Figure 1. Beacon Wind Project Overview Showing Lease Area and the Location of the Offshore Substation Facilities for BW1 and BW2.

The purpose of the Project is to generate renewable electricity from an offshore wind farm(s) located in the Lease Area. The Project addresses the need identified by northeastern states to achieve offshore renewable energy targets: New York (9,000 megawatts [MW]), Connecticut (2,000 MW), Rhode Island (up to 1,000 MW), and Massachusetts (5,600 MW). The BW1 wind farm has a 25-year offtake agreement with the New York State Energy Research and Development Authority (NYSERDA) to deliver the power to its identified Point of Interconnection (POI) in Queens, New York.

The Project will involve two developments: BW1, located in the northern 56,535 ac (229 km^2) of the Lease Area with landfall at the Astoria Power Complex in Queens, New York; and a second phase, BW2, located in the southern 51,611 ac (209 km^2) of the Lease Area with landfall at the Millstone Power Complex in Waterford, Connecticut, or at the Astoria Power Complex. An overlap in the Lease Area, comprising 20,665 ac (84 km^2), could be used for BW1 or BW2. BW1 and BW2 will be constructed independently and will operate as electrically isolated transmission systems that will connect the individual offshore substation facilities to their respective onshore POIs by way of submarine export cable routes. BW1 will connect to the New York Independent System Operator via an existing substation owned by the Consolidated Edison Company of New York, Inc. BW2 is being developed to addresses the need for renewable energy identified by states across the region, including New York, Massachusetts, Rhode Island, and Connecticut. The interconnectedness of the New England transmission system, managed by the New England Independent System Operator, allows a single point of interconnection in the region to deliver offshore wind energy to all of the New England states (Connecticut, Rhode Island, Massachusetts, Vermont, New Hampshire, and Maine). The magnitude of regional targets for offshore wind and the limited amount of developable area, given current and reasonably foreseeable BOEM leasing activity, demonstrates a need for full build-out of the Lease Area.

The components of BW1 electric transmission system that are discussed in this offshore EMF assessment report include:

- Landfall at the Astoria Power Complex, Queens, New York.
- HVAC Interarray Cables—Multiple high-voltage alternating current (HVAC) interarray cables that will be installed below the seafloor, or on the seafloor covered with rock, rock bags, or concrete mattresses to connect the 61 to 94 wind turbines to the BW1 offshore substation facility.
  - Wind Turbines—a proposed 61 to 94 wind turbines (including 33 wind turbines located in the Overlap Area). Specifically, the HVAC interarray cables traveling vertically along the monopiles of the wind turbines.
- Offshore Substation Facilities—a single offshore substation facility that will convert the alternating current (AC) signal generated by the wind turbines to high-voltage direct current (HVDC) that will travel through the HVDC submarine export cable.

Specifically, the HVAC interarray cables and the HVDC submarine export cables extending vertically along the offshore substation facility support structure.

- HVDC Submarine Export Cable—One 320 kV HVDC submarine export cable circuit (two cable conductors) installed below the seafloor, or on the seafloor covered with protective mattresses, from the BW1 offshore substation facility to landfall adjacent to the Astoria Power Complex (approximately 202 nm [374 km]) in Queens, New York.

The components of BW2 electric transmission system that are discussed in this offshore EMF assessment report include:

- Landfall at the Millstone Power Complex, Waterford, Connecticut or the Astoria Power Complex, Queens, New York.
- Wind Turbines—A proposed 61 to 94 wind turbines (including 33 wind turbines located in the Overlap Area). Specifically, the HVAC interarray cables travelling vertically along the monopiles of the wind turbines.
- HVAC Interarray Cables—Multiple HVAC interarray cables that will be installed below the seafloor, or on the seafloor covered with protective mattresses to connect the 61 to 94 wind turbines to the BW2 offshore substation facility.
- Offshore Substation Facilities—A single offshore substation facility that will convert the AC signal generated by the wind turbines to HVDC that will travel through the HVDC submarine export cable. Specifically, the HVAC interarray cables and the HVDC submarine export cables extending vertically along the offshore substation facility support structure.
- HVDC Submarine Export Cable—One 320 kV HVDC submarine export cable circuit (two cable conductors) installed below the seafloor, or on the seafloor covered with protective mattresses, from the BW2 offshore substation facility to landfall adjacent to the Millstone Power Complex (approximately 113 nm [209 km]), and approximately 202 nm (374 km) in length if routed to the Astoria Power Complex.

1.2 ELECTRIC AND MAGNETIC FIELDS

EMFs are ubiquitous in the environment, and occur as a result of a variety of natural and man-made sources. EMFs are generated as a result of electrical currents flowing through a conductor. The offshore portions of the BW1 and BW2 transmission systems will include direct current (DC) conductors (i.e., the HVDC submarine export cables) and AC conductors (i.e., the HVAC interarray cables), and the HVDC and HVAC cables along the wind turbines and offshore substation facilities, generating both DC and AC EMFs, respectively. Electric, magnetic, and induced electric fields generally may occur with electrical current flowing through conductors.

1.2.1 Magnetic Fields

Earth has a geomagnetic field, which creates a background DC magnetic field that is present everywhere on earth. Earth's geomagnetic field is a result of the magnetism of the minerals in the earth's crust and core. The DC current flowing through a cable will produce a DC magnetic field. The strength of this magnetic field will vary based on the proximity of the cable conductors, the direction of the cable path relative to earth's geomagnetic field, the loading, and the cable burial depth. This cable-induced DC magnetic field can combine with earth's background magnetic field resulting in increasing or decreasing of total magnetic field strength.

The current flowing through an AC cable will produce an AC magnetic field and its strength will vary based on the configuration of the 3-phase AC cable, and the current loading. No naturally occurring background AC magnetic fields exist.

1.2.2 Electric Fields

Electric fields come in two forms: regular electric fields and induced electric fields. Regular electric fields are generated by the electric current flowing through a conductor. Induced electric fields are generated by charged ions passing through a magnetic field. The Project cables will be covered in grounded metallic sheaths and have steel armoring. As a result, electrical fields are entirely shielded from the marine environment.

However, the altered magnetic fields as a result of DC cables, combined with electrically charged ions in seawater or marine species moving through those magnetic fields, will generate an induced DC electric field. An induced AC electric field can also occur as a result of AC cables and their associated magnetic fields. The induced AC electric field will have a frequency related to the frequency of the AC cable, resulting from the rotation of the AC magnetic field.

1.3 ENVIRONMENTAL RISK ASSESSMENT PROCESS

The Project's offshore electric transmission system will produce EMFs in the surrounding marine environment where they will diminish rapidly with distance. EMFs can potentially be sensed by certain marine organisms that are present and have specialized sensory systems for detecting particular signatures of EMF. These organisms include varieties of fish, such as sharks and skates, and crustaceans, such as crabs and lobsters.

In order to assess the potential for EMF to effect marine life, a systematic evaluation of several factors is necessary. The strength of EMF from the cables must be determined based on location of the cables in the marine environment, the type of current (DC or AC) carried by the cables, the cable characteristics, the power transmitted, and surrounding environmental factors. It is also necessary to understand which marine organisms can detect EMF and may be exposed to EMF associated with the cables. The levels of EMF suspected to cause harm to those marine

organisms are also needed. Lastly, the area over which EMF from cables can occur relative to the total area where populations and communities of species occur regionally must be considered.

Given the number and variety of factors, the assessment of EMF presented in this report was performed using the process of "environmental risk assessment," or more commonly known as "risk assessment." Risk assessment has been in use for nearly five decades and is considered the standard for how to evaluate risks that may be posed to an environment. The National Research Council describes the risk assessment process as a systematic and scientific framework for assessing, communicating, and managing risk (NRC 1983). While risk assessment is considered the accepted state-of-the-science, the paradigm has not been fully integrated into the assessment of EMF. A number of authors, notably Hutchison et al. (2018), have recommended that a risk assessment approach be adopted to better inform the understanding offshore wind project EMF effects on marine life.

Risk assessment is used worldwide by health, environment and other regulatory agencies, and in the U.S. Examples are:

- U.S. Department of Commerce (e.g., National Oceanic and Atmospheric Administration)
- U.S. Environmental Protection Agency
- U.S. Department of the Interior (e.g., U.S. Fish & Wildlife Service)
- U.S. Department of Health and Human Services
- U.S. Department of Labor
- U.S. Department of Agriculture
- U.S. Food and Drug Administration
- U.S. Department of Defense

Risk is generally defined as the chance of harmful effects to humans or to ecological receptors resulting from exposure to an environmental stressor.[2] While the term is generally synonymous with "impact," risk entails not only a description of the magnitude of an effect, but also provides insight on the probability that the effect may occur to a given individual, population, community, or ecosystem.

The standard risk assessment process consists of the following steps: 1) a Problem Formulation is presented describing the

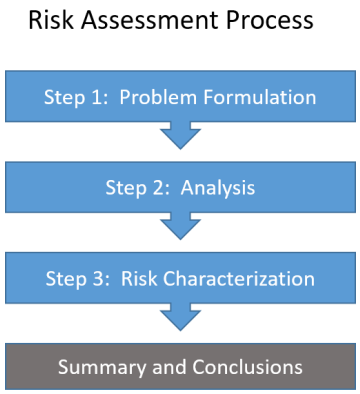

[2] The term "receptor" is generally used to describe the particular entity (e.g., for human health a resident or worker, and for ecological health a given species, population, community or ecosystem) selected for assessment with the goal of protection.

project, the environmental stressor[3] (e.g., EMF) that may be present, and what human and/or ecological receptors could be exposed to the stressor; 2) an Analysis is performed to evaluate potential exposure to the stressor and the effects that could occur to humans and/or ecological receptors; and 3) Risk Characterization is completed by combining the information about exposure and effects. The risk assessment process is designed to be flexible as more information may be needed or new questions arise.

The assessment of EMF associated with the Project's offshore electric transmission system was evaluated following the above three-step process. The remainder of this report is therefore organized in the following sections:

- **Section 2—Problem Formulation.** A description of the Project's offshore electric transmission system is provided, a background overview of EMF is presented, human and ecological receptors that may be exposed to EMF associated with the offshore system are discussed, spatial and temporal considerations of EMF exposure are described, and EMF effect threshold levels for receptors are identified.
- **Section 3—Methods of Analysis.** The conceptual approach and numerical methods used to model EMF associated with the Project's offshore electric transmission system are presented and discussed.
- **Section 4—Results of Analysis.** Calculations of the levels of EMF that may be associated with a variety of scenarios for the proposed configurations of the Project's offshore electric transmission system are presented.
- **Section 5—Risk Characterization.** Information on the calculated levels of EMF and potential exposures to those levels by ecological receptors are combined and presented relative to EMF levels known to be safe or cause effects in order to characterize potential risk associated with the Project's offshore electric transmission system.
- **Section 6—Summary and Conclusions.** A summary of the findings and the conclusions of the EMF risk assessment for the Project's offshore electric transmission system are presented.

[3] A variety of stressors that can be evaluated in risk assessment include chemical stressors (e.g., toxic pollutants), physical stressors (e.g., climate change, flooding, EMF), or biological stressors (e.g., disease, invasive species, parasites) in the environment (USEPA 1992, 1998).

2 PROBLEM FORMULATION

This section presents the problem formulation portion of the risk assessment for EMF. The section begins with a discussion on the general occurrence of natural and anthropogenic sources of EMF in the environment, the EMF associated with the BW1 and BW2 offshore electrical transmission system, and the human and ecological receptors that may be exposed to the system's EMF.

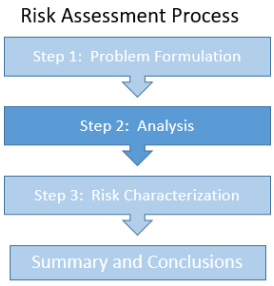

2.1 EMF IN THE ENVIRONMENT

EMFs are naturally occurring in the environment. EMFs are also generated through various man-made activities, including when electricity is produced, transported, or used. Those natural and anthropogenic sources are discussed below.

2.1.1 Natural Sources of EMF

The main sources of naturally occurring EMF in the marine environment are:

- **Earth's geomagnetic field** is a static DC magnetic field that originates from the flow of liquid metal in the earth's core and from local anomalies in earth's crust (Normandeau et al. 2011; NYSERDA 2017; Snyder et al. 2019; Tetra Tech 2021). Along the southern New England coast and in relation to the Project location, the earth's magnetic field ranges in strength from approximately 507 to 514 milliGauss (mG) (Chulliat et al. 2020).
- **Naturally induced electric fields from motion** can occur in seawater based on its conductivity in combination with the earth's geomagnetic field and through movement of ocean currents or by a marine organism. This combination results in the generation of a weak static electric field, referred to as a motion-induced electric field (Normandeau et al. 2011; Gill and Desender 2020). While the actual strength is dependent on the speed and direction of movement or a current or organism, it generally does not exceed 0.075 millivolt per meter (mV/m) (Normandeau et al. 2011; Snyder et al. 2019).
- **Bioelectric fields** are generated by all living marine organisms through the presence of mucous, heartbeats, gill movements, nerve impulses, and uneven distributions of electric charge along their bodies created by muscle contractions (Bedore and Kajiura 2013; Normandeau et al. 2011; Snyder et al. 2019). These electric fields are predominant as static DC, but AC components can be added from rhythmic movement, for example, of gills (lower frequency of <10 Hertz [Hz]) or muscle contractions (higher frequency of >20 Hz). Molluscs produce up to 10 mV, crustaceans and elasmobranchs (cartilaginous fish that include sharks) produce up to 50 mV, and teleosts (bony fish) produce up to

500 mV (Bedore and Kajiura 2013). Predators that can detect bioelectric fields, notably sharks, are thought most capable of detecting frequencies ≤2 Hz, and no more than 20 Hz (Bedore and Kajiura 2013). DC bioelectric fields may reach strengths of 500 mV/m at the organism's body, but quickly drop to much lower levels within 4 to 8 in. (10 to 20 cm) of the source (Wilkins and Hoffman 2005; Bedore and Kajiura 2013; Snyder et al. 2019). Some marine organisms use these fields to find each other and sense other species nearby, including prey.

Naturally occurring AC EMF are identified by their oscillation frequency, or the number of times the strength and direction of the field alternates per second. DC fields are static (i.e., they have a constant direction with no oscillations) and have a frequency of 0 Hz, while AC fields change direction many times per second and mostly occur at frequencies less than 10 Hz in the natural marine environment (Snyder et al. 2019). This distinction for AC is important because electricity in the U.S., including the AC portions of the Project's offshore electric transmission system, is transmitted at a frequency of 60 Hz.

BASIC UNITS OF ELECTRICITY AND EMF

Units of Electricity

Electrical strength, such as generated by a utility power line, is expressed in volts or kilovolts (1 kV = 1,000 V). Voltage is the "pressure" of the electricity and is sometimes described as being similar to the pressure of water in a plumbing system.

Electric current describes the movement of electric charges and is expressed in units of amperes (A). Current is the "flow" of the electricity and is sometimes described as being similar to the flow of water in a plumbing system.

Units of EMF

An "electric field" can be generated by a voltage difference between power lines and ground. Electric field is expressed in units of millivolts per meter (mV/m). The size of the electric field depends on the voltage, the separation between lines and ground, and other factors. Because the cables used for BW1 and BW2 are covered in metallic sheathing, electric fields are insulated within the cable and are prevented from entering the marine environment.

A "magnetic field" can be generated around electrical lines. The magnetic field produced by an electric current is usually expressed in units of gauss (G) or milligauss (mG) (1 G = 1,000 mG). Another unit for magnetic field levels is the microtesla (μT) (1 μT = 10 mG). The size of the magnetic field depends on the electric current, the distance to the current-carrying conductor, and other factors. Seawater or marine organisms moving within a magnetic field can also create a weak motion-induced electrical field.

2.1.2 Man-made Sources of EMF

EMFs are created by variety of electrical devices used daily by humans. They include electric home appliances (e.g., blenders, refrigerators, clothes washers, toasters, vacuums, pencil sharpeners, televisions), personal care products (e.g., electric shavers, hair dryers), indoor wiring, grounding currents on pipes and ground wires, and outdoor distribution or transmission circuits.

Any human activity that uses electrical cables in the marine environment will act as an additional source of EMF. In the marine environment, man-made sources of EMF are nearly

ubiquitous and include bridges, ships, certain kinds of pipelines, and submarine cables used for telecommunications and electrical transmission (Hutchison et al. 2018; Normandeau et al. 2011; European Offshore Wind Deployment Centre 2011; Gill and Desender 2020).

2.2 EMF FROM THE PROJECT'S OFFSHORE ELECTRICAL TRANSMISSION SYSTEM

The BW1 and BW2 offshore electric transmission system consists of wind turbines generating AC electricity, HVAC interarray cables that transmit the electricity from the wind turbines to offshore substation facilities within the Lease Area to convert AC to DC electricity, and then the HVDC submarine export cables that transmit the renewable energy from the offshore substation facilities towards landfall for connection to an onshore substation facility and then transmission to the existing electric grid POI (see **Figure 2**). The flow of electric currents in the collective Project's offshore electric transmission system, specifically the HVAC interarray cables and the HVDC submarine export cables, will be new sources of EMF in the marine environment.

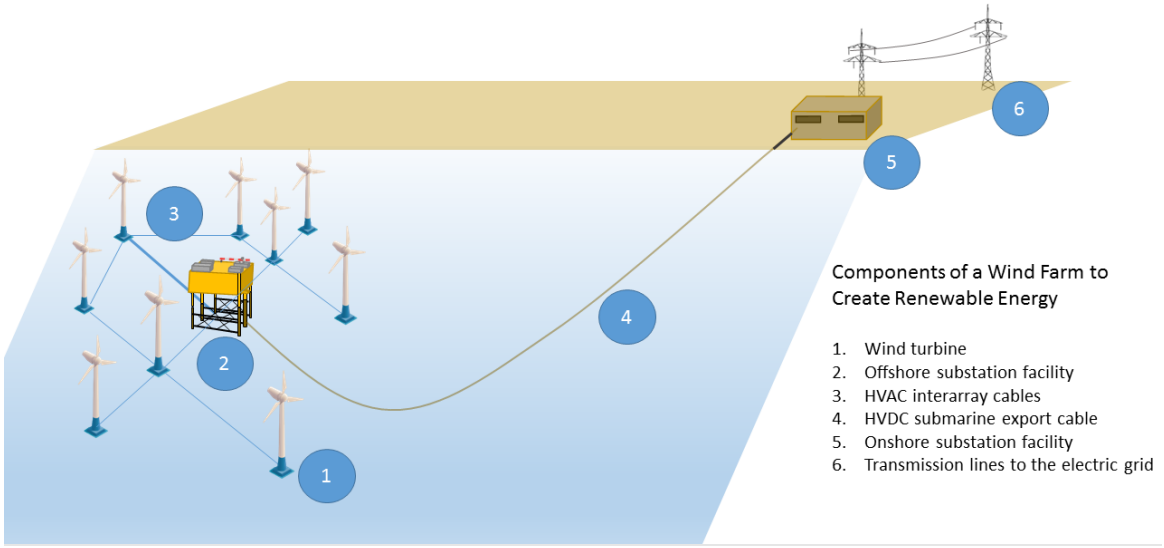

Figure 2. Generalized Illustration of the Components of an Offshore Wind Farm.

While the system is considered as a whole for this assessment, the individual systems for BW1 and BW2 themselves are not electrically connected and are independent from one another.

2.2.1 HVAC Interarray Cables

The HVAC interarray cables will be used to connect up to a maximum of 155 wind turbines in an array to the offshore substation facilities (**Figure 3**). The wind turbines are projected to generate 15 to 20 MW of electricity and at an individual wind turbine, a maximum of two 66-kV HVAC cables within the wind turbine monopile will convey this electricity generated to its base at the seafloor. There the cables will exit the monopile in cable protection systems (e.g., J-tubes) outside the monopile at a height of approximately 16 ft (5 m) above the seafloor. At the point of initial burial at the base of the wind turbines, the cables will be covered by a secondary layer of protection (typically consisting of rock, rock bags, or concrete mattresses). The cables will then be joined to other buried cables in a larger array, one array for BW1 and one array for BW2, and 18–22 cables will terminate at their respective offshore substation facilities (**Figure 3**). The HVAC interarray cables will be buried to a target burial depth of 3 to 6 ft (0.9 to 1.8 m), though other depths may be used based on a cable burial risk assessment (see **Section 3.2** for additional discussion). The collective length of the interarray cables for both BW1 and BW2 will be 162 nm (300 km).

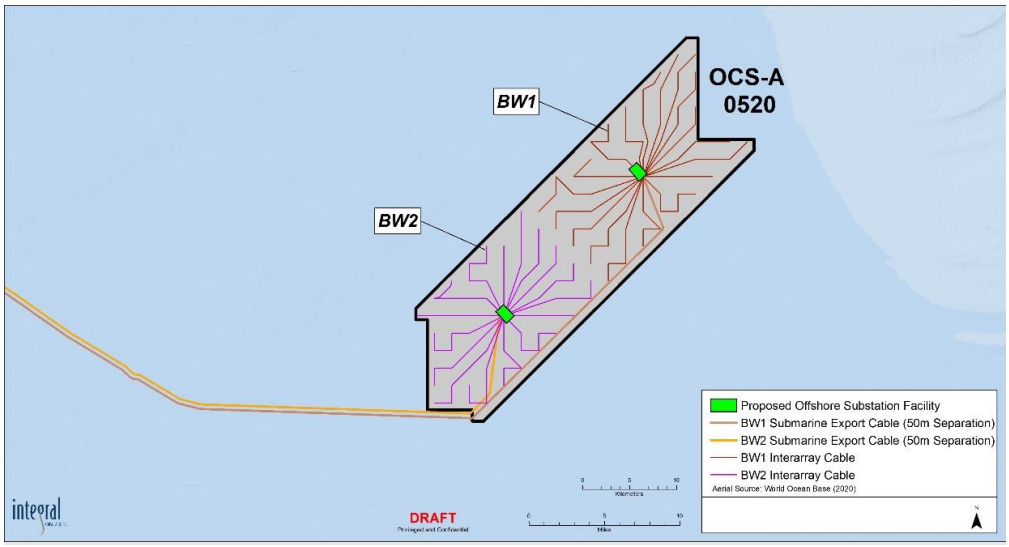

Figure 3. BW1 and BW2 HVAC Interarray Cables, Offshore Substation Facilities, and HVDC Submarine Export Cables.

The HVAC interarray cables themselves will consist of three smaller conductors ("cores") that are bundled together to carry three-phase currents. The overall diameter of the cable is 6.8 in. (17.4 cm), with each individual conductor having a diameter of 1.4 in. (3.6 cm). **Figure 4** shows

an example illustration of an HVAC submarine cable.[4] The AC current associated with the HVAC interarray cables will produce AC magnetic fields due to the flow of electric charge along the cables. The AC magnetic fields alternate strength and direction in a continuous cycle that repeats 60 times each second (i.e., a frequency of 60 Hz).

Figure 4. Illustrative Example of an HVAC Submarine Cable.

The electric field produced by the voltage on the current-carrying conductors inside the cable is shielded from the marine environment by the grounded metallic sheath and armoring encircling the three cables (Snyder et al. 2019; Normandeau et al. 2011; Claisse et al. 2015; Dunlop et al. 2016). However, these metal sheaths/armoring do not shield the environment from the magnetic field produced by the cables. The out-of-phase magnetic field emitted by each conductor of the cable causes a rotation in the magnetic emission; this oscillating magnetic field generates a weak, secondary induced electric field in the surrounding marine environment that is unrelated to the voltage of the cable (Snyder et al. 2019; Gill and Desender 2020). The 60-Hz AC magnetic fields will induce 60-Hz AC electric fields. Electric fields in the marine environment are measured in units of millivolts per meter (mV/m).

2.2.2 HVDC Submarine Export Cables

The HVDC submarine export cables will be used to transmit HVDC electricity from the individual offshore substation facilities located in the center of the BW1 and BW2 Lease Area to

[4] The cables will be similarly designed between BW1 and BW2, and so the descriptions provided are applicable to both BW1 and BW2 HVAC cables.

their respective landfall locations. Each export cable will consist of one 320-kV circuit.[5] Independent submarine export cables will be used for BW1 and BW2, as they have separate offshore substation facilities and separate landfall locations (i.e., Queens, New York, and/or Waterford, Connecticut). The cables will exit the offshore substation facility and travel vertically within J-tubes inside of the jacketed support structures and exit the support structure at a proposed height above the seafloor. At the base of the offshore substation facility, the J-tubes will be on the exterior of the support structure, extending vertically to where the cables will be covered by a secondary layer of protection (typically consisting of rock, rock bags, or concrete mattresses) and then buried below the seafloor. When buried, the cables are proposed to be placed at a target depth of 3 to 6 ft (0.9 to 1.8 m), though other burial depths may be used (see **Section 3.1** for additional discussion).

From the Lease Area, the BW1 and BW2 submarine export cables will be placed in parallel trenches below the seafloor and separated by up to 160 ft (50 m) (**Figure 3**), extending from their respective offshore substation facilities to the mouth of Long Island Sound. At that point, the submarine export cables will either diverge towards their separate landfall locations (BW1 will make landfall at the Astoria Power Complex in Queens, New York; BW2 will make landfall in Waterford, Connecticut at the Millstone Power Complex), or both BW1 and BW2 will continue in parallel trenches to the Astoria Power Complex in Queens, New York. Over the course of their lengths, the individual cables will occur as a bundled bi-pole configuration, or the bundled cable may be separated (i.e., two separate cables, one for each pole). Under the bundled configuration, the cables will have a total width of 10 in. (25.4 cm) (each pole with a 5 in. [12.7 cm] diameter), including the conductors, sheathing, and armoring. **Figure 5** shows an example illustration of an HVDC submarine cable.

[5] The cables will be similarly designed between BW1 and BW2, and so the descriptions provided are applicable to both BW1 and BW2 submarine export cables.

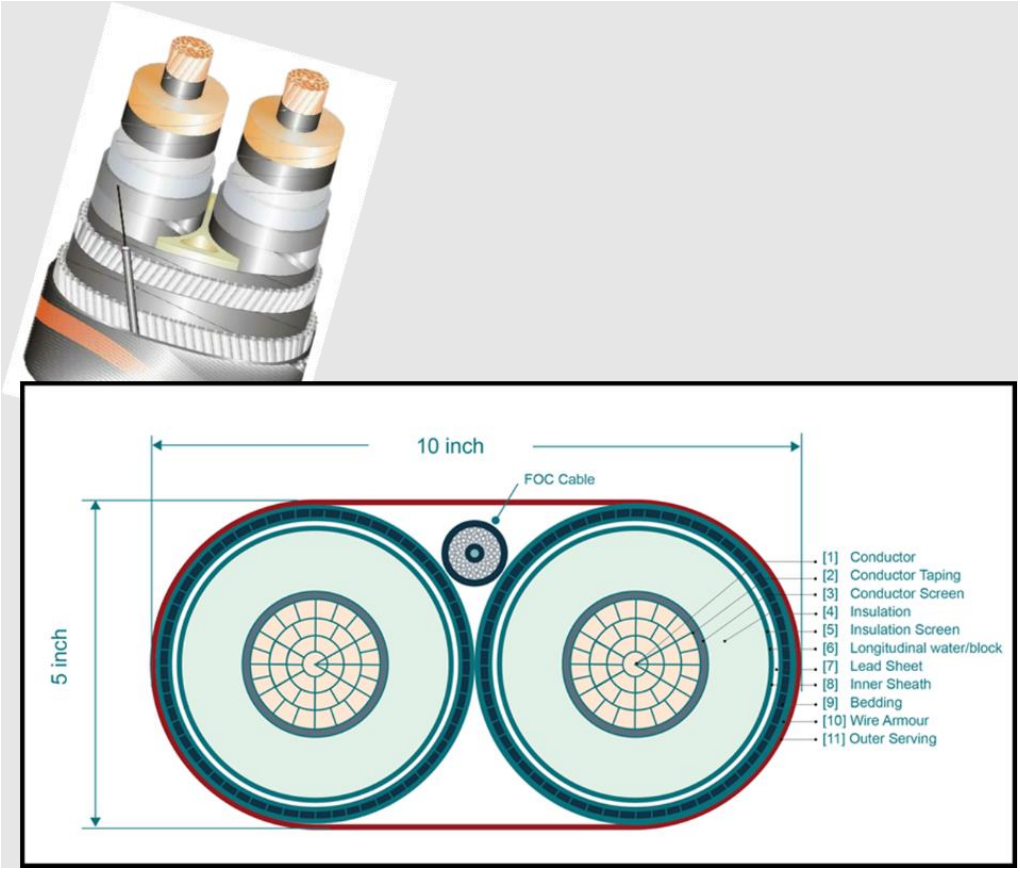

Figure 5. Illustrative Example of a Bundled HVDC Submarine Cable.

At landfall in either Queens, New York, or Waterford, Connecticut, the submarine export cables will be installed via horizontal directional drilling (HDD) at a target burial depth of 3 to 6 ft (0.9 to 1.8 m), though burial depths of approximately 15 ft (4.6 m) below the U.S. Army Corps of Engineers authorized dredge depth are proposed for within navigation channels. Once on land, the cables will subsequently be connected underground to an onshore substation facility, which will then transfer the renewable energy to the electrical grid POI.

The DC current associated with the HVDC submarine export cables will produce an altered magnetic field beyond the cables, but unlike the AC magnetic field, it will not alternate and instead will be a static DC magnetic field (i.e., at a frequency of 0 Hz). As described above, the earth's natural geomagnetic field occurs naturally in the marine environment (the earth's geomagnetic field is also a static [i.e., DC, 0 Hz] magnetic field). The DC magnetic field generated from the submarine export cable will create an altered magnetic field when combined with earth's geomagnetic field. In addition, when electrically charged ions in seawater or

marine species move through the static DC magnetic field created by the submarine export cables, as well as earth's background geomagnetic field, a weak, motion-induced DC electrical field may also be created.

As in the case of HVAC interarray cables, while an electric field is created by the voltage applied to the conductors inside the HVDC submarine export cables, the electrical fields themselves are entirely shielded from the marine environment by grounded metallic sheaths and steel armoring around the cable (Snyder et al. 2019; Normandeau et al. 2011; Claisse et al. 2015; Dunlop et al. 2016).

2.3 HUMAN AND ECOLOGICAL RECEPTORS

As discussed, the cables associated with the Project's offshore electric transmission system may create: 1) magnetic fields produced by current flow through either the HVAC (60 Hz) or static HVDC (0 Hz) cables; 2) an indirect AC electric field induced by alternating magnetic fields from the HVAC cables; or 3) an induced DC electric field caused by movement (through either ocean currents or marine species) through the DC magnetic field of the HVDC cables.

While humans and marine life are known to respond differently to EMF, there are important differences related to how these receptors may be exposed to EMF.

2.3.1 Humans and Potential Exposure to Project-Related EMF

For risk assessment, exposure is initially assessed by considering the likelihood that an individual may be present and exposed to a given stressor. When potential exposure is considered likely, the "exposure pathway" is judged complete and more detailed assessment of risk is required. In instances where exposure is limited in a way that risks are considered below levels of concern, the exposure pathway is judged incomplete and a detailed assessment is not performed.

Human exposure to Project-related EMF is expected to be limited. The general public will unlikely be exposed because the Project's electric transmission system is located offshore far away from residences.[6] Near the shoreline, the HVDC submarine export cables will be installed far below the seafloor and shoreline as part of the constructed HDD. Offshore fishermen and boaters may visit areas adjacent to the Lease Area and the areas along the route of the HVDC submarine export cables. Because the cables are buried below the seafloor or covered by protective mattresses in water depths of approximately 98–197 ft (30–60 m), individuals will be

[6] Potential exposure of the general public to onshore components of the Project's electric transmission system is also anticipated to be limited, as both landfall locations (i.e., Astoria Power Complex and Millstone Power Complex) will occur at industrial properties away from residential housing. An in-depth assessment is provided for the Project's onshore electric transmission system in a separate report prepared for this COP entitled "Onshore Electric and Magnetic Field Assessment – Beacon Wind Project" (Integral 2022).

at distance and have limited exposure to Project-related EMF. Exclusion zones will limit public access to the Lease Area and the wind turbines, offshore substation facilities, and associated HVAC interarray cables. It is assumed workers engaged in operations and maintenance activities of the offshore electric transmission system will be subject to separate workplace safety requirements to protect worker health and safety (e.g., Occupational Safety and Health Administration requirements).

While it is possible that scuba divers may utilize some offshore areas along the routes of the HVDC submarine export cables, their time immediately above the cables is anticipated to be minimal relative to the breadth of dive areas of interest off southern New England and within Long Island Sound.

Overall, the potential human health exposure pathway for Project-related offshore EMF is considered incomplete and a detailed risk assessment is therefore not performed.

2.4 MARINE LIFE AND POTENTIAL EXPOSURE TO PROJECT-RELATED EMF

Many different forms of marine life exist in the areas where the cables will be present. Some select species of marine life have evolved the ability to detect magnetic and electric fields, though not all species are equipped with such capabilities.

The degree to which risk to Project-related EMF may occur to marine life receptors is based on a consideration of 1) the areas where Project-related EMF may occur; 2) the types of marine life that may be present in those areas and the degree to which those species may or may not be capable of sensing EMF; 3) the spatial scale and duration of exposure; and 4) the kinds of effects to marine life that are possible given the levels of EMF that might occur. These considerations are discussed below. The discussion is then followed by a visual depiction of these considerations in a conceptual site model diagram.

2.4.1 Potential Areas for Project-Related EMF Marine Life Exposure

The BW1 and BW2 offshore electrical transmissions may result in exposure to Project-related EMF to marine life. These include the following:

- HVAC interarray cables will be housed in J-tubes on the lower portion of the wind turbine monopiles. The base of the wind turbines will have rock, rock bags, or concrete mattresses covering the cables that will provide hard surface and reef-like habitat that may attract certain bottom-associated (i.e., "demersal") species. These areas are estimated to be a maximum of 4.2 ac (0.02 km^2) in area for each wind turbine, assuming a suction bucket jacket foundation, and are proposed to be 6.5 to 13 ft (2 to 4 m) in height above the seafloor. As the individual wind turbines will be separated by distance, these

areas will be distinct and will not constitute a continuous habitat patch. The total area of these individual patches will be a maximum of 651 ac (2.6 km^2) in area for the proposed 155 wind turbines for BW1 and BW2.

- The buried HVAC interarray cables will be buried below soft-bottom, sand habitats in the Lease Area typical of the surrounding seafloor habitat in the region. The proposed target burial depth will be 3 to 6 ft (0.9 to 1.8 m). The interarray cables will occur across a continuous total area for both BW1 and BW2 of approximately 128,811 ac (521 km^2) (the size of the Lease Area). These areas may be utilized as part of the continuum of the larger regional area used by demersal species.
- HVAC interarray cables leading to and HVDC submarine export cables leading from the offshore substation facilities will be housed in J-tubes on the lower portion of the offshore substation facility support structures. The base of the offshore substation facilities located in the center of each of the BW1 and BW2 Lease Area will also have secondary layers of protection (i.e., rock, rock bags, or concrete mattresses) that will cover both the HVAC interarray cables and HVDC submarine export cables. The estimated diameter of these areas at each of the individual BW1 and BW2 offshore substation facilities will be approximately 5.2 ac (0.02 km^2) and are proposed to be 6.5 to 10 ft (2 to 3 m) in height above the seafloor. As the stations will be separated by distance, these areas will be distinct and will not represent a continuous habitat.
- Along the areas comprising the HVDC submarine export cables corridor routes from the offshore substation facilities along their respective landfall locations, the cables are proposed to be buried over the majority (approximately 90%) of their routes at a proposed target depth of 3 to 6 ft (0.9 to 1.8 m). In areas where burying the cables is not possible, protective mattresses will be placed over the cables.

The above areas are each associated with conditions at the seafloor, as opposed to the open water column (i.e., "pelagic") environment. Accordingly, demersal species typically living at or near the bottom are those that have the highest potential to be exposed to Project-related EMF. In particular, demersal species that are less mobile and could spend longer timeframes in close proximity to these areas are most likely to have the greatest potential for exposure.

2.4.2 Demersal Receptors Exposure to Project-Related EMF

Select demersal receptors may be exposed to Project-related EMF in the areas described above (i.e., the base of individual wind turbines, areas of HVAC interarray cables, base of offshore substation facilities, and along the corridor routes of the HVDC submarine export cables). Species within these receptor groups include varieties attracted to or dependent upon hard surfaces or reef structure near the seafloor, as well as species that utilize open, predominantly sand, or mixed-sand and gravel seafloor habitat.

The new structure presented is anticipated to provide an "artificial reef effect" with the new habitat leading to locally increased production and biodiversity, as described for other offshore structures in the U.S. and Europe (e.g., Hutchison et al. 2020a; Degraer et al. 2020; Quigel and Thornton 1989; Petersen and Malm 2006).

Colonization begins with aggregations adhering to vertical surfaces and hard surfaces at the bottom, such as algae, sponges, amphipods, mussels, and barnacles. As many of these organisms are suspension feeders, they act as "biofilters" for the surrounding water column, while their organic waste provides a nutrient source for the surrounding seafloor. The introduction of rock, for example at the base of wind turbines and offshore substation facilities, affects seafloor habitat complexity, particularly in mobile sediments, expanding the habitats available to serve as refuges and to support food sources for biota (**Figure 6**; Degraer et al. 2020).

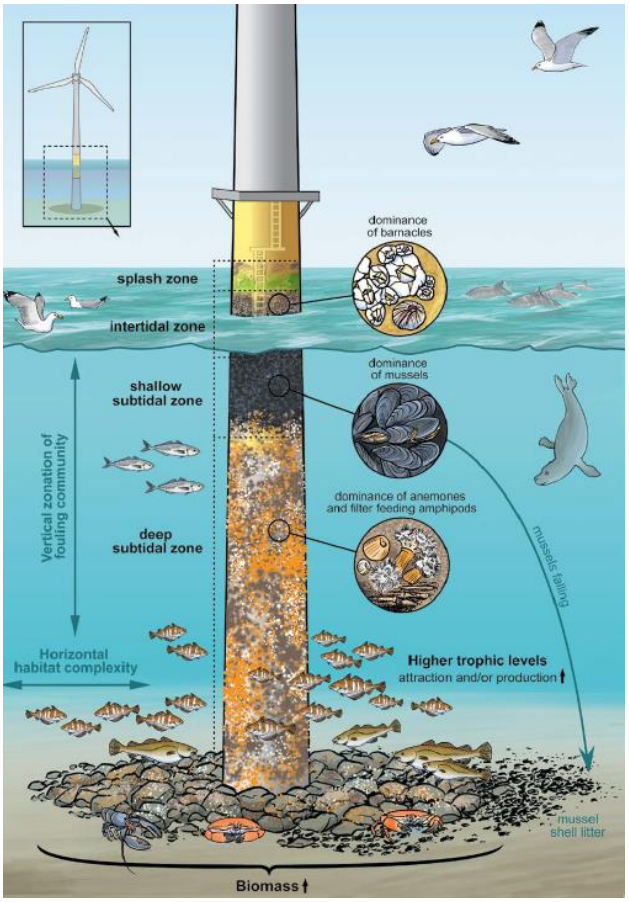

Figure 6. Reef Effect of an Offshore Wind Turbine Providing Increased Habitat, Biodiversity, and Production (Source: Degraer et al. 2020).

Larger species such as anemones, crabs, and lobsters take advantage of increased food availability and shelter (Krone et al. 2017; Degraer et al. 2020). Over time, the surrounding seafloor communities become increasingly complex and diverse, and by locally increasing food availability, support higher trophic levels (fish, birds, marine mammals). Fish species known to take particular advantage of this new habitat include pelagic species such as mackerel and demersal species such as Atlantic cod (*Gadus morhua)* and black sea bass (*Centropristis striata)* (Reubens et. al. 2014; Dannheim et al. 2020; Wilber et al. 2020). While some information needs to remain regarding potential effects (e.g., potential changes in carbon cycling at local and regional ecosystem scales) (Degraer et al. 2020), the structures presented by wind turbines and offshore substation facilities are anticipated to provide ecological benefits.

For the risk assessment of Project-related EMF, the demersal species present will be those that utilize habitat around the base of the wind turbines and offshore substation facilities, as well habitat associated with the open-bottom areas where the HVAC interarray cables and HVDC submarine export cables will be located. Species may be entirely sessile (i.e., attached, not mobile) or are otherwise considered to generally be less mobile (i.e., not highly migratory). The demersal receptor groups selected for evaluation in the risk assessment are as follows:

Invertebrates. This receptor group includes benthic species such as encrusting molluscs (e.g., blue mussels [*Mytilus edilus* complex] and eastern oyster [*Crassotra virginica*]), sea scallops (*Placopecten magellanicus*), ocean quahog (*Artica islandica*), certain varieties of sea sponges, bryozoans and sea stars, varieties of crustaceans (e.g., Atlantic rock crab [*Cancer irroratus*], Jonah crab [*Cancer borealis*], American lobster [*Homarus americanus*], and horseshoe crab [*Limulus Polyphemus*]), and certain varieties of squid (e.g., longfin inshore squid [*Doryteuthis pealeii*]). **Table 1** presents a summary listing of demersal species expected to occur within southern New England waters and included in the Invertebrates group. The table includes information on habitat preference and ability to detect EMF. None of the species are listed under the Endangered Species Act (ESA).

Table 1. Summary of Demersal Invertebrates Expected to Occur in Southern New England Waters.

Species	Zonal Group	Preferred Habitat[a]	Sensitivity to EMF	EMF-related Sensory Functions	ESA Listed Species
American Lobster (*Homarus americanus*)	Demersal	Rocky to mixed sandy or mud substrates, occasional burrower.	M	Navigation	--
Atlantic rock crab (*Cancer irroratus*)	Demersal	Mixed substrate types throughout coastal waters to continental rise.	--		--
Atlantic sea scallop (*Placopecten magellanicus*)	Demersal	Soft bottom, sand-to-gravel	--		--
Atlantic surf clam (*Spisula solidissima*)	Demersal	Juveniles found in finer, shallow soft bottom, sandy substrate. Adults found in coarser sandy substrates in shallow to deep water.	--		--
Jonah crab (*Cancer borealis*)	Demersal	Near-shore to offshore seasonal migrations, mixed substrates.	--		--
Longfin inshore squid (*Doryteuthis paeleii*)	Demersal/Benthic	Diurnal migrations through water column, adults can be found at depths up to 1,300 ft (400 m). Seasonal migrations from continental shelf to continental slope. Eggs deposited on sandy to rocky substrate	--		--
Northern shortfin squid (*Illex illecebrosus*)	Demersal/Benthic	Seasonal migrations from open ocean, deep waters, to shallow, continental shelf waters. Eggs deposited in mid-water column.	--		--
Ocean quahog (*Artica islandica*)	Demersal	Cold water, benthic, sandy substrates, up to 1,300 ft (400 m).	--		--
Eastern oytser (*Crassotrea virginica*)	Demersal	Brackish and salty waters from 8–35 ft (2–11 m) deep attaching to firm bottom areas and to each other to grow into reefs	--		--

Notes:
Dashes indicate no known magnetosensitivity or electrosensitivity noted within scientific literature.
M = magnetosensitive

Elasmobranchs. This receptor group includes demersal sharks (e.g., Atlantic spiny dogfish [*Squalus acanthias*] and sandbar shark [*Carcharhinus plumbeus*]), skates (e.g., little skate [*Leucoraja erinacea*]), and rays (e.g., cownose ray [*Rhinoptera bonasus*]). **Table 2** presents a summary listing of demersal species included in the Elasmobranchs group.

Table 2. Summary of Demersal Elasmobranchs Expected to Occur in Southern New England Waters.

Species	Zonal Group	Preferred Habitat[a]	Sensitivity to EMF	EMF-related Sensory Functions	ESA Listed Species
Barndoor skate (*Dipturus laevis*)	Demersal/Benthic	Marine; demersal; oceanodromous	E, M	Orientation	--
Blacktip shark (*Carcharhinus limbatus*)	Reef-associated	Marine; brackish; reef-associated; amphidromous	E	Prey detection, predator avoidance	--
Clearnose skate (*Rostroraja eglanteria*)	Demersal	Marine; brackish; demersal; oceanodromous	E	Prey detection, predator avoidance	--
Little skate (*Leucoraja erinacea*)	Demersal/Benthic	Marine; demersal; oceanodromous	E	Prey detection, predator avoidance	--

Notes:
[a] Information from fishbase.org
E = electrosensitive
M = magnetosensitive

Finfish. This receptor group includes several demersal finfish species, including summer flounder (*Paralichthys dentatus*), black sea bass, sand lance (*Ammodytes americanus*), Atlantic cod, and shortnosed sturgeon (*Acipenser brevirostrum*). **Table 3** presents a summary listing of the demersal species included in the Finfish group.

Table 3. Summary of Demersal Finfish Expected to Occur in Southern New England Waters.

Species	Zonal Group	Preferred Habitat[a]	Sensitivity to EMF	EMF-related Sensory Functions	ESA Listed Species
Atlantic cod (*Gadus morhua*)	Demersal/Benthic	Marine; brackish; benthopelagic; oceanodromous	E	Foraging, predator avoidance	--
Atlantic halibut (*Hippoglossus hippoglossus*)	Demersal/Benthic	Marine; demersal; oceanodromous	M		--
Atlantic sturgeon (*Acipenser oxyrinchus oxyrinchus*)	Demersal/Benthic	Marine; freshwater; brackish; demersal; anadromous	E	Navigation, foraging, predator avoidance	Endangered*
Shortnosed sturgeon (*Acipenser brevirostrum)*	Demersal/Benthic	Marine; freshwater; brackish; demersal; anadromous	E	Navigation, foraging, predator avoidance	Endangered
Atlantic wolffish (*Anarhichas lupus*)	Demersal/Benthic	Marine; demersal; oceanodromous	--		--

Species	Zonal Group	Preferred Habitat[a]	Sensitivity to EMF	EMF-related Sensory Functions	ESA Listed Species
Black sea bass (*Centropristis striata*)	Reef-associated	Marine; reef-associated; oceanodromous	--		--
Conger eel (*Conger oceanicus*)	Demersal/Benthic	Marine; demersal; oceanodromous	E, M	Navigation, foraging	--
Haddock (*Melanogrammus aeglefinus*)	Demersal/Benthic	Marine; demersal; oceanodromous	E		--
Monkfish (Lophius americanus)	Demersal/Benthic	Marine; demersal; oceanodromous	--		--
Northern searobin (*Prionotus carolinus*)	Demersal/Benthic	Marine; brackish; demersal	--		--
Ocean pout (*Zoarces americanus*)	Demersal	Marine; brackish; demersal; oceanodromous	--		--
Pollock (*Pollachius virens*)	Demersal/Benthic	Marine; demersal; oceanodromous	E		--
Red hake (*Urophycis chuss*)	Demersal/Benthic	Marine; demersal; oceanodromous	--		--
Sand lance (*Ammodytes americanus*)	Demersal/Benthic	Marine; brackish; demersal	--		--
Scup (*Stenotomus chrysops*)	Demersal/Benthic	Marine; demersal; oceanodromous	--		--
Silver hake (*Merluccius bilinearis*)	Demersal/Benthic	Marine; demersal; oceanodromous	--		--
Spot (*Leiostomus xanthurus*)	Demersal/Benthic	Marine; brackish; demersal; oceanodromous	--		--
Spotted hake (*Urophycis regia*)	Demersal/Benthic	Marine; demersal; non-migratory	--		--
Striped bass (*Morone saxatilis*)	Demersal/Benthic	Marine; freshwater; brackish; demersal; anadromous	--		--
Striped searobin (*Prionotus evolans*)	Reef-associated	Marine; brackish; reef-associated	--		--
Summer flounder (*Paralichthys dentatus*)	Demersal/Benthic	Marine; brackish; demersal; oceanodromous	--		--
Tautog (*Tautoga onitis*)	Reef-associated	Marine; brackish; reef-associated	--		--
Weakfish (*Cynoscion regalis*)	Demersal/Benthic	Marine; brackish; demersal; oceanodromous	--		--
White hake (*Urophycis tenius*)	Demersal/Benthic	Marine; demersal; oceanodromous	--		--
Windowpane flounder (*Scophthalmus aquosus*)	Demersal/Benthic	Marine; brackish; demersal	--		--
Winter flounder (*Pseudopleuronectes americanus*)	Demersal/Benthic	Marine; demersal; oceanodromous	M		--
Witch flounder (*Glyptocephalus cynoglossus*)	Demersal/Benthic	Marine; demersal; oceanodromous	M		--
Yellowtail flounder (*Limanda ferruginea*)	Demersal/Benthic	Marine; demersal	M		--

Notes:
* At least one distinct subspecies is considered endangered in all or part of species' distribution.
Dashes indicate no known magnetosensitivity or electrosensitivity noted within scientific literature.
[a] Information from fishbase.org

E = electrosensitive
M = magnetosensitive

2.4.3 Pelagic Receptors Exposure to Project-Related EMF

Pelagic species, including many varieties of highly mobile fish as well as species utilizing the sea surface such as seabirds and waterbirds, are expected to have relatively limited exposure to Project-related EMF.

Fish species include Atlantic bluefin tuna (*Thunnus thynnus*), bluefish (*Pomatomus saltatrix*), Atlantic salmon (*Salmo salar*), shortfin mako (*Isurus oxyrinchus*), and Atlantic common thresher shark (*Alopias vulpinus*).

Avian species using the sea surface include sea ducks[7], shearwaters and petrels[8], and grebes[9] (NYSERDA 2010; BRI 2015). Species such as cormorants[10] and loons[11] may utilize the sea surface and seek out prey underwater (NYSERDA 2010; BRI 2015).

Exposure to Project-related EMF is expected to occur only in the immediate vicinity of buried or covered cables associated with the BW1 and BW2 electric transmission systems. This is because EMF levels dissipate rapidly in the environment with distance from the cables (Bull and Helix 2011; CMACS 2003; Taormina et al. 2018; Gill and Desender 2020; Tetra Tech 2021; Snyder et al. 2019). Pelagic species, because they reside in the open water column or at the sea surface, will be physically separated from seafloor areas where Project-related EMF will occur.

While pelagic species are not of central focus in this risk assessment given their limited potential exposure, information regarding potential effects of EMF to a number of pelagic species are included for consideration in **Section 2.5** below.

2.4.4 Marine Mammals and Sea Turtles

Several marine mammals and species of sea turtles inhabit the western Atlantic, including the areas along the coastline and the Lease Area where the Project's electric transmission systems will be located. Some species have migratory ranges expanding across multiple oceans. Humpback whales (*Megaptera novaeangliae*), for example, may travel up to 5,000 mi (8,047 km) annually migrating between high-latitude summer feeding grounds and winter mating and

[7] For example, common eider (*Somateria mollissima*), surf scoter (*Melanitta perspicillata*), white-winged scoter (*Melanitta deglandi*), and Black Scoter (*Melanitta americana*).
[8] For example, northern Fulmar (*Fulmarus glacialis*), Cory's shearwater (*Calonectris borealis*), greater shearwater (*Puffinus gravis*), sooty shearwater (*Puffinus griseus*), manx shearwater (*Puffinus puffinus*), Wilson's storm petrel (*Oceanites oceanicus*), and Leach's storm petrel (*Oceanodroma leucorhoa*).
[9] For example, red-necked grebe (*Podiceps grisegena*) and horned grebe (*Podiceps auritus*).
[10] Double-crested cormorant (*Phalacrocorax auritus*) and great cormorant (*Phalacrocorax carbo*).
[11] Common loon (*Gavia immer*) and red-throated loon (*Gavia stellata*).

calving areas in tropical waters.[12] For sea turtles, a metasynthesis of maximum migration distances for adults reported by Hays and Scott (2013) shows ranges between approximately 620 and 1,864 mi (1,000 and 3,000 km) for green sea turtles (*Chelonia mydas)*, loggerhead turtles (*Caretta caretta*), and hawksbill turtles (*Eretmochelys imbricate*), with a maximum distance for leatherback turtles (*Dermochelys coriacea*) associated with large body mass of 6,213 mi (10,000 km).

Within these groups exist species that are federally or state-listed as endangered, threatened, or rare under state protection and conservation acts, ESA, and international law. Marine mammals in the U.S. are additionally protected under the Marine Mammal Protection Act of 1978.

In general, marine mammals are not considered to possess electroreceptive capabilities[13], though some evidence for magnetosensitivity exists. Sightings published by Walker et al. (1992) of migrating fin whales along the U.S. Atlantic coasts and mathematical extrapolation of those sightings predicted a relationship with seasonal movement (winter and fall) during corresponding periods and areas of low geomagnetic fields from the earth. No relationship was identified across all sightings across seasons. A study involving free-ranging bottlenose dolphins (*Tursiops truncates*) by Hui (1994) showed no association between earth's geomagnetic field and patterns of dolphin movement, but did find agreement between bottom topography and patterns of dolphin movement. A later study by Kremers et al. (2014) involving caged bottlenose dolphins exposed to high levels of static DC magnetic fields of 510,000 to 2,400,000 mG showed no significant effect on time spent in proximity to the magnetic field source, but the time to approach the magnetic field source was significantly shorter versus the control condition. The high levels of magnetic fields that dolphins were exposed to in this study were several orders of magnitude above low levels associated with earth's geomagnetic fields (ranging from approximately of 507–514 mG found in the vicinity of the Project location) or fields realistically associated with the HVDC submarine export cables or HVAC interarray cables for BW1 and BW2 (see **Section 4**). To this point, Kremers et al. (2014) concluded that it was unclear if, or to what degree, dolphins could detect lower intensity anthropogenic magnetic fields.

For sea turtles, there appears to exist more evidence related to magnetosensitivity and use of earth's geomagnetic field for migration (Lohmann et al. 2008). Luschi et al. (2001, 2007) described homing behaviors being influenced by magnetic sense of green sea turtles. Later work by Benhamou et al. (2011) refined this understanding by describing that use of geomagnetic fields might only be important in final locating of home areas within 30 mi (50 km), though not for long-distance migration. Brothers and Lohmann (2018) described differences in magnetic fields to predict genetic differences between loggerhead sea turtles at

[12] See https://www.fisheries.noaa.gov/species/humpback-whale
[13] The only marine mammal known to be electroreceptive is Guiana dolphin (*Sotalia guianensis*), which inhabits estuaries and the coastal waters to the north and east of South America, and east of Central America.

different nesting beaches. Collectively, these studies provide evidence that the relationship between geomagnetic fields and movement by sea turtles, though the degree to which turtles may respond to magnetic fields at very small scales, such as within immediate proximity to the HVDC submarine export cables and HVAC interarray cables, is not fully understood.

For both marine mammals and sea turtles, exposure to Project-related EMF is assumed to be negligible. While both groups show some degree of magnetosensitivity, species are highly mobile and travel significant distances, meaning that the time spent in proximity to the HVDC submarine export cables or HVAC interarray cables will be limited.

2.4.5 Spatial Scale of Potential Exposure

The areas where Project-related EMF may occur make up a small fraction of the total ecosystem utilized by the populations of marine life in the offshore waters ecosystem. The area comprising the BW1 and BW2 electric transmission system includes the Lease Area (wind turbines, HVAC interarray cables, and offshore substation facilities), an area of 128,811 ac (521 km^2), and the HVDC submarine export cables route corridors, an area of 2,190 ac (9 km^2) (the total for both cables assuming the length of each cable route and a buffer of 50 ft [15.2 m] on either side of corridor route for each cable). The HVDC submarine export cable route corridor area increases to 2,810 ac (11 km^2) with the BW2 submarine export cable routed to the Astoria Power Complex. The combined acreage of this area is approximately 131,001 ac (530 km^2) with the BW2 submarine export cable routed to the Millstone Power Complex and 131,621 ac (533 km^2) with the BW2 submarine export cable routed to the Astoria Power Complex.

In its modeling of populations of commercial and non-target species, the National Marine Fisheries Service has adopted an ecosystem-based fisheries management approach using the Northeast U.S. (NEUS) Continental Shelf Ecosystem. This ecosystem is divided into the southern New England, Gulf of Maine, Georges Bank, and the Mid-Atlantic Bight ecoregions. The ecoregions are based largely on the availability of long-term biological survey data on a variety of target and non-target species, including data for fish, sharks, skates, crabs, lobsters, other crustaceans, molluscs, and plankton, as well as marine mammals. The combined acreage of NEUS Ecosystem is approximately 61,000,000 ac (247,000 km^2; Link et al. 2006).

Based on the above summary of acreages, the BW1 and BW2 electric transmission area represents approximately 0.21% or 0.22%, based on the routing of the BW2 submarine export cable, of the total NEUS Ecosystem (**Figure 7**). The values presented in **Figure 7** are assuming the BW2 submarine export cable is route to the Millstone Power Complex. If only the southern New England Area was considered, the total BW1 and BW2 electric transmission area represents approximately 0.83% of the regional ecosystem.

Careful ecological judgment is needed when drawing conclusions about such comparisons, including consideration of relative differences in animal density across individual ecoregions,

special status of vulnerable species, availability of connected habitat, and the actual spatial scale of local and meta-populations (e.g., Hutchison et al. 2018; Dunne et al. 2002; Ebenman and Jonsson 2005; Kramer et al. 2011; Hanski 1998; Preziosi and Durda 1999; Pastorok and Preziosi 2011; Suter et al. 2005; Spromberg et al. 1998). However, at a simplistic level the comparison shows that the spatial extent of the area where Project-related EMF may occur is a relatively small portion of the overall area utilized by populations of demersal and pelagic species inhabiting the regional NEUS Ecosystem.

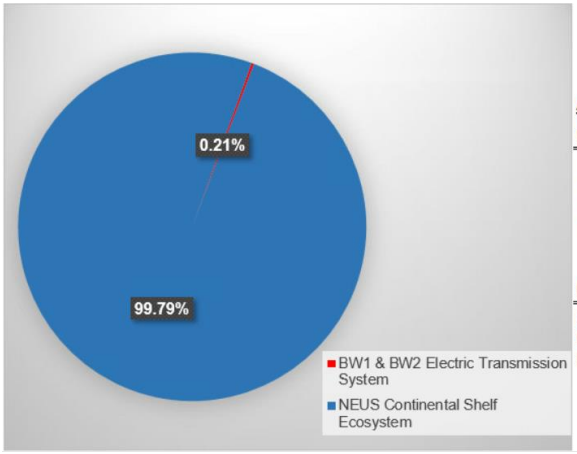

Area	Acres	Square Kilometers
NMFS Ecosystem-based Fisheries Management		
Southern New England	15,822,820	64,033
George's Bank	10,785,502	43,647
Gulf of Maine	19,544,616	79,094
Mid Atlantic Bight	14,772,329	59,782
NEUS Continental Shelf Ecosystem	60,925,267	246,556
BW1 & BW2 Electric Transmission System		
Lease Area OCS-A 0520	128,811	521
BW1 HVDC Submarine Export Cable corridor	1,405	6
BW2 HVDC Submarine Export Cable corridor	785	3
BW1 & BW2 Subtotal	131,001	530

Figure 7. Comparison of BW1 and BW2 Electric Transmission System Area Relative to the Northeast U.S. Continental Shelf Ecosystem.

2.4.6 Duration of Potential Exposure

The duration over which exposure may occur is an important consideration when assessing risk (USEPA 1992, 1998; Suter 2007, 2008). This is because impacts from stressors in the environment manifest themselves over differing timeframes of exposure. For example, a species may show limited, long-term effects resulting from high levels of exposure over very brief periods, referred to as "acute" exposures that occur over the course of seconds, minutes, or hours. The same species, however, may experience long-term effects from low levels of exposure from the same stressor but over an extended period, referred to as "chronic" exposures that occur over the course of days, months, and years.

For the assessment of Project-related EMF risks, both acute and chronic exposure conditions were considered. In general, exposure to the buried HVDC submarine export cables and HVAC interarray cables are assumed to be of shorter, acute exposure timeframes (such as when a fish may be passing above cables buried at target depths of 3.3 to 6.6 ft [1 to 2 m]). In instances when these cables are covered by rock, rock bags, or concrete mattresses, individual organisms may congregate over longer, chronic exposure timeframes (e.g., crustaceans seeking out and inhabiting hard bottom and structures). These congregations over time are similarly assumed

to occur for the base of the wind turbines and offshore substation facilities where rock, rock bags, or concrete mattresses are proposed for placement.

2.5 SENSITIVITY OF MARINE LIFE TO EMF

Several marine species across various taxa are known to have specialized sensory organs or physiological systems that interact with EMFs produced from both natural and anthropogenic sources.

Species within the elasmobranch group are known to be both electrosensitive and magnetosensitive. Elasmobranchs possess electroreceptive capabilities through the presence of specialized, gel-filled organs referred to as Ampullae of Lorenzini. These small, pore-like organs are located predominantly across their heads and pectoral fins and are believed to be used in the detection of prey and mates (Murray 1960). Elasmobranch electrosensitivity allows for the detection of low frequency electric fields of 1 to 10 Hz. This ability to detect electric fields is used when foraging to detect prey items at close proximity (Bedore and Kajiura 2013). The magnetosensitivity of certain elasmobranchs is thought to aid in migration. Scalloped hammerhead sharks (*Sphyrna lewini*) have been documented as being able to perceive naturally occurring alterations in the geomagnetic field through tagging studies that show disproportional distribution along boundaries (Klimley 1993).

While a variety of fish throughout the world show electroreceptive abilities, at the regional level and in relation to the Project's electric transmission systems, only the federally endangered Atlantic sturgeon (*Acipenser oxyrinchus oxyrinchus*)[14] and shortnose sturgeon[15] are known to be electroreceptive. Electroreception in sturgeon is believed to aid along with olfactory cues in the detection of prey (Zhang et al. 2012). Sturgeon have also shown to possess magnetoreceptive abilities. An investigation of Atlantic sturgeon migrations in the New York area indicated that these were predictable and governed by a series of environmental cues, including photoperiod and water temperature (Ingram et al. 2019).

A number of fish species demonstrate some level of magnetosensitivity, likely as a result of physiological adaptions such as the presence of particles of magnetite in bones and organs (Harrison et al. 2002). Fish including tuna, carp, salmonids, and eels are able to perceive changes in the geomagnetic field and use these to guide migrations (Hanson and Westerberg 1987; Tański et al. 2011; Walker et al. 1988), though this ability is likely used in conjunction with multiple other environmental variables, including photoperiod, changes in temperature and currents, and olfactory cues (Leggett 1977). Only a very few fish have demonstrated the

[14] See https://www.fisheries.noaa.gov/species/atlantic-sturgeon
[15] See https://www.fisheries.noaa.gov/species/shortnose-sturgeon

capacity to detect low-level electric fields, an ability that is mediated by specialized and sensitive electroreceptors (Ampullae of Lorenzini).

Plausible evidence of either magneto- or electroreceptivity has been demonstrated for marine molluscs, arthropods, and echinoderms. While there is evidence to suggest that invertebrates can detect magnetic fields, support for electroreception is lacking for this group. Patullo and Macmillan (2007) found that two species of crayfish (*Cherax destructor* [Australian freshwater crayfish], and *Procambarus clarkii* [freshwater crayfish]) showed behavioral responses to electric field stimulus of 20 mV/cm. When tested in conjunction with other stimulus (mechanical and olfactory), the responses suggested that the sensory mechanisms triggered were not due to highly specialized electro-sensory organs, comparable to the Ampullae of Lorenzini seen in elasmobranchs. The suggested functional role of electroreception in invertebrates is to aid in prey detection and predator avoidance (Patullo and Macmillan 2007). However, a response to the Patullo and Macmillan (2007) study by Steullet et al. (2007) refutes previous claims that the two species of crayfish are able to use electroreception in any meaningful way to respond to electric field stimuli that are environmentally relevant, and also showed a clear lack of a specialized electro-sensory systems within these two invertebrate species (Steullet et al. 2007). No specialized biological electro-sensory system has been identified for any invertebrate species.

The ability of organisms to detect and orient themselves along geomagnetic lines for navigation has been demonstrated across various clades and numerous species. Nordmann et al. (2017) discusses the three leading hypotheses that explain the mechanisms that organisms may use to sense and act upon magnetic stimuli. The three mechanisms of sensory systems discussed include: 1) a magnetite-based receptor that functions through mechanical stimulus; 2) a chemical-based mechanism that responds to light-induced biochemical reactions; and 3) electro-magnetic induction through other accessory structures. These three systems for interpreting magnetic stimuli are not mutually exclusive and could be used in conjunction with one another to allow an organism to orient itself along magnetic fields (Nordmann et al. 2017).

2.5.1 Effect Reference Values

Effect reference values (ERVs) were used for the risk assessment as representative field strength levels associated with EMF impacts to species within each of the demersal invertebrate, elasmobranch, and finfish groups. The values were identified for DC magnetic and AC magnetic and electric fields based on the available literature on EMF effects for species within each of the groups. The ERVs were then used in comparison to the predicted Project-related EMF that receptors may be exposed to for the characterization of risk (**Section 5**).

The ERVs were selected based on established ecological risk assessment procedures for selection of toxicity reference values and ecological screening benchmarks used in chemical risk

assessment (e.g., Sample et al. 1996; USEPA 2005; Durda and Preziosi 2000). ERVs were selected from the available literature based upon the following prioritization:

- Preference was given to effect studies of EMF performed in controlled laboratory settings reflecting environmentally realistic exposure conditions
- Priority was placed on studies incorporating test species relevant to waters of southern New England, or otherwise considered taxonomic and functional surrogates
- Experimental design used in the studies included multiple exposure levels to define dose response, including a characterization of shape of the dose–response curve
- Measurement endpoints included in the studies that examined effects in test species related to growth, survival, and reproduction as corollaries to population level impacts, with behavioral and biomarker-based effects considered secondarily
- Effects levels were observed at 20% or greater relative to control, and differences were determined statistically significant
- Replicate testing was performed to account for potential variability in test species response
- Methods, materials, and analysis performed for the experimental studies are sufficiently documented and considered reproducible.

The below presents a summary of relevant literature of EMF sensitivity and effects for demersal invertebrates, elasmobranchs, and finfish. For completeness, additional discussion is provided where relevant data are available for select pelagic species (such as sharks, dolphins, and sea turtles). Upon review of the literature and guided by the hierarchy above, ERVs were then selected for each of these receptor groups.

2.5.2 EMF Sensitivity and Effects for Demersal Invertebrates

This section presents an overview of information obtained from the scientific literature on the sensitivity of demersal invertebrates to static DC magnetic fields and AC magnetic fields. As presented in **Section 2.4**, demersal invertebrates associated with offshore waters of southern New England are not known to exhibit electroreceptive abilities. Two invertebrate species, freshwater crayfish and Australian freshwater crayfish, have shown potential electroreceptive abilities (Patullo and Macmillan 2007; Steullet et al. 2007), however these species are not known to occur in offshore U.S. waters (Normandeau et al. 2011).

2.5.2.1 DC Magnetic Fields

Bochert and Zettler (2004) showed that static magnetic fields have no significant effect on several behavioral characteristics of isopod (*Saduria entomon*), common shrimp (*Crangon crangon*), dwarf crab (*Rhithropanopeus harrisii*), common starfish (*Asterias rubens*), or ragworm

(*Nereis diversicolor*) when exposed in tanks to static magnetic fields of 27,000 mG. Another study (Woodruff et al. 2012) showed that there was an effect of DC magnetic fields on the variability of behavior of Dungeness crab (*Metacarcinus magister*) when exposed to 10,000-mG fields. However, the authors found no effect on the behavior of American lobster under similar conditions (Woodruff et al. 2012).

Field studies that exposed American lobster to EMF produced by HVDC cables associated with the Cross Sound Cable in Long Island Sound (Hutchison et al. 2018, 2020b) concluded that the behavior of American lobsters was altered as a response to EMF exposure. Lobsters collected near the study area were housed in cages at sites adjacent to a HVDC cable that emitted a total magnetic field of 653 mG and control sites with no cable present. Both the treatment and control groups exhibited a distributional preference for the ends of the cages. Relative to one another, the non-exposed individuals were more likely to be found near the perimeter of the cages, whereas the exposed group more often inhabited the middle of the cages. The number of large turns performed by the lobsters increased when the cages housing the groups were relocated between control and cable sites. Although the behavior of lobster was noted as being influenced by the cable-related EMF, the cable and EMF did not create a barrier to movement by lobster across the cable. The significance of the behavioral differences between control and treatment group lobsters (e.g., differences in where lobsters congregate in cages and the number of large turns) is not fully known. Additional information is required, for example, that elucidates the probability than an individual will encounter a cable (Hutchison et al. 2018), given that the study utilized caged individuals intentionally placed in proximity to the cable. Hutchison et al. (2018) also suggested the need for environmental risk assessment to be used to reduce uncertainties to better inform the understanding of potential impacts of EMF, both at the scale of individual cables and cumulatively where multiple cables may exist.

Harsanyi et al. (2022) found that anthropogenic sources of DC EMF produce adverse effects on sensitive life stages of edible crab (*Cancer pagurus*) and European lobster (*Homarus gammarus)*. Under laboratory conditions, egg-bearing females were exposed static EMF at 28 mG during egg development and larval release. European lobster showed increased rates of larval deformities at a rate of 3% versus control at 1%. Exposed lobster larvae failed more vertical swim trials (11%) than the control (4%), though the average of successful swim speeds was comparable. Edible crab showed decreased egg volumes between stages 2 and 4, increased egg volume at stage 6, but no difference in rates of larval deformities or mortality, and no differences in swim parameters. While differences were identified for lobster larvae, the ecological significance of differences between exposed and control of 2% and 7% for deformities and vertical swim trials, respectively, is not presently understood. As suggested by the Harsanyi et al. (2022), additional study is required to further understand population level significance of the findings. In a previous study performed by Taormina et al. (2020), when European lobster were exposed to static magnetic fields up to 2,300 mG there were no observed impacts to behavioral endpoints including movement, time spent finding and staying within shelter, and overall activity levels.

Higher intensity magnetic fields have been shown to impact behavior of other commercially valuable edible crab (Scott et al. 2018). Crabs were exposed to static magnetic fields of 28,000 to 400,000 mG for 24 hours. During this exposure time, the exposed crabs preferred shelters adjacent to the source of the magnetic field, and spent less time foraging.

A recent study by Scott et al. (2021) examined the effects of lower strength EMF on edible crab. Static DC EMF strengths of 2,500 mG, 5,000 mG, and 10,000 mG were used to examine the dose–response relationship between DC EMF and behavioral and physiological endpoints. Physiological responses included D-Glucose, L-Lactate, and total haemocyte count (THC) as biomarkers of stress response resulting from exposure to the different treatment levels of EMF. Edible crab D-Glucose levels were significantly increased in individuals when exposed to EMF levels of 5,000 mG and 10,000 mG; there were no changes in D-Glucose levels resulting from exposure to 2,500 mG. Levels of L-Lactate were significantly decreased in crabs exposed to each treatment level, with crabs showing decreased levels throughout the 24-hour period at 10,000 mG, decreased levels after the 24-hour period at 5,000 mG, and decreased levels 4 hours after exposure at 2,500 mG. There were no changes in THC after exposure to 2,500 mG, significant increases after 8 hours of exposure to 5,000 mG, and a non-significant, slight increase after exposure to 10,000 mG (Scott et al. 2021). D-Glucose and THC levels returned to baseline concentrations were not significantly different than controls at 24 hours of exposure. Taken together, the authors conclude differences in these biomarkers are indicative of relative stress. However, while the experimental design included multiple levels of increasing exposure, typical dose response (i.e., increasing effects with increasing exposures) in the biomarkers was not consistently observed (see Figures 2 through 4 of Scott et al. [2021]).

Behavioral responses of edible crab described by Scott et al. (2021) included time spent in and out of shelter and shelter selection. At 2,500 mG and 5,000 mG, there were no significant differences between treatment of individuals and controls when examining time spent in and out of shelter. There was a significant increase in time spent in shelter when individuals were exposed to 10,000 mG. The dual shelter experiment showed that edible crabs will preferentially select shelters with 5,000 mG and 10,000 mG exposures, with an increased time in the EMF exposed shelter, and a decreased time spent roaming (Scott et al. 2021). The authors suggest that less time spent roaming while being attracted to EMF could come at the cost of time spent foraging for food and seeking mates. However, the authors do not consider the potential compensatory offset for less roaming, notably the lesser chance of being preyed upon while remaining in shelter. While no universally consistent dose response was observed, the data indicate increasing time spent in shelter or not roaming with increasing magnetic field exposure (see Figure 5 of Scott et al. [2021]).

Dive surveys conducted by Sherwood et al. (2016) over a 3-year period concluded that no impacts to benthic invertebrates were produced as a result of exposure to DC EMF produced by buried portions of the Basslink DC cable (Bass Strait, Australia). Unburied cables and cable

structures were noted as creating a "reef effect," producing suitable habitat and substrate for encrusting benthic invertebrates.

The Monterey Accelerated Research System, operated by the Monterey Bay Aquarium Research Institute, is composed of 60 km of 10-kV cables that provide power to various research instruments placed throughout the submarine canyon located in the Monterey Bay, California. Ecological surveys were performed from 2004 to 2015 that showed there were negligible impacts to benthic communities due to the construction and operation of the submerged cables (Kuhnz et al. 2015). The researchers found that the natural variation of benthic organisms was greater than any effects produced by the installation and energization of the Monterey Accelerated Research System cable.

Based upon the above summary, the value of 10,000 mG was selected based on the study of Scott et al. (2021) as a conservative ERV for DC magnetic levels for demersal invertebrates. While the population level significance of more time in shelter and less roaming by crabs associated with this level is not fully known, the study's use of dose–response experimental design supports selection of the value.

2.5.2.2 AC Magnetic Fields

Field studies conducted by Love et al. (2015, 2017a) investigated the effects of EMFs produced from 60-Hz AC submerged cables off of the coasts of Washington and California. Both studies were designed to show if large, mobile crustaceans would be impacted by traversing the EMF produced by AC cables powered at 60 Hz and if there could be any adverse effects due to impacts on migration. Both studies showed no changes in distribution or impediments to movement due to either the presence of the cable or the EMF produced when energized.

Red rock crab (*Cancer productus*) and yellow rock crab (*Metacarcinus anthony*) were placed adjacent to unburied AC cables, both unpowered and powered at 60 Hz, by Love et al. (2015) to determine if there was an effect on crab distributions due to produced EMF emitting from the cables. The EMF produced ranged from 462 mG to 800 mG when energized and decreased to 9 mG at the maximum extent of the cage. Results showed that crab distribution was unaffected by the EMF produced by both energized and non-energized cables.

Love et al. (2017a) studied crustacean movement in response to submerged 60-Hz cables by placing cages with Dungeness crabs and red rock crabs across the cables. The Dungeness crab field study was conducted off the coast of Washington, whereas the red rock crab was conducted off the coast of California. For the Washington study, 428 mG was measured. The California study incorporated a cable with more current and a greater EMF strength of 1,168 mG. The researchers noted no variation in the ability of either species of crabs to traverse the energized 60-Hz cables and concluded that EMF produced by 60-Hz AC cables does not create a barrier to migration or produce an impact on distribution.

Another study by Love et al. (2017b) investigated whether there are any impacts from submerged AC cables on benthic communities. Cephalopods (East Pacific red octopus; *Octopus rubens*) and California spot prawns (*Pandalus platyceros*) were noted to occur at similar rates at both cable and non-cable sites. The benthic invertebrate communities at all cable sites differed from the non-cable sites due to the structural habitat provided by the cables themselves. The authors concluded that the 60-Hz EMF produced (1,100 mG) did not impact cephalopods or crustaceans.

A laboratory study assessing the effects of 50-Hz magnetic fields of 10 mG exposure on the behavior and physiology of the common ragworm (*Hediste diversicolor*) found that the polychaete maintained a positive energy balance and high amount (85% of assimilated energy) of energy available for individual production (scope for growth) after exposure to EMF (Jakubowska et al. 2019). The polychaetes did exhibit enhanced burrowing activity. In addition, food consumption and respiration rates were not affected, but ammonia excretion was reduced in exposed animals, with plausible consequences for their metabolism; however, knowledge about the biological relevance of this response is currently absent (Jakubowska et al. 2019).

Based on the above summary, no identifiable effect threshold for AC magnetic fields is available from existing studies. For the purposes of this assessment, the effect threshold level for DC magnetic fields of 10,000 mG based on the study of Scott et al. (2021) is selected as surrogate value for AC magnetic fields for demersal invertebrates.

2.5.3 EMF Sensitivity and Effects of Demersal Elasmobranchs

This section presents an overview of information obtained from the scientific literature on the sensitivity of demersal elasmobranchs to static DC magnetic fields and AC magnetic and electric fields.

2.5.3.1 DC Magnetic Fields

Laboratory and field studies performed with elasmobranch species have documented behavioral response to static magnetic fields produced from DC sources. Sandbar sharks have shown the ability to detect changes between 25 mG and 1,000 mG (Nestler et al. 2010; Anderson 2018).

Hutchison et al. (2018, 2020b) included little skate among the field experiments of caged organisms placed adjacent to the Cross Sound Cable in Long Island Sound. The submerged cables emitted a total magnetic field of 653 mG. Relative to the control group, caged skates placed adjacent to the cable traveled longer average distance (1.1 mi [1.7 km] [control] versus 2 mi [3.2 km] [adjacent to cable]), had larger average proportions of large turns (21% [control] versus 29% [adjacent to cable], and swam at lower heights (26 in. [65 cm] [control] versus 17 in.

[42 cm] [adjacent to cable]). Skates used the full available space in both enclosures, and they spent most of their time at the ends of the enclosure. However, skates spent more time in the central space of the control enclosure compared to the treatment enclosure. The ecological significance of the behavioral differences between control and treatment group skates to population level impacts, particularly resulting from changes in individual energy budgets, is not fully known.

The above studies indicate available information relating to elasmobranch sensitivity for detecting levels of static magnetic fields as low as 25 mG. While these studies are informative for relating physical mechanisms and limits for identification of prey and orientation, they are not relatable to deleterious effects of DC electric fields for this receptor group. With respect to the 46% greater average difference traveled (i.e., (1.1 mi [1.7 km] [control] versus 2 mi [3.2 km] [adjacent to cable]) for little skate as reported in Hutchison et al. (2018, 2020b), these differences are pronounced and could result in shifts in energy allocation for individuals if encounters are continuous and prolonged over time. However, in the context of the overall population of little skate in the NEUS Continental Shelf Ecosystem, exposures at the population scale are considered negligible (see **Figure 7** above and accompanying discussion) relative to the spatial scale of Project-related EMF exposure conditions.

Based on the available literature and above considerations, an ERV could not be identified for DC magnetic fields and elasmobranchs.

2.5.3.2 DC Electric Fields

Behavior of Eastern shovelnose ray (*Aptychotrema rostrata*) and common shovelnose ray (*Glaucostegus typus*) were tested for electrosensitivity in experimental laboratory tanks fitted with electrodes connected to a DC battery source (Wueringer et al. 2012). The electric fields caused changes in a variety of behaviors, including approaches towards the battery source. The authors reported that the median DC electric-field strength at the point of response initiation ranged between approximately 5e-4 mV/m and 8e-3 mV/m. Bedore et al. (2014) reported detection sensitivity for cownose rays of 1.1e-2 mV/m and sensitivity for yellow stingrays (*Urobatis jamaicensis*) of 2.2e-3 mV/m. Bedore and Kajiura (2013) reported DC electric-field sensitivities for elasmobranchs ranged from 5e-4 to 4.8e-3 mV/m at maximum distances up to 1.3 ft (0.4 m) when produced by a static power source.

Spiny dogfish and smooth dogfish (*Mustelus canis*) ability to detect electric fields from a static magnetic-field source were determined to be 1.4e-3 mV/m and 2.9e-3 mV/m, respectively (Jordan et al. 2011). Gill and Taylor (2001) obtained field-collected lesser spotted dogfish (*Scyliorhinus canicular*) and tested their electrosensitivity under laboratory settings. Electric fields of 100 mV/m produced by a static power source caused avoidance behaviors, although these behaviors were observed to be highly variable among tested individuals. Juvenile scalloped hammerhead and sandbar sharks both showed altered orientation within their tanks

in response electric fields generated by a static source, 2e-3 mV/m electric field (Kaijura and Holland 2002).

The above studies indicate significant research has been performed to identify the exceptionally low levels of static electric fields that can be detected by elasmobranchs. For example, these studies document the ability to detect levels as low as 5e-4 mV/m. Under natural conditions in the ocean environment, however, organisms are regularly exposed to induced electric fields at this level. For example, using earth's geomagnetic field of 512 mG for the waters of southern New England, and a low current velocity of 0.2 ft/s (5 cm/s), results in a predicted induced electric field in the ocean environment of 2.6e-3 mV/m. This example underscores that data relevant to the low levels of sensitivity achievable by elasmobranchs are not equivalent to levels that would result in effects.

In light of the available literature and these considerations, an ERV was not selected for DC electric fields for elasmobranchs. However, as discussed in **Section 2.5.4**, the ERV derived for electric fields for demersal finfish based on a sturgeon species is used as the surrogate ERV for elasmobranchs.

2.5.3.3 AC Magnetic and Electric Fields

As described above, bioelectric fields generated by all living marine organisms through the presence of mucous, heartbeats, gill movements, nerve impulses, and uneven distributions of electric charge along their bodies created by muscle contractions (Bedore and Kajiura 2013; Normandeau et al. 2011; Snyder et al. 2019). These electric fields are predominant as static DC, but AC components can be added from rhythmic movement of gills (lower frequency of <10 Hz) or muscle contractions (higher frequency > 20 Hz). Predators that can detect bioelectric fields, notably elasmobranchs, are thought most capable of detecting frequencies ≤2 Hz, and no more than 20 Hz (Bedore and Kajiura 2013). As frequencies increase above these ranges, elasmobranchs are less able to detect EMF (Andrianov et al. 1984).

Electrosensitivity in shark species has been shown to aid in foraging, but at more sensitive life stages (e.g., embryonic stages) the same electrosensitivity has been shown to aid in predator avoidance (Kempster et al. 2013). Bamboo shark (*Chiloscyllium punctatum*) embryos showed greatest response associated with frequencies ranging from 0.25 to 1.0 Hz, with responses diminishing above this range (Kempster et al. 2013).

A study performed by Love et al. (2016) found that there were no impacts to elasmobranch species along submerged cables off of the coast of California. Transects were performed along cable impacted habitat and non-impacted habitat to assess if elasmobranchs were repelled or attracted to energized cables.

Gill et al. (2009) constructed 130 ft (40 m) circular experimental tanks (i.e., mesocosms) within shallow, sheltered coastal waters of Scotland to evaluate demersal elasmobranch response to

HVAC cables[16] added to the tanks. The cables were buried at a depth of 1.6 to 3.3 ft (0.5 to 1 m). Thornback ray (*Raja clavata*), small-spotted catshark (*Scyliorhinus canicula*), and spurdog (*Squalus acanthias*) were fitted with telemetry tags to record real-time movements. Analysis of the movements showed that there were inconsistent findings for the numbers of individual fish near the cables. Overall, catshark were found to be more likely located near an energized cable and less mobile (Gill et al. 2009). For all other comparisons there was no statistically significant difference. After extensive study, the authors concluded "there is no evidence from the present study to suggest any positive or negative effect on elasmobranchs of the EMF encountered."

Other field surveys to evaluate potential EMF near HVAC cables versus background areas off the coast of California showed no significant impacts on elasmobranch assemblages (Love et al. 2016).

Collectively, these studies indicate that elasmobranchs are unlikely to detect EMF frequencies above 20 Hz. As the Project's HVAC cables are 60 Hz, outside the frequency detectable by elasmobranchs, effects are not anticipated. As this information demonstrates a lack of evidence for significant effects, no ERV is selected.

2.5.4 EMF Sensitivity and Effects of Demersal Finfish

This section presents an overview of information obtained from the scientific literature on the sensitivity of demersal finfish to static DC magnetic fields and AC magnetic and electric fields.

2.5.4.1 DC Magnetic Fields

While numerous studies have been performed to identify levels of static magnetic fields detectable by finish, studies have also been performed to attempt to identify levels associated with potential effects.

Bochert and Zettler (2004, 2006) reported on exposure of European flounder (*Platichthys flesus*) in a laboratory setting to a 27,000-mG static magnetic field and determined there was no effect on the positioning of flounder within the experimental laboratory tank.

Eggs of salmonid species, including Atlantic salmon, were field collected and subjected to a 20,000-mG static magnetic field in the laboratory. Rate of sinking and permeability of eggs to water was measured in an osmotically active solution in artificial water columns (Sadowski et al. 2007). Based on the exposure level, the permeability of eggs was significantly increased by approximately 26% relative to control eggs ($p \leq 0.025$). Other short term-exposures to 50,000 to

[16] The HVAC cables had a conductor cross section of 16 mm^2 and could carry 600–1,000 V and was rated from 25 to 730A (Gill et al. 2009).

100,000 mG were found to significantly increase the oxygen uptake in rainbow trout (*Oncorhynchus mykiss*) embryos (Formicki and Perkowiski 1998).

Woodruff et al. (2012) evaluated EMF effects under laboratory conditions associated with marine and hydrokinetic devices. The authors used measurement endpoints focused on developmental changes (i.e., growth and survival from egg or larval stage to juvenile), exposure markers indicative of physiological responses, or behavioral responses (e.g., detection of EMF, interference with feeding behavior, avoidance or attraction to EMF). Using exposures of up to 30,000 mG showed no significant effects relative to control for growth and development of larvae.

Striped bass, when exposed to magnetic fields up to 364,000 mG under laboratory settings, showed no difference in activity or distribution relative to control (Cada et al. 2012).

Studies on effects of DC magnetic fields have also been performed for sturgeon. McIntyre et al. (2016) performed laboratory experiments with Atlantic sturgeon and did not identify any behavioral changes across multiple exposures conditions of 50 mG, 1,000 mG, and 10,000 mG. Kavet et al. (2016) investigated potential effects to green sturgeon (*Acipenser medirostris*) resulting from the Trans Bay Cable in San Francisco Bay. The cable had varying effects identified for outbound and inbound migratory sturgeon: outbound migration times were significantly prolonged, while inbound migration times were shortened by the presence of the energized Trans Bay Cable (Kavet et al. 2016). The authors additionally identified that bridges spanning the San Francisco Bay were associated with up to an order-of-magnitude higher magnetic-field distortions than the Trans Bay Cable. A subsequent study by Klimley et al. (2017) concluded that magnetic-field distortions associated with the bridges in the San Francisco Bay indicated that these did not constitute a "strong barrier" to fish migration (Klimley et al. 2017). This conclusion was reached for a variety of fish, and notably green sturgeon and Chinook salmon (*Oncorhynchus tshawytscha*).

For other highly migratory fish, Westerberg and Begout-Anras (1999) monitored the movements of migratory European eel (*Anguilla anguilla*) in relation to potential effects associated with 450-kV Baltic DC submarine and found the cable did not act as a barrier or obstruction to migration for the species.

Based on the above summary, limited effects have been documented for finfish exposed to DC magnetic fields. The lowest effect level identified was for Atlantic salmon based on reproductive effects associated with changes in egg permeability of 26% relative to control following exposure to 20,000 mG (Sadowski et al. 2007). While dose response was not examined in this study, the value was conservatively selected as the ERV for DC magnetic fields for finfish.

2.5.4.2 AC Magnetic Fields

Atlantic salmon exposed to 50-Hz magnetic fields up to 950 mG exhibited no significant change in swim behavior (Armstrong et al. 2015). Similarly, European eels were exposed to a 960 mG 50-Hz magnetic field, which elicited no significant effects on swimming behavior, orientation, or passage through the tank system (Orpwood et al. 2015).

In research performed by the U.S. Department of Energy, Oak Ridge National Laboratory, Cada et al. (2012) performed laboratory experiments to evaluate EMF effects potentially associated with hydrokinetic devices for rivers. Tests were performed using lake sturgeon (*Acipenser fulvescens*) with multiple exposures up to 66,000 mG 60-Hz AC magnetic field under laboratory conditions. Exposure levels of 100%, 50%, 25%, 5%, 4%, and 1% maximum magnetic field strength were tested and observations were made for multiple replicates in the experiment. Initial examination of potential dose response was examined by comparing exposures to proportions of fish showing effects. Behaviors observed most frequently in response to the 66,000-mG exposure level included pectoral fin flare (30.5% of all observations), slowing or gliding (22.6%), body spasms (20%), remaining in area of the source (15.5%), and sudden stops near the magnet (14.2%). Differences were identified to be significantly different than control treatments ($p = 0.002$).

In other studies involving sturgeon, swimming behavior and distribution of pallid sturgeon (*Scaphirhynchus albus*) were unaffected by 18,000 to 24,500 mG 60-Hz AC magnetic fields (Bevelhimer et al. 2013).

Overall, there is limited evidence to suggest effects to finish associated with environmentally realistic exposures to AC magnetic fields. The lowest effect level identified was for lake sturgeon based on effects associated with changes in swimming behavior greater than 20% relative to control at an exposure level of 60,000 mG (Cada et al. 2012). While only temporary and reversible changes in swimming behavior were observed, and not long-term changes in growth, survival and reproduction, the value of 60,000 mG was conservatively selected as the ERV for AC magnetic fields for finfish.

2.5.4.3 DC and AC Electric Fields

While a variety of fish throughout the world show electroreceptive abilities, at the regional level and in relation to the Project's electric transmission systems, only the federally endangered Atlantic sturgeon[17] and shortnose sturgeon[18] are known to be electroreceptive.

As is the case for elasmobranchs, numerous studies have been performed on a variety of sturgeon species to document abilities to detect static DC electric fields, while less attention has

[17] See https://www.fisheries.noaa.gov/species/atlantic-sturgeon
[18] See https://www.fisheries.noaa.gov/species/shortnose-sturgeon

been placed on evaluated potential effects to electric fields. For example, shovelnose sturgeon (*Scaphirhynchus platorynchus*), the smallest freshwater sturgeon in North America, can detect static electric fields as low 10 to 20 mV/m (Teeter et al. 1980), within comparable ranges of elasmobranchs.

With respect to sensitivity to AC electric fields, Basov (2007) reported responses (based on a previous study performed by Basov [1999]) to 50-Hz AC electric fields using Russian sturgeon (*Acipenser gueldenstaedtii*) and sterlet (*Acipenser ruthenus*). At levels above 50 mV/m, the author reported avoidance behaviors in both species (Basov 2007). Limited information was presented by the author regarding experimental design and statistical analysis of the data, and the significance of observed differences relative to control treatments.

While a number of significant uncertainties exist with respect to the reported levels by Basov (2007), the value of 50 mV/m 50-Hz AC electric field level is conservatively selected as the ERV for both AC and DC electric fields for finfish. The value is additionally used as a surrogate ERV for elasmobranchs, as the mechanism of electroreception between the taxa are considered analogous based on the common presence of Ampullae of Lorenzini.

2.5.5 Summary of Selected ERVs

Table 4 below summarizes the ERVs selected for the demersal invertebrate, elasmobranch and finfish receptor groups as described above. The calculated levels of Project-related EMF are described in **Sections 3 and 4**. The calculated levels are then compared to the ERVs in the risk characterization presented in **Section 5**.

Table 4. ERVs Selected for Demersal Invertebrates, Elasmobranchs and Finfish.

	DC Magnetic Field			AC Magnetic Field			DC Electric Field			AC Electric Field		
Receptor group	mG	Endpoint	Source	mG	Endpoint	Source	mV/m	Endpoint	Source	mV/m	Endpoint	Source
Invertebrates	10,000	B	Scott et al. (2021)	10,000	B	Scott et al. (2021)	NA	--	--	NA	--	--
Elasmobranchs	653	B	Hutchison et al. (2018)	ND	--	--	50	B	Basov (2007)	ND	--	--
Finfish	20,000	R	Sadowski et al. (2007)	60,000	B	Cada et al. (2012)	50	B	Basov (2007)	50	B	Basov (2007)

Notes:
B = Behavioral
ERV = Effect reference value
G = Growth
ND = ERV not derived due to documented lack of evidence of effects or limited data
NA = Not applicable (receptor group known to not be magento- or electrosensitive)
R = Reproduction

3 METHODS OF ANALYSIS

The methods for modeling the potential EMF levels from the proposed BW1 and BW2 DC and AC Project cables are discussed below. The methods applied for the evaluation of potential EMF from the BW1 and BW2 wind turbines and offshore substation facilities are also discussed.

Integral Consulting Inc. (Integral) relied upon data provided by Beacon Wind (e.g., details on the configuration, construction, phasing, rating, location of routing, and burial depth of cables) to calculate magnetic field levels. The calculations assumed that all conductors are parallel to one another and infinite in length, the load on the phase conductors is balanced, there is no attenuation of magnetic fields from any surrounding material, and there are no unbalanced currents flowing along the outer sheaths of the cables.

3.1 HVDC SUBMARINE EXPORT CABLES

The DC current flowing through the HVDC submarine export cables will produce a DC magnetic field. The strength of this static magnetic field will vary based on the proximity of the two cable conductors or poles, the direction of the cable path relative to earth's geomagnetic field, the loading, and the cable burial depth. Along the proposed route of the BW1 and BW2 HVDC submarine export cables, earth's DC magnetic field is variable. This ever-present DC magnetic field can influence the DC magnetic field generated by the DC cables. The strength of the DC magnetic field along the cables was calculated using the Biot-Savart Law. Earth's geomagnetic field was added to the magnetic field from the DC cables, using vector addition, to calculate the total DC magnetic field. Magnetic field values are reported as magnetic flux density in mG and were calculated as the strength of the magnetic field along the major axis of the ellipse.

In addition, Integral evaluated the extent to which the BW1 and BW2 HVDC submarine export cables magnetic fields may influence magnetic compass direction, referred to as compass deflection. A compass needle typically points along the direction of the earth's geomagnetic field, but a new DC magnetic field source may cause a local deviation in the apparent direction of magnetic north. This deviation was calculated as the compass deflection, which is the difference in angular direction in degrees between the horizontal component of the ambient geomagnetic field and the horizontal component direction of the combined geomagnetic field from the earth and the DC field from the cables.

The metallic and dielectric insulation surrounding the BW1 and BW2 HVDC submarine export cables will inhibit any electric field from the current flowing through the cable being exposed to

the marine environment (Snyder et al. 2019). However, a DC electric field is induced by electric charges, or ions, such as those in seawater and marine species, flowing through a static DC magnetic field. Earth's DC geomagnetic field will cause a background induced electric field to be produced, a result of electric charges flowing through it. That induced electric field will be altered as a result of the magnetic field being altered around and above the export cable. The magnitude of the motion-induced DC electric field was calculated using an assumed ocean current velocity, or swimming speed of a marine organism, and applying a modified version of the Lorentz force equation. The magnitude of the motion-induced DC electric field, E in $\mu V/m$, is computed by:

$$E = vB \sin\theta$$

where v is the velocity of the seawater or marine organism in m/s, B is the vertical component magnitude of the magnetic field vector, in μT, resultant from the combination of Earth's geomagnetic field and the HVDC submarine export cable, and $\sin\theta$ is the angle between vectors v and B.

3.1.1 BW1—HVDC Submarine Export Cable

The BW1 HVDC submarine export cable will consist of one 320-kV circuit and will be approximately 202 nm (374 km) in length. The cables will extend from the BW1 offshore substation facility and will make landfall at Lawrence Point at the Astoria Power Complex in Queens, New York (**Figure 8**).

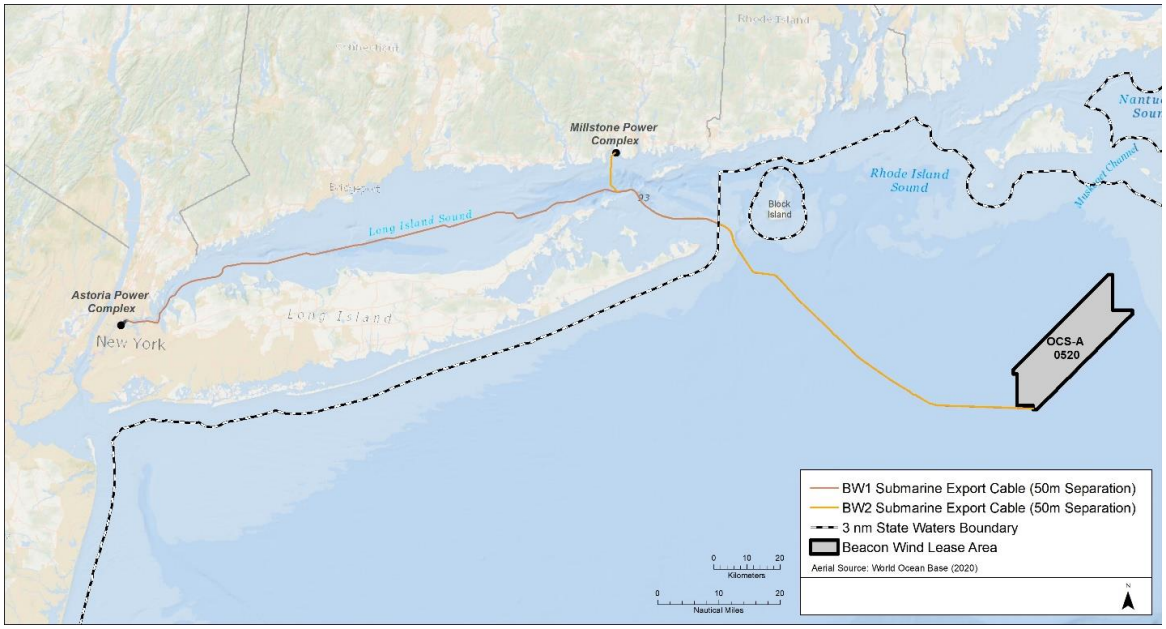

Figure 8. Beacon Wind Project Overview including Lease Area and Proposed Route of BW1 Submarine Export Cable to the Astoria Power Complex in Queens, New York, and BW2 Submarine Export Cable to the Millstone Power Complex in Waterford, Connecticut.

Along the proposed route of the BW1 HVDC submarine export cable, the earth's DC magnetic field has a strength of 507–514 mG (**Figure 9**; Chulliat et al. 2020). For the DC magnetic field analysis presented below, the average value along the cable route was used, equal to 512 mG.

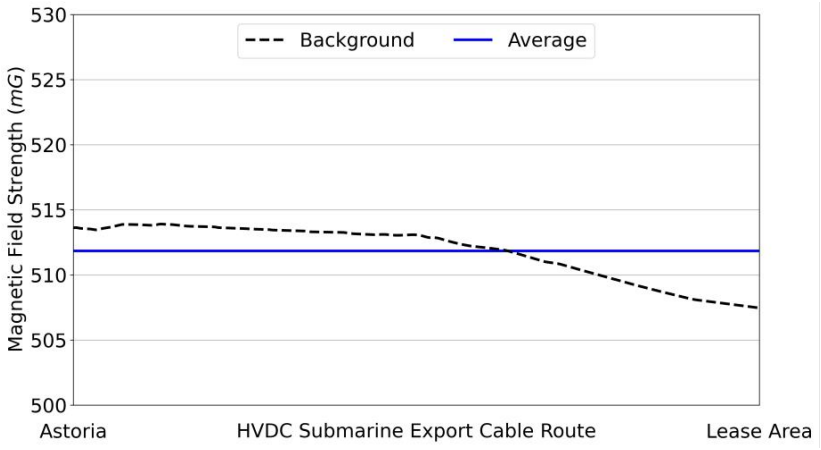

Figure 9. Background Magnetic Field Strength along BW1 Submarine Export Cable Route from Earth's Geomagnetic Field Predicted by the World Magnetic Model.[19]

This cable may occur in a variety of pole separations and burial depth configurations along its route. The poles may occur as a bundled cable, or the poles may be separated by a distance of up to 33 ft (10 m). Along a majority length of the HVDC submarine export cables, the proposed target burial depth will be between 3 and 6 ft (0.9 and 1.8 m), though some portions will be buried deeper, when within a navigation channel. Where the target burial depth cannot be achieved those portions will not be buried and rock, rock bags, or concrete mattresses will cover the cables. Within a navigation channel, the burial depth is planned for at least 15 ft (4.6 m) below existing or the U.S. Army Corps of Engineers authorized dredge depth, whichever is deeper.

The orientation of the proposed BW1 HVDC submarine export cable route was measured as 308° and 256°, corresponding to the cable route from the Lease Area to the mouth of Long Island Sound and as it enters Long Island Sound on route to Queens, New York (**Figure 8**). The magnetic field, compass deflection, and induced electric field as a result of the HVDC submarine export cables were computed for the single amperage, the bundled and separated configurations, and the four proposed burial depths shown in **Table 5**. As a note, the burial, or cover depth of 1 ft (0.3 m) is conservatively shallow compared to the proposed target cover depth of 5 ft (1.5 m). Model results were evaluated using the assumed winter normal conductor (WNC) rating of the cable.

[19] https://www.ngdc.noaa.gov/geomag/WMM/back.shtm

Table 5. BW1 Submarine Export Cables Parameters Used for the EMF Assessment.

Cable Parameter	Values
Voltage	±320 kV
Cable Ampacity Rating	2,190 A
Cable Route Heading	308°, 256°
Cable Pole Separation	Bundled, 33 ft (10 m)
Proposed Burial Depths	1, 3, 6, 15 ft (0.3, 0.9, 1.8, 4.6 m)

3.1.2 BW2—HVDC Submarine Export Cable

The BW2 HVDC submarine export cable will consist of one 320-kV HVDC cable circuit and will be approximately 113 nm (209 km) in length if routed to Waterford, Connecticut, and the same distance as the BW1 submarine export cable if routed to Queens, New York. The cables will extend from the BW2 offshore substation facility and will make landfall at the Millstone Power Complex in Waterford, Connecticut (**Figure 8**).

Along the proposed route of the BW2 HVDC submarine export cable to the Millstone Power Complex, the earth's DC magnetic field has a strength of 507–513 mG (**Figure 10**; Chulliat et al. 2020). For the DC magnetic field analysis presented below, the average value along the cable route was used, equal to 510 mG.

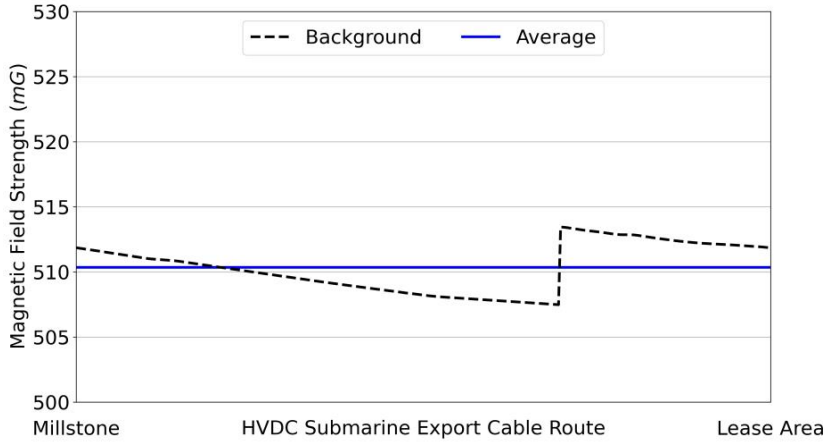

Figure 10. Background Magnetic Field Strength along BW2 Submarine Export Cable Route from Earth's Geomagnetic Field Predicted by the World Magnetic Model.[20]

The BW2 HVDC submarine export cable is proposed to have the same possible configurations as the BW1 cable, with respect to the cable separation and the burial depths. The orientation of

[20] https://www.ngdc.noaa.gov/geomag/WMM/back.shtm

the proposed BW2 HVDC submarine export cable route was measured as 308° and 359°, corresponding to the cable route from the Lease Area to the mouth of Long Island Sound and as diverges from a parallel track with the BW1 submarine export cable in route to the Millstone Power Complex in Waterford, Connecticut. If the BW2 submarine export cable landfall is at the Astoria Power Complex in Queens, New York, the cable route will be identical to that of the BW1 cable; therefore, the BW1 submarine export cable methods of analysis will be applied to the BW2 submarine export cable. The magnetic field, compass deflection, and induced electric field as a result of the HVDC submarine export cables were computed for the single amperage, the bundled and separated configurations, and the four proposed burial depths shown in **Table 6**. Model results were evaluated using the assumed WNC rating of the cable.

Table 6. BW2 Submarine Export Cables Parameters Used for the EMF Assessment.

Cable Parameter	Values
Voltage	±320 kV
Cable Ampacity Rating	2,190 A
Cable Route Heading	308°, 359°
Cable Pole Separation	Bundled, 33 ft (10 m)
Proposed Burial Depths	1, 3, 6, 15 ft (0.3, 0.9, 1.8, 4.6 m)

3.2 HVAC INTERARRAY CABLES

Current flowing through AC cables will produce an AC magnetic field. The strength of this magnetic field will vary based on the configuration of the 3-phase AC cable, the loading, and the burial depth.

The Project will include multiple 60-Hz AC cables making up the HVAC interarray cables that connect the wind turbines to the offshore substation facility. The AC voltage flowing through these cables will produce an AC magnetic field and an induced AC electric field. The magnetic field and induced electric fields generated as a result of these cables were computed for the single voltages and amperage, and other parameters shown in **Table 7**. Some portions of the HVAC interarray cables will not be buried and rock, rock bags, or concrete mattresses will be used to cover the cables. As a note, the burial, or cover depth of 0.7 ft (0.2 m) is conservatively shallow compared to the proposed target cover depth of 5 ft (1.5 m). The methods discussed below will apply to both the BW1 and BW2 HVAC interarray cables.

Table 7. Interarray Cable Parameters Used for the EMF Assessment.

Cable Parameter	Values
Voltage	66 kV
Amperage	744 A
Proposed Burial Depths	0.7 ft (0.2 m) and 6.6 ft (2 m)

3.2.1 AC Magnetic Fields

AC magnetic fields were computed using the Ansys Maxwell software, which is an EMF solver for electric machines, transformers, wireless charging, permanent magnet latches, actuators, and other electromechanical devices. It solves static, frequency-domain, and time-varying magnetic and electric fields.

As mentioned above, the AC current flowing through the HVAC interarray cables will produce an AC magnetic field. The strength of this magnetic field will vary based on the configuration of the 3-phase AC cable, the loading, and the burial depths. Unlike the DC magnetic field generated by the HVDC submarine export cables, AC magnetic fields will not create any compass deflection.

3.2.2 Induced AC Electric Fields

The metallic and dielectric insulation surrounding the HVAC interarray cable conductors will inhibit any electric field from being exposed to the marine environment (Snyder et al. 2019). However, the alternating current flowing through these cables will generate an induced AC electric field. The strength of this induced electric field will be dependent on the loading of the cables, based on the Project design recommendations. The Ansys Maxwell software was also used to model induced AC electric fields.

3.3 WIND TURBINES

Up to 155 wind turbines will generate electricity as HVAC and transfer that electric current to the respective offshore substation facilities by way of the HVAC interarray cables. The wind turbine support structures and any rock or protective mattresses at their bases will create new benthic habitat for marine species (see **Section 2.4.2** above), possibly exposing them to prolonged periods of EMF. The methods discussed below apply to the BW1 and BW2 wind turbines.

The wind turbines will be supported by monopoles. The HVAC interarray cables travel vertically through the water column within the monopile for a certain distance before exiting and running within J-tubes along the exterior of the monopile before contacting the seafloor and being buried. The exposed portion of these cables has the potential for the generation of AC EMF within the marine environment. Each wind turbine will house a maximum of two interarray cables spaced at a minimum of 6.6 ft (2 m) apart within and along the exterior of the monopile as the cables approach the seafloor. Each interarray cable consists of three conductors, as detailed in **Section 2.2.1** and shown in **Figure 3**. At the base of the wind turbine monopiles, the HVAC interarray cables will be covered by protective mattresses, to the point where trenching can be conducted and bury the cables to their proposed target burial depth of 3

to 6 ft (0.9 to 1.8 m). The EMFs as a result of the HVAC interarray cables running along the wind turbines were calculated using the parameters shown in **Table 8**.

Table 8. Wind Turbine Interarray Cable Parameters Used for the EMF Assessment.

Cable Parameter	Values
Voltage	66 kV
Cable Ampacity Rating	744 A
Number of Cables	2 per Wind Turbine (maximum)
Cable Separation	6.6 ft (2 m)
Proposed Burial Depths[a]	0.2 ft (5 cm)

Notes:
[a] The proposed burial depths for the wind turbine evaluation are a proxy for the cables within steel J-tubes.

AC magnetic fields were computed for the HVAC interarray cables within J-tubes along the lower portion of the wind turbine monopiles using the Ansys Maxwell software, which is an EMF solver for electric machines, transformers, wireless charging, permanent magnet latches, actuators, and other electromechanical devices. It solves static, frequency-domain, and time-varying magnetic and electric fields. The cables were evaluated as a cross section of the cable where it is on the exterior of the monopile, assuming a minimal separation between adjacent cables to produce a conservative result. When the interarray cables reach the seafloor and are covered by protective mattresses, the burial depth is assumed to be at the proposed target depth of 6.6 ft (2 m), where the methods of analysis presented in **Section 3.2.1** are applied.

3.4 OFFSHORE SUBSTATION FACILITIES

The above seafloor transmission structures proposed for the Project include two offshore substation facilities: one for BW1 and one for BW2 (**Figure 3**). The wind turbines will generate electricity and transfer that electric current to the offshore substation facilities. The offshore substation facilities will then convert the HVAC signal from multiple wind turbines into an HVDC signal that will be transmitted to shore-based power stations via the HVDC submarine export cables. The methods discussed below apply to the BW1 and BW2 offshore substation facilities.

3.4.1 Offshore Substation Facility AC Cables

The offshore substation facilities will be supported by a jacketed structure and the HVAC interarray cables will travel vertically through the water column within J-tubes along the exterior of the support structure before contacting the seafloor and being buried. A subset of the 18–22 HVAC interarray cables, separated by 8.2 ft (2.5 m), were modeled to determine the AC EMF generated at the offshore substation facilities. The cables are assumed to be separated into groups on the offshore substation facility support structure, utilizing the large footprint of the support structure to space out the 18–22 HVAC interarray cables. The offshore substation facilities were modeled as a single offshore substation station, representing a portion of the

HVAC interarray cables entering the structure. The exact numbers and position of all the individual cables terminating at the offshore substation facility are not known at this time and therefore could not be precisely modeled. The offshore substation facilities interarray cables were evaluated as a cross section of the cables along the supporting structure. At the base of the offshore substation facilities, the HVAC interarray cables will be buried either by rock, rock bags, or concrete mattresses to where trenching can be conducted and bury the cables to their proposed target burial depth of 3 to 6 ft (0.9 to 1.8 m). The EMFs as a result of the HVAC interarray cables running along the offshore substation facilities were calculated using the parameters shown in **Table 9**.

Table 9. Offshore Substation Facility Interarray Cable and Submarine Export Cable Parameters Used for the EMF Assessment.

Cable Parameter	AC Values	DC Values
Voltage	66 kV	±320 kV
Cable Ampacity Rating	744 A	2,190 A
Number of Cables	18–22	2
Cable Separation	8.2 ft (2.5 m)	20 ft (6 m)
Proposed Burial Depths[a]	0.2 ft (5 cm)	1 ft (0.3 m)

Notes:
[a] The proposed burial depths for the offshore substation facility evaluation are a proxy for the cables within steel J-tubes.

AC magnetic fields were also computed for the HVAC interarray cables within J-tubes along the lower portion of the offshore substation facility support structure using the Ansys Maxwell software. Prior to the interarray cables reaching the offshore substation facility, they are buried or covered by protective mattresses and the burial depth is assumed to be at the proposed target depth of 3 to 6 ft (0.9 to 1.8 m) where the methods of analysis presented in **Section 3.2.1** are applied.

3.4.2 Offshore Substation Facility DC Cables

The HVDC submarine export cables will travel vertically through the water column within J-tubes along the exterior of the support structures before contacting the seafloor and being buried. Two conductors for BW1 and two conductors for BW2 will comprise the HVDC transmission lines exiting the offshore substation facility in route to their respective landfalls. For the DC EMF modeling, the offshore substation facilities were modeled as a single offshore substation facility, representing a cross section of the submarine export cables exiting the structure. At the base of the offshore substation facilities, the submarine export cables will be buried either by rock, rock bags, or concrete mattresses to where trenching can be conducted and bury the cables to their proposed target burial depth of 3 to 6 ft (0.9 to 1.8 m). If laid at the surface, they will be covered by rocks, rock bags, or concrete mattresses. The EMFs as a result of the submarine export cables running along the offshore substation facilities were calculated using the parameters shown in **Table 9**. For the base of the offshore substation facility where

the cables reach the seafloor, the results of the submarine export cables in **Section 4.1** are applicable.

The strength of the DC magnetic field along the submarine export cable was calculated using the Biot-Savart Law, the same method as discussed in **Section 3.1**. Earth's geomagnetic field was added to the magnetic field from the DC cables, using vector addition, to calculate the total DC magnetic field.

Lastly, the magnitude of the motion-induced DC electric field was calculated for the submarine export cables running along the offshore substation facility support structure, using an assumed ocean current velocity, or swimming speed of a marine organism, and applying a modified version of the Lorentz force equation. The details of these calculations are discussed in more detail in **Section 3.1**.

4 RESULTS OF ANALYSIS

EMF levels for the BW1 and BW2 offshore electric transmission systems are presented below. Discussion is additionally provided to describe potential compass deflection in the immediate vicinity of Project-related magnetic fields. Model results are presented specifically for the HVDC submarine export cables, the HVAC interarray cables, the wind turbines, and the offshore substation facilities.

4.1 HVDC SUBMARINE EXPORT CABLES

Model results for DC magnetic fields, compass deflection, and induced electric fields for the BW1 and BW2 HVDC submarine export cables are presented below.

4.1.1 BW1—HVDC Submarine Export Cables

The BW1 HVDC submarine export cable will consist of one 320-kV circuit and will be approximately 202 nm (375 km) in length. The cable will extend from the BW1 offshore substation facility to the landfall point at Lawrence Point at the Astoria Power Complex in Queens, New York. A majority of the offshore portion of the BW1 HVDC submarine export cable is proposed to be in a bundled configuration, then separated by 33 ft (10 m) as it approaches the landfall point. The evaluation of the magnetic field, compass deflection, and induced electric field as a result of this cable is presented below.

4.1.1.1 DC Magnetic Fields

The strength of the DC magnetic fields generated by the current flowing through the submarine export cables will vary based on the proximity of the two conductors or poles, whether a bundled or separated configuration, the direction of the cable path relative to earth's geomagnetic field, and the cable burial depth.

Bundled Cable Configuration

The strength of the magnetic field from the bundled BW1 HVDC submarine export cable was evaluated at four burial depths: 1 ft (0.3 m), representing a conservatively shallow burial by rock, rock bags, or concrete mattresses; 3 ft (0.9 m); 6 ft (1.8 m); and 15 ft (4.6 m) (**Figure 11**). In addition, the figure below shows the strength of the magnetic field at the seafloor and 3.3 ft (1 m) above the seafloor, directly above the cable and out to 100 ft (30 m) on either side of the cable centerline. In this scenario, earth's geomagnetic field was set at 512 mG, and the cable is oriented at 308°, representative of the HVDC submarine export cable as it leaves the BW1 offshore substation facility in route to the mouth of Long Island Sound. The largest predicted magnetic field strength was 4,240 mG, at the seafloor, directly over the cable for the surface laid

cover depth of 1 ft (0.3 m), representing a conservatively shallow burial by rock, rock bags, or concrete mattresses. However, at 3.3 ft (1 m) above the seafloor, directly over the cable, the magnetic field strength is reduced to 709 mG, a reduction of 83% and a deviation of less than 200 mG from earth's background geomagnetic field. When the cable is buried to a depth of 3 ft (0.9 m), the shallowest proposed target burial depth, the maximum magnetic field strength is 917 mG at the seafloor, directly over the cable centerline. This value drops to 603 mG at 3.3 ft (1 m) above the seafloor. At burial depths of 6 ft (1.8 m), the proposed target depth, and 15 ft (4.6 m) below the U.S. Army Corps of Engineers authorized dredge depth, the maximum magnetic field strength at the seafloor, directly over the cable centerline is 615 and 527 mG, respectively. These results show that the magnetic field strength decreases rapidly as the distance above the seafloor increases, within tens of feet on either side of the cable centerline, and as the burial depth increases (**Table 10**).

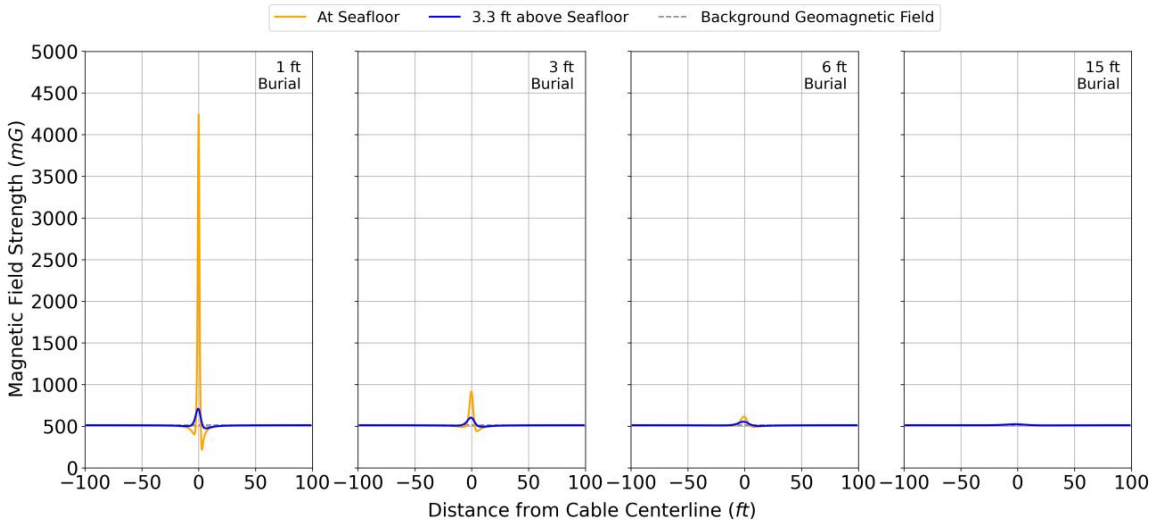

Figure 11. Magnetic Field Strength along the BW1 Submarine Export Cable for the Bundled Configuration. Earth's Background Magnetic Field is Shown as a Gray Dashed Line. The Cable is Oriented at 308°.

Table 10. Maximum Magnetic Field Strength along the BW1 Submarine Export Cable for the Bundled Configuration.

Burial Depth (ft [m])	Maximum Magnetic Field Strength (mG) at Seafloor		Maximum Magnetic Field Strength (mG) at 3.3 ft (1 m) Above Seafloor	
Cable Route Heading	308°	256°	308°	256°
1 [0.3]	4,240	4,240	709	705
3 [0.9]	917	911	603	600
6 [1.8]	615	612	554	553
15 [4.6]	527	526	522	522

Figure 12 illustrates the minimal difference in the calculated magnetic field strength as a result of the change in the cable route heading. In this scenario, earth's geomagnetic field was set at 512 mG, and the cable is oriented at 256°, representative of the HVDC submarine export cable as it enters the mouth of Long Island Sound in route to the landfall point. The largest predicted magnetic field strength is 4,240 mG, at the seafloor, directly over the cable with a surface laid cover depth of 1 ft (0.3 m). At 3.3 ft (1 m) above the seafloor, directly over the cable, the magnetic field strength is reduced to 705 mG, a reduction of 83% and a deviation of less than 200 mG from earth's background geomagnetic field. The same trend in rapid reduction of the magnetic field strength as burial depth and distance above the seafloor increases, as discussed for the previous cable route heading, is exhibited in **Table 10**.

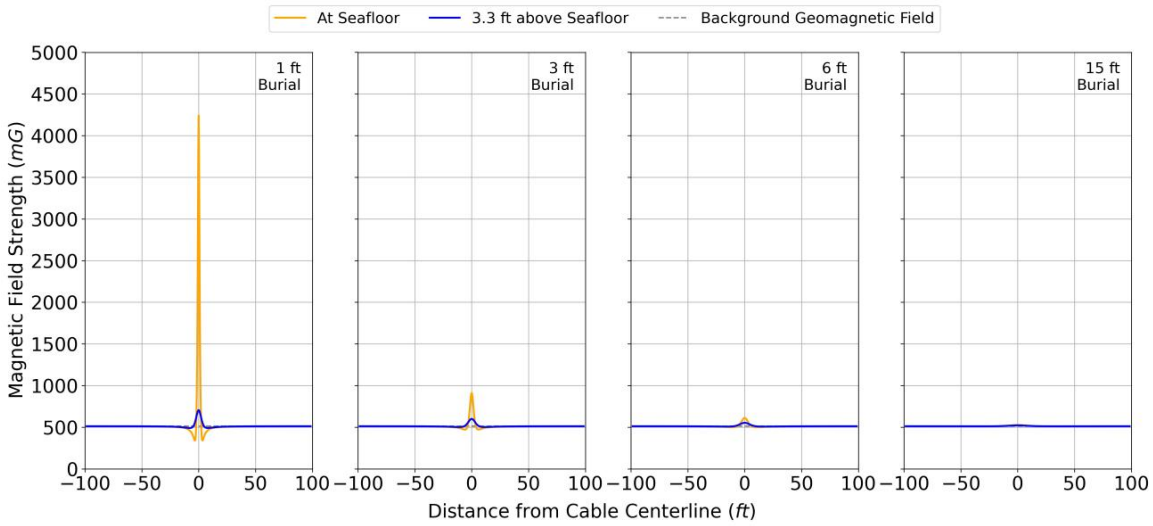

Figure 12. Magnetic Field Strength along the BW1 Submarine Export Cable for the Bundled Configuration. Earth's Background Magnetic Field is Shown as a Gray Dashed Line. The Cable is Oriented at 256°.

While the figures above provide a snapshot of the magnetic field strength from the BW1 HVDC submarine export cable, **Figure 13** illustrates spatially how the magnetic field strength rapidly declines above and to either side of the cable centerline for the conservative, surface laid cover depth scenario of 1 ft (0.3 m) for a bundled configuration. Given the conservative cable burial scenario, within 26 ft (8 m) on either side of the cable centerline, at the seafloor, the magnetic field strength has declined to within 1% of earth's geomagnetic field. Moving above the cable, through the water column, at 10 ft (3 m) above the cable centerline, the magnetic field strength has declined to within 6% of earth's geomagnetic field.

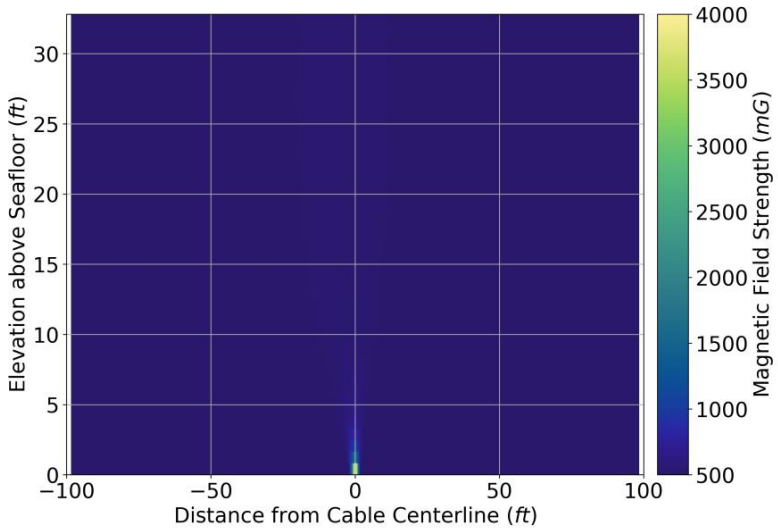

Figure 13. Magnetic Field Strength of the BW1 Submarine Export Cable for a Burial Depth of 1 ft (0.3 m) for the Bundled Configuration. The Cable is Oriented at 308°.

Separated Cable Configuration

In this section, the strength of the magnetic field from the BW1 HVDC submarine export cable with the poles separated by 33 ft (10 m) was evaluated at the same four burial depths and elevations at and above the seafloor as the bundled configuration (**Figure 14**). Earth's background geomagnetic field was set at 512 mG, and the cable is oriented at 308°, representative of the HVDC submarine export cable as it leaves the BW1 offshore substation facility in route to the mouth of Long Island Sound. The largest predicted magnetic field strength was 11,800 mG, at the seafloor, directly over one pole of the cable for a surface laid cover depth of 1 ft (0.3 m). The magnetic field strength decreases to 2,318 mG at the proposed target burial depth of 6 ft (1.8 m), a reduction of 80%. While the benefits of a bundled configuration are illustrated by the difference in the magnetic field strength in the figures below, the magnetic field strength for the separated cable configuration does still decline rapidly as the burial depth and distance above the seafloor increases (**Table 11**).

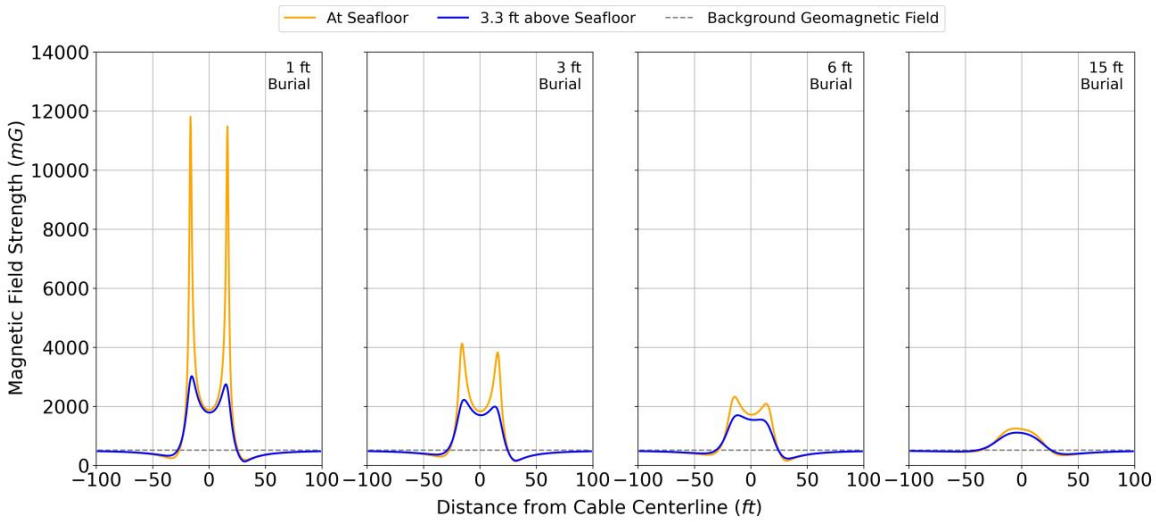

Figure 14. Magnetic Field Strength along the BW1 Submarine Export Cable for the Separated Configuration. Earth's Background Magnetic Field is Shown as a Gray Dashed Line. The Cable is Oriented at 308°.

Table 11. Maximum Magnetic Field Strength along the BW1 Submarine Export Cable for the Separated Configuration.

Burial Depth (ft [m])	Maximum Magnetic Field Strength (mG) at Seafloor		Maximum Magnetic Field Strength (mG) at 3.3 ft (1 m) Above Seafloor	
Cable Route Heading	308°	256°	308°	256°
1 [0.3]	11,800	11,640	3,014	2,882
3 [0.9]	4,120	3,975	2,215	2,103
6 [1.8]	2,318	2,201	1,695	1,615
15 [4.6]	1,243	1,225	1,106	1,094

Figure 15 illustrates the minimal difference in the calculated magnetic field strength as a result of the change in the cable route heading. In this scenario, earth's geomagnetic field was set at 512 mG, and the cable is oriented at 256°, representative of the HVDC submarine export cable as it enters the mouth of Long Island Sound in route to the landfall point. The largest predicted magnetic field strength was 11,640 mG, at the seafloor, directly over the cable with a surface laid cover depth of 1 ft (0.3 m) and reduces to 1,615 mG using the proposed target burial depth of 6 ft (1.8 m) and evaluated at 3.3 ft (1 m) above the seafloor. The same trend in rapid reduction of the magnetic field strength as burial depth and distance above the seafloor increases, as discussed for the previous cable route heading, is exhibited in **Table 11**.

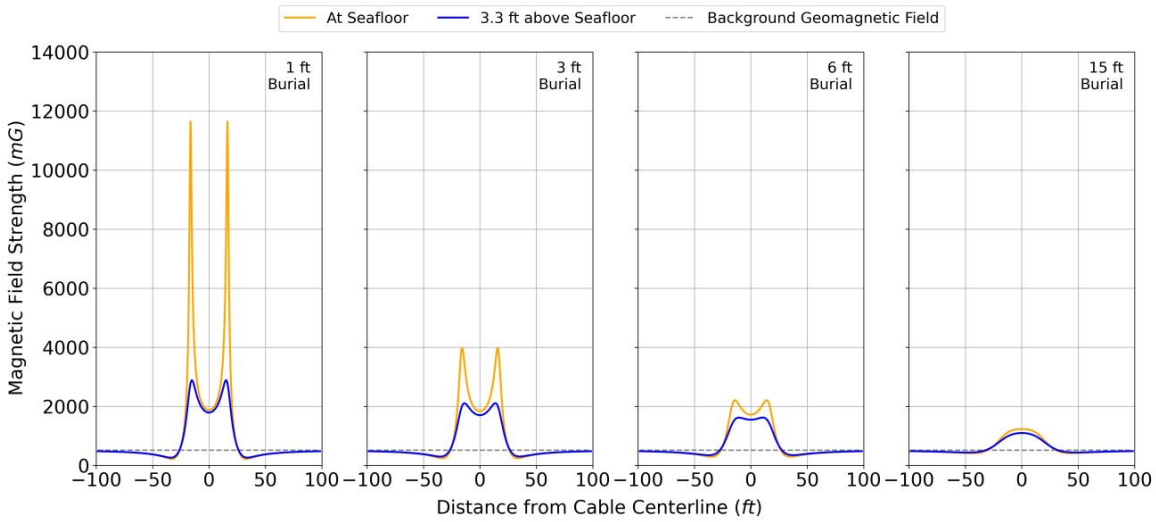

Figure 15. Magnetic Field Strength along the BW1 Submarine Export Cable for the Separated Configuration. Earth's Background Magnetic Field is Shown as a Gray Dashed Line. The Cable is Oriented at 256°.

Figure 16 illustrates spatially how the magnetic field strength rapidly declines above and to either side of the cable centerline for the conservative, surface laid cover depth scenario of 1 ft (0.3 m) for the separated configuration. Within 10 ft (3 m) on either side of the separated cable poles, at the seafloor, the magnetic field strength has declined to within 1% of earth's background geomagnetic field. Moving above the cable, through the water column, the magnetic field strength is elevated, but rapidly declines.

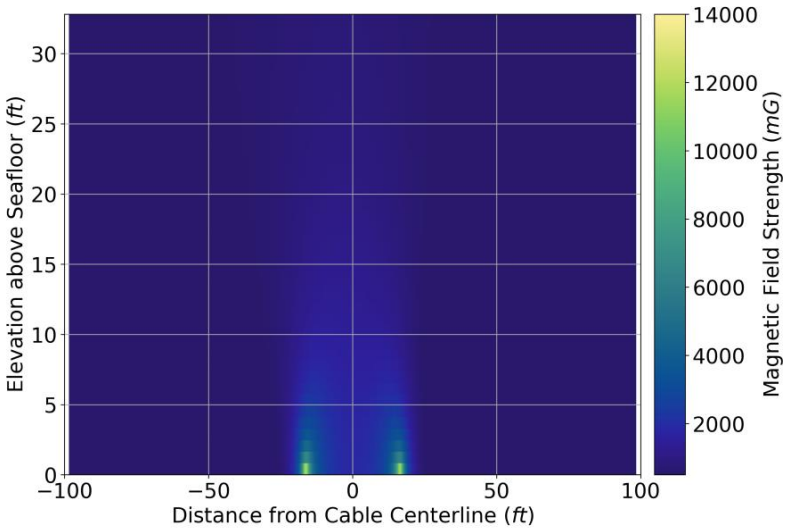

Figure 16. Magnetic Field Strength of the BW1 Submarine Export Cable for a Burial Depth of 1 ft (0.3 m) for the Separated Configuration. The Cable is Oriented at 308°.

4.1.1.2 Compass Deflection

The amount of compass deflection as a result of the altered DC magnetic fields due to the BW1 HVDC submarine export cable is presented below. It is important to note that modern navigational instruments (e.g., LORAN-C, global positioning system [GPS]) will not be impacted by the altered magnetic field along the cable, or any other Project cables.

Bundled Cable Configuration

The amount of compass deflection as a result of the magnetic field from the bundled BW1 HVDC submarine export cable was evaluated at the same four burial depths used above (**Figure 17**). The amount of compass deflection is directly dependent on the magnetic field strength and the cable route heading. The maximum compass deflection is -244° from magnetic north, however this maximum value only occurs on the seafloor directly over the cable. Within 6 ft (1.8 m) on either side of the bundled cable, on the seafloor, the compass deflection has decreased to 10° or less. Moving up into the water column, and as the burial depth increases, the amount of compass deflection quickly decreases as well (**Table 12**).

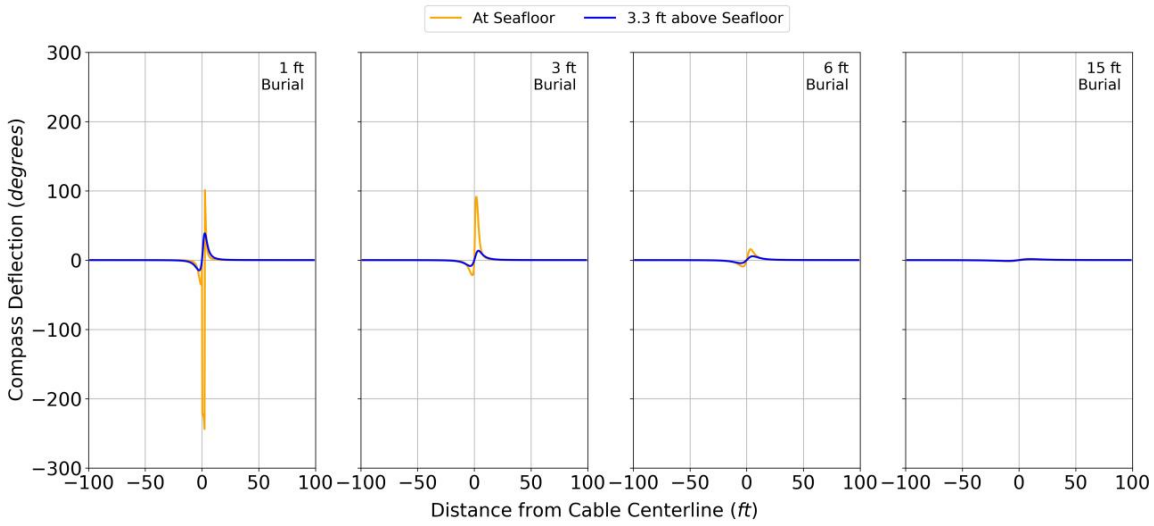

Figure 17. Magnetic Compass Deflection along the BW1 Submarine Export Cable for the Bundled Configuration. The Cable is Oriented at 308°.

Table 12. Maximum Compass Deflection along the BW1 Submarine Export Cable for the Bundled Configuration.

Burial Depth (ft [m])	Maximum Compass Deflection (°) at Seafloor		Maximum Compass Deflection (°) at 3.3 ft (1 m) Above Seafloor	
Cable Route Heading	308°	256°	308°	256°
1 [0.3]	-244	86	38	33
3 [0.9]	91	53	14	17
6 [1.8]	16	19	6	8
15 [4.6]	2	3	1	2

Given the proposed route of the submarine export cable has multiple different headings, the compass deflection was calculated for the portion of the submarine export cable routed from the mouth of Long Island Sound to the landfall point at the Astoria Power Complex, a heading of 256° (**Figure 18**). The differing cable route headings have an impact on how the magnetic field from the cable interacts with earth's background geomagnetic field. While there is not much of an observable difference in the magnetic field strength between the two cable route headings, the impact on compass deflection is more pronounced. The maximum compass deflection, at the seafloor directly over the cable poles is 86°, 65% lower compared to a cable route heading of 308°. Moving up into the water column, and as the burial depth increases, the amount of compass deflection quickly decreases as well (**Table 12**).

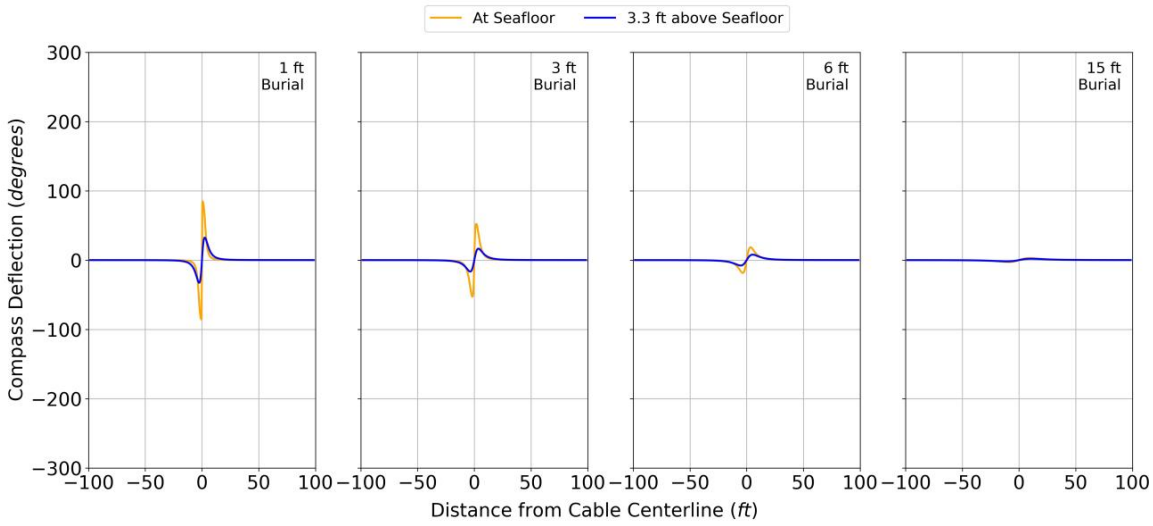

Figure 18. Magnetic Compass Deflection along the BW1 Submarine Export Cable for the Bundled Configuration. The Cable is Oriented at 256°.

Separated Cable Configuration

In this section, the compass deflection from the BW1 HVDC submarine export cable with the poles separated by 33 ft (10 m) (**Figure 19**). Without the benefit of the bundled cables, the compass deflection directly over and between the poles of the cable is elevated across all burial depths, resulting in a maximum deflection of -256° from magnetic north. However, within 50 ft (15 m) from the cable centerline between the two separated cable poles, the compass deflection has decreased to 10° or less. For both cable route heading scenarios, moving up into the water column, and as the burial depth increases, the compass deflection is minimally reduced as compared to the bundled configuration (**Table 13**). However, at 33 ft (10 m) above the seafloor, for the most conservative burial depth, the compass deflection has been reduced to 60°. At the maximum proposed burial depth of 15 ft (4.6 m) below the U.S. Army Corps of Engineers authorized dredge depth within navigation channels, the compass deflection at 33 ft (10 m) above the seafloor is 11°.

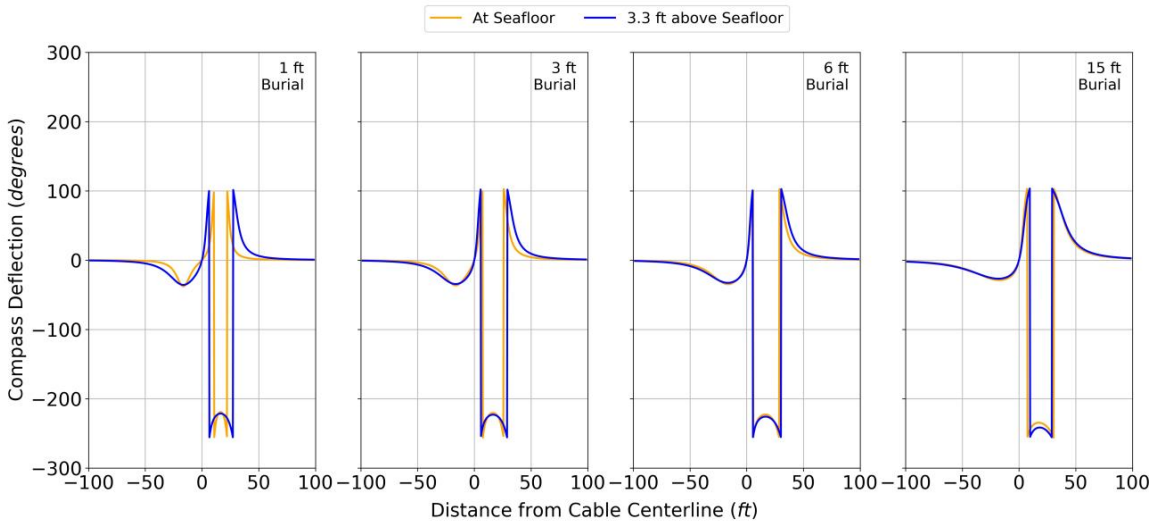

Figure 19. Magnetic Compass Deflection along the BW1 Submarine Export Cable for the Separated Configuration. The Cable is Oriented at 308°.

Table 13. Maximum Compass Deflection along the BW1 Submarine Export Cable for the Separated Configuration.

Burial Depth (ft [m])	Maximum Compass Deflection (°) at Seafloor		Maximum Compass Deflection (°) at 3.3 ft (1 m) Above Seafloor	
Cable Route Heading	308°	256°	308°	256°
1 [0.3]	-256	89	-256	86
3 [0.9]	-256	87	-256	84
6 [1.8]	-255	84	-256	80
15 [4.6]	-256	72	-256	66

The compass deflection under the separated configuration was also evaluated for the portion of the cable routed from the mouth of Long Island Sound to the landfall point at the Astoria Power Complex, a heading of 256° (**Figure 20**). The maximum compass deflection, at the seafloor directly over the cable poles is 89°, 65% lower compared to a cable route heading of 308°. While the progressively deeper proposed burial depths have a minimal impact on the compass deflection, moving 33 ft (10 m) vertically into the water column, the compass deflection is reduced to 20°.

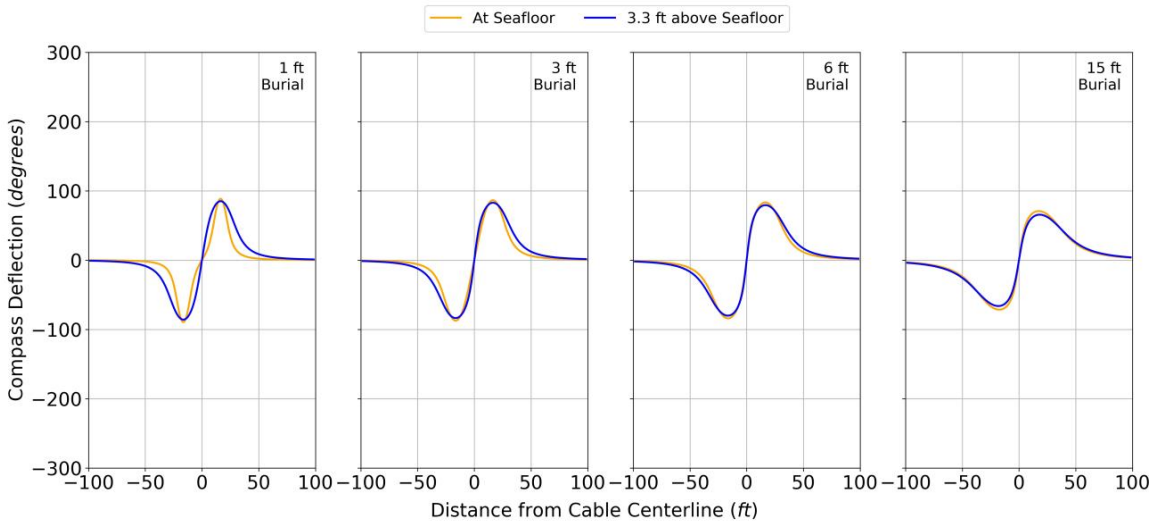

Figure 20. Magnetic Compass Deflection along the BW1 Submarine Export Cable for the Separated Configuration. The Cable is Oriented at 256°.

4.1.1.3 Induced DC Electric Fields

A motion-induced DC electric field is generated by electric charges, or ions, such as those in seawater and marine organisms, flowing through a static DC magnetic field, such as that generated by earth's geomagnetic field and the BW1 HVDC submarine export cable. The strength of this electric field is directly proportional to the strength of the magnetic field and the speed of the charged ions moving through the field. Given that relationship, as the burial depth of the cable increases and moving away from the cable poles into the water column or to either side of the cable centerline, the induced electric field will be reduced. In addition, a faster or slower flowing ocean current or a faster swimming marine organism will result in an increased or decreased induced electric field. The strength of the motion-induced DC electric field was calculated for the bundled and separated cable configurations assuming an ocean current velocity of 2 ft/s (0.6 m/s) (**Table 14** and **Table 15**). For the bundled cable configurations, the electric field values are the same for both cable route headings, a result of the similar magnetic field strengths shown in **Section 4.1.1.1**. The separated cable configuration induced electric fields were higher than the bundled configuration, a result of the higher magnetic field strengths, though the values still decline as the proposed burial depths increase. Similar to the magnetic field trends, the induced electric fields are strongest at the seafloor, directly over the cable poles, and decline rapidly moving to either side of the cable pole and into the water column.

Table 14. Maximum Induced DC Electric Field along the BW1 Submarine Export Cable for the Bundled Configuration.

Burial Depth (ft [m])	Maximum Motion-Induced Electric Field (mV/m) at Seafloor		Maximum Motion-Induced Electric Field (mV/m) at 3.3 ft (1 m) Above Seafloor	
Cable Route Heading	308°	256°	308°	256°
1 [0.3]	0.25	0.25	0.04	0.04
3 [0.9]	0.05	0.05	0.03	0.03
6 [1.8]	0.03	0.03	0.03	0.03
15 [4.6]	0.03	0.03	0.03	0.03

Table 15. Maximum Induced DC Electric Field along the BW1 Submarine Export Cable for the Separated Configuration.

Burial Depth (ft [m])	Maximum Motion-Induced Electric Field (mV/m) at Seafloor		Maximum Motion-Induced Electric Field (mV/m) at 3.3 ft (1 m) Above Seafloor	
Cable Route Heading	308°	256°	308°	256°
1 [0.3]	0.40	0.40	0.13	0.13
3 [0.9]	0.17	0.17	0.11	0.11
6 [1.8]	0.11	0.11	0.09	0.09
15 [4.6]	0.07	0.07	0.06	0.06

4.1.2 BW2—HVDC Submarine Export Cables

The BW2 HVDC submarine export cable will consist of one 320-kV circuit and will be approximately 113 nm (209 km) in length if routed to Waterford, Connecticut, and the same distance as the BW1 submarine export cable if routed to Queens, New York. The cable will extend from the BW2 offshore substation facility to the landfall point at the Millstone Power Complex in Waterford, Connecticut, or the Astoria Power Complex in Queens, New York. A majority of the offshore portion of the BW2 HVDC submarine export cable is proposed to be in a bundled configuration, then separated by 33 ft (10 m) as it approaches the landfall point. An important note, while the BW2 HVDC submarine export cable is proposed to be spaced up to 164 ft (50 m) apart from the BW1 cable while traveling from the offshore substation facilities, the two cables are independent circuits and electronically isolated from one another. The BW1 and BW2 cables are proposed to be spaced far enough apart to not create any compound EMF effects. The evaluation of the magnetic field, compass deflection, and induced electric field produced by this cable is presented below, assuming a landfall at Waterford, Connecticut. If the landfall for the BW2 submarine export cable is at Queens, New York, the results for BW1, presented in **Section 4.1.1**, are applied.

4.1.2.1 DC Magnetic Fields

The strength of the DC magnetic fields will vary based on the proximity of the two poles, whether a bundled or separated configuration, the direction of the cable path relative to earth's geomagnetic field, and the cable burial depth.

Bundled Cable Configuration

The strength of the magnetic field from the bundled BW2 HVDC submarine export cable was evaluated at four burial depths: 1 ft (0.3 m), representing a conservatively shallow burial by rock, rock bags, or concrete mattresses; 3 ft (0.9 m); 6 ft (1.8 m); and 15 ft (4.6 m) (**Figure 21**). In addition, the figure below shows the strength of the magnetic field at the seafloor and 3.3 ft (1 m) above the seafloor, directly above the cable and out to 100 ft (30 m) on either side of the cable centerline. In this scenario, earth's geomagnetic field was set at 510 mG, and the cable is oriented at 359°, representative of the BW2 HVDC submarine export cable as it approaches the landfall point at the Millstone Power Complex. The largest predicted magnetic field strength was 4,238 mG, at the seafloor, directly over the cable for the conservative, surface laid cover depth of 1 ft (0.3 m). However, at 3.3 ft (1 m) above the seafloor, directly over the cable, the magnetic field strength is reduced to 710 mG, a reduction of 83%. These results show that the magnetic field strength decreases rapidly as the distance above the seafloor increases, within tens of feet on either side of the cable centerline, and as the burial depth increases (**Table 16**).

The second cable route heading of 308°, representative of the BW2 HVDC submarine export cable as it leaves the offshore substation facility in route to the mouth of Long Island Sound, where it is parallel to the BW1 HVDC submarine export cable, was also evaluated (**Table 16**). The magnetic field strengths for the second cable route heading are within 0.5% of the 359° cable route heading scenario displayed below.

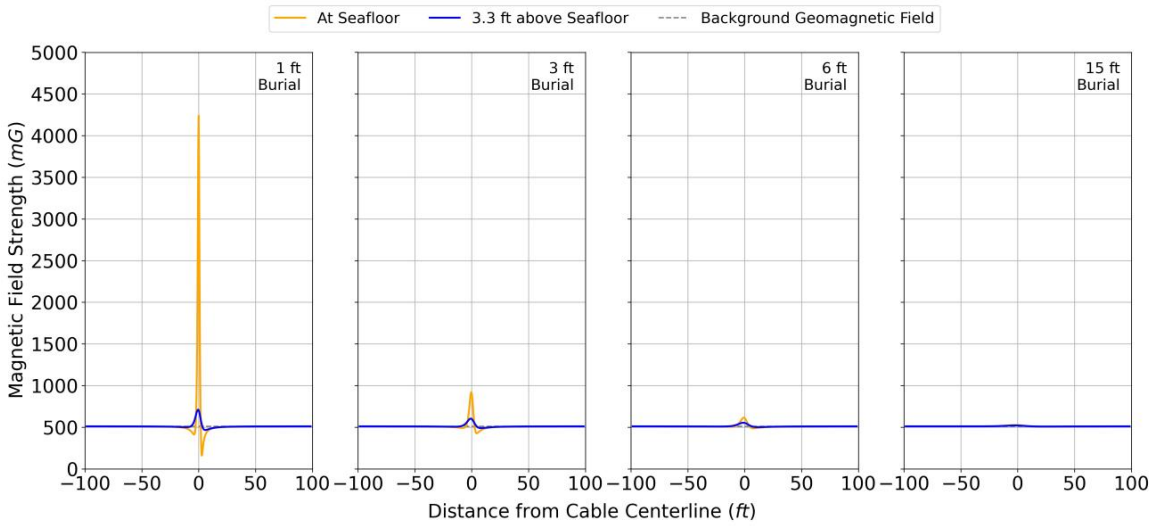

Figure 21. Magnetic Field Strength along the BW2 Submarine Export Cable for the Bundled Configuration. Earth's Background Magnetic Field is Shown as a Gray Dashed Line. The Cable is Oriented at 359°.

Table 16. Maximum Magnetic Field Strength along the BW2 Submarine Export Cable for the Bundled Configuration.

Burial Depth (ft [m])	Maximum Magnetic Field Strength (mG) at Seafloor		Maximum Magnetic Field Strength (mG) at 3.3 ft (1 m) Above Seafloor	
Cable Route Heading	308°	359°	308°	359°
1 [0.3]	4,238	4,238	708	710
3 [0.9]	916	920	601	603
6 [1.8]	613	615	553	553
15 [4.6]	525	526	521	521

Separated Cable Configuration

In this section, the strength of the magnetic field from the BW2 HVDC submarine export cable with the poles separated by 33 ft (10 m) was evaluated at the same four burial depths and elevations at and above the seafloor as the bundled configuration (**Figure 22**). The largest predicted magnetic field strength was 11,841 mG, at the seafloor, directly over one pole of the cable for a surface laid cover depth of 1 ft (0.3 m). The magnetic field strength decreases to 2,346 mG at the proposed target burial depth of 6 ft (1.8 m), a reduction of 80%. While the benefits of a bundled configuration are illustrated by the difference in the magnetic field strength in the figure below, the magnetic field strength for the separated cable configuration does still decline rapidly approaching the background value of 510 mG as the burial depth and distance above the seafloor increases (**Table 17**).

The second cable route heading of 308° was also evaluated for the separated cable configuration. Similar to the bundled cable configuration, the magnetic field strengths for the second cable route heading are within 1% of the 359° cable route heading (**Table 17**).

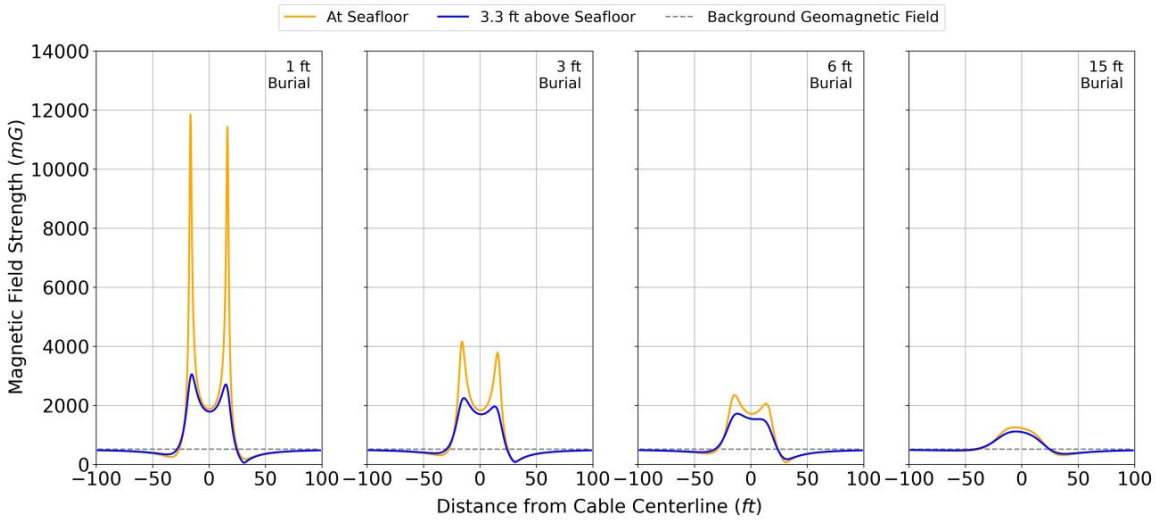

Figure 22. Magnetic Field Strength along the BW2 Submarine Export Cable for the Separated Configuration. Earth's Background Magnetic Field is Shown as a Gray Dashed Line. The Cable is Oriented at 359°.

Table 17. Maximum Magnetic Field Strength along the BW2 Submarine Export Cable for the Separated Configuration.

Burial Depth (ft [m])	Maximum Magnetic Field Strength (mG) at Seafloor		Maximum Magnetic Field Strength (mG) at 3.3 ft (1 m) Above Seafloor	
Cable Route Heading	308°	359°	308°	359°
1 [0.3]	11,802	11,841	3,014	3,047
3 [0.9]	4,121	4,155	2,215	2,243
6 [1.8]	2,318	2,346	1,694	1,714
15 [4.6]	1,242	1,250	1,104	1,110

4.1.2.2 Compass Deflection

The amount of compass deflection as a result of the altered DC magnetic fields due to the BW2 HVDC submarine export cable is presented below. It is important to note that modern navigational instruments (e.g., LORAN-C, GPS) will not be impacted by the altered magnetic field along the cable, or any other Project cables.

Bundled Cable Configuration

The amount of compass deflection as a result of the magnetic field from the bundled BW2 HVDC submarine export cable was evaluated at the same four burial depths used above (**Figure 23**). The amount of compass deflection is directly dependent on the magnetic field strength and the cable route heading. For a cable route heading of 359°, the maximum compass deflection is -166° from magnetic north, however this maximum value only occurs on the seafloor directly over the bundled cable. For a cable route heading of 308°, the maximum compass deflection is -244° from magnetic north, identical to the compass deflection from the BW1 HVDC submarine export cable. Within 3.3 ft (1 m) on either side of the bundled cable, on the seafloor, the compass deflection has declined to 10° or less. Moving up into the water column, and as the burial depth increases, the amount of compass deflection is further decreased below a deflection of 10° (**Table 18**). The compass deflection for the BW2 cable with a route heading of 308° is within 4% of the BW1 cable with the same route heading.

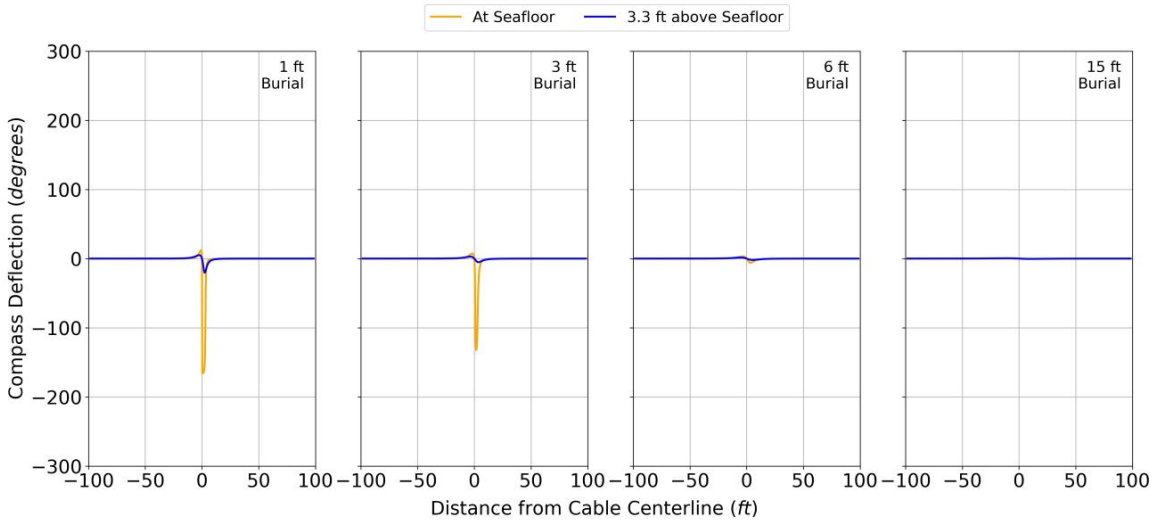

Figure 23. Magnetic Compass Deflection along the BW2 Submarine Export Cable for the Bundled Configuration. The Cable is Oriented at 359°.

Table 18. Maximum Compass Deflection along the BW2 Submarine Export Cable for the Bundled Configuration.

Burial Depth (ft [m])	Maximum Compass Deflection (°) at Seafloor		Maximum Compass Deflection (°) at 3.3 ft (1 m) Above Seafloor	
Cable Route Heading	308°	359°	308°	359°
1 [0.3]	-244	-166	38	-20
3 [0.9]	91	-132	13	-5
6 [1.8]	16	-6	5	-2
15 [4.6]	2	0.7	1	0.4

Separated Cable Configuration

In this section, the compass deflection from the BW2 HVDC submarine export cable with the poles separated by 33 ft (10 m) (**Figure 24**). Without the benefit of the bundled cables, the compass deflection directly over and between the poles of the cable is elevated across all burial depths, resulting in a maximum deflection of -256° from magnetic north for a cable route heading of 308° and a maximum deflection of -167° for a cable route heading of 359°. However, within 50 ft (15 m) from the cable centerline between the two separated cable poles, the compass deflection has declined to within 10° of magnetic north. The effect of the cable route heading on the amount of compass deflection is shown in **Table 19**. A similar trend to the BW1 cables is shown with the BW2 cable, where at 3.3 ft (1 m) above the seafloor, there is a minimal change in the compass deflection; however, moving up into the water column, and to either side of the separated cable poles, the amount of compass deflection is reduced.

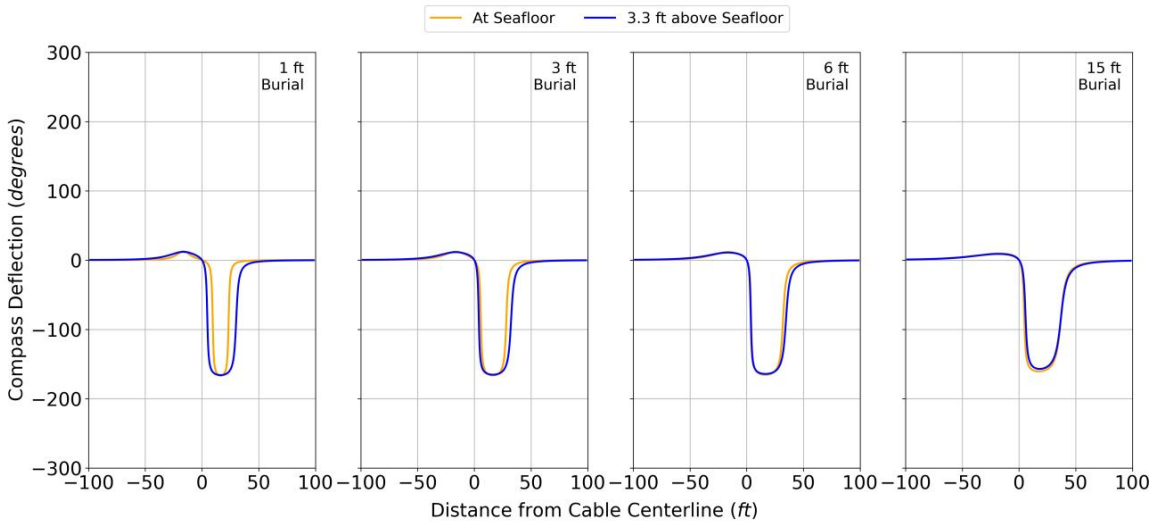

Figure 24. Magnetic Compass Deflection along the BW2 Submarine Export Cable for the Separated Configuration. The Cable is Oriented at 359°.

Table 19. Maximum Compass Deflection along the BW2 Submarine Export Cable for the Separated Configuration.

Burial Depth (ft [m])	Maximum Compass Deflection (°) at Seafloor		Maximum Compass Deflection (°) at 3.3 ft (1 m) Above Seafloor	
Cable Route Heading	308°	359°	308°	359°
1 [0.3]	-255	-167	-256	-166
3 [0.9]	-256	-166	-256	-165
6 [1.8]	-255	-166	-255	-164
15 [4.6]	-256	-161	-256	-157

4.1.2.3 Induced DC Electric Fields

A motion-induced DC electric field is generated by electric charges, or ions, such as those in seawater and marine organisms, flowing through a static DC magnetic field, such as that generated by earth's geomagnetic field and the BW2 HVDC submarine export cable. The strength of this electric field is directly proportional to the strength of the magnetic field and the speed of the charged ions moving through the field. Given that relationship, as the burial depth of the cable increases and moving away from the cable poles either into the water column or to either side of the cable centerline, the electric field will be reduced. In addition, a faster or slower flowing ocean current or a faster swimming marine organism will result in an increased or decreased motion-induced electric field. The strength of the motion-induced DC electric field was calculated for the bundled and separated cable configurations assuming an ocean current velocity of 2 ft/s (0.6 m/s) (**Table 20** and **Table 21**). For the bundled cable configurations, the electric field values are the same for both cable route headings, a result of the similar magnetic field strengths shown in **Section 4.1.2.1**. The separated cable configuration induced electric fields were higher than the bundled configuration, a result of the higher magnetic field strengths, though the values still decline as the proposed burial depths increase.

Table 20. Maximum Induced DC Electric Field along the BW2 Submarine Export Cable for the Bundled Configuration.

Burial Depth (ft [m])	Maximum Motion-Induced Electric Field (mV/m) at Seafloor		Maximum Motion-Induced Electric Field (mV/m) at 3.3 ft (1 m) Above Seafloor	
Cable Route Heading	308°	359°	308°	359°
1 [0.3]	0.25	0.25	0.04	0.04
3 [0.9]	0.05	0.05	0.03	0.03
6 [1.8]	0.03	0.03	0.03	0.03
15 [4.6]	0.03	0.03	0.03	0.03

Table 21. Maximum Induced DC Electric Field along the BW2 Submarine Export Cable for the Separated Configuration.

Burial Depth (ft [m])	Maximum Motion-Induced Electric Field (mV/m) at Seafloor		Maximum Motion-Induced Electric Field (mV/m) at 3.3 ft (1 m) Above Seafloor	
Cable Route Heading	308°	359°	308°	359°
1 [0.3]	0.40	0.40	0.13	0.13
3 [0.9]	0.17	0.17	0.11	0.11
6 [1.8]	0.11	0.11	0.09	0.09
15 [4.6]	0.07	0.07	0.06	0.06

4.2 HVAC INTERARRAY CABLES

Model results for AC magnetic fields, and induced electric fields for the BW1 and BW2 HVAC interarray cables, are presented below. The HVAC interarray cables are not differentiated between BW1 and BW2, though they are independent circuits and electrically isolated.

4.2.1 AC Magnetic Fields

The strength of the magnetic field from the HVAC interarray cables was evaluated at two burial depths: 0.7 ft (0.2 m), representing the cable covered by rock, rock bags, or concrete mattresses, and 6.6 ft (2 m), slightly deeper than the maximum proposed target burial depth of 6 ft (1.8 m) (**Figure 25** and **Figure 26**). In addition, the figures below show the strength of the magnetic field at the seafloor and 3.3 ft (1 m) above the seafloor, directly above the cable and out to 100 ft (30 m) on either side of the cable centerline.

When the cables cannot reasonably be buried, they are assumed to be covered by 0.7-ft (0.2-m) thick rock bags or concrete mattresses. **Figure 25** shows the predicted magnetic field strength from the HVAC interarray cable, at the assumed WNC rating, when it is covered by protective mattresses. The largest predicted magnetic field strength was 600 mG, at the seafloor. At a height of 3.3 ft (1 m) above the seafloor, the magnetic field strength decreases to less than 34 mG, a reduction of 94%. At both heights evaluated (at the seafloor and 3.3 ft [1 m] above the seafloor), the predicted magnetic field strength decreases to below 0.9 mG at a distance of 25 ft (7.6 m) from the centerline of the cable.

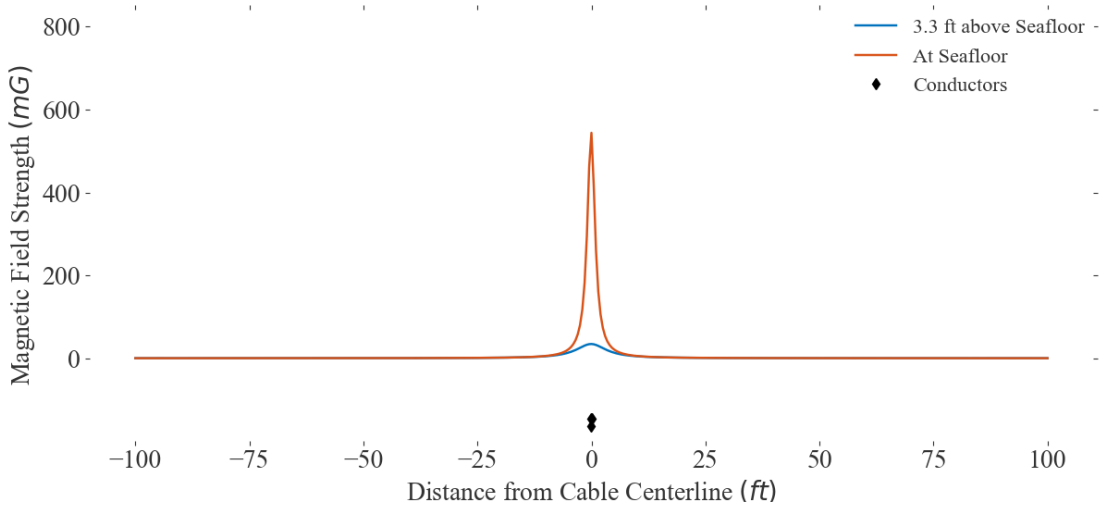

Figure 25. Magnetic Field Strength along the Interarray Cables. The Burial Depth is 0.7 ft (0.2 m).

Using a burial depth of 6.6 ft (2 m), at the assumed WNC rating for the HVAC interarray cables, the largest predicted magnetic field strength was 17 mG at the seafloor and decreased to 7 mG at 3.3 ft (1 m) above the seafloor, a reduction of 59% (**Figure 26**). As the distance away from the cable centerline increases, beyond 25 ft (7.6 m), the magnetic field strength drops below 0.9 mG. These results show that the magnetic field strength decreases rapidly as the distance above the seafloor increases, within tens of feet on either side of the cable centerline, and as the burial depth increases (**Table 22**).

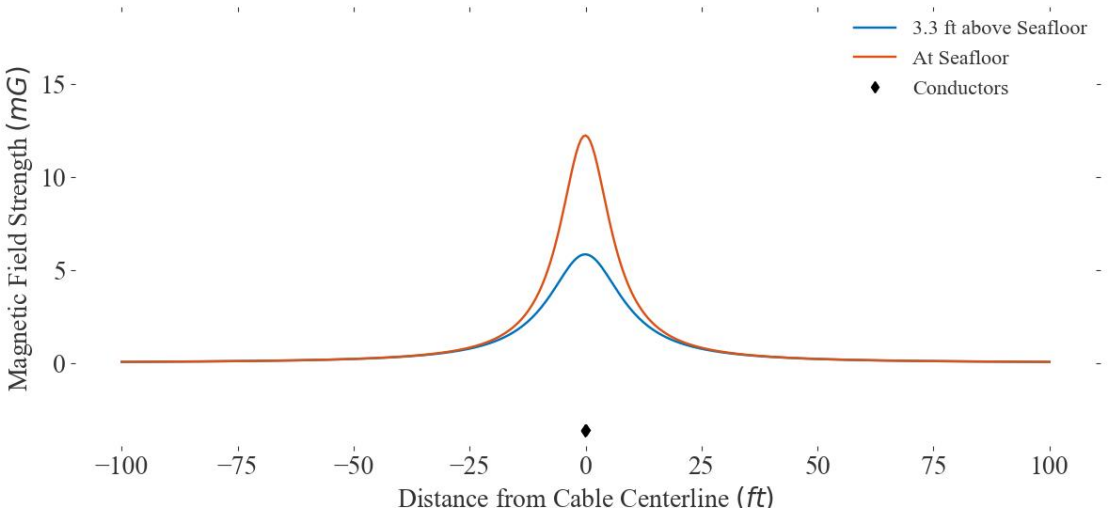

Figure 26. Magnetic Field Strength along the Interarray Cables. The Burial Depth is 6.6 ft (2 m).

Table 22. Maximum Magnetic Field Strength along the Interarray Cables.

Burial Depth (ft [m])	Maximum Magnetic Field Strength (mG) at Seafloor	Maximum Magnetic Field Strength (mG) at 3.3 ft (1 m) Above Seafloor
0.7 [0.2]	600	34
6.6 [2]	17	7

4.2.2 Induced AC Electric Fields

An induced AC electric field can be generated from the alternating current flowing through the HVAC interarray cables. In addition, the induced AC electric field will have a frequency related to the frequency of the AC cable, resulting from the rotation of the AC magnetic field. The strength of this induced electric field will be dependent on the strength of the AC magnetic field and the loading of the cables, based on the Project design recommendations. Given that relationship, as the burial depth of the cable increases and moving away from the cable poles into the water column or to either side of the cable centerline, the induced electric field will be reduced. Similar to the magnetic field trends, the induced electric fields are strongest at the seafloor, directly over the cables, and decline rapidly moving to either side of the cable centerline and into the water column.

The strength of the induced electric field from the HVAC interarray cables was evaluated at the same two burial depths as the magnetic field. When the cables cannot reasonably be buried, they are assumed to be covered by 5-ft (1.5-m) thick rock, rock bags, or concrete mattresses. **Error! Reference source not found.** shows the predicted induced electric fields when an HVAC interarray cable is covered by rock, rock bags, or concrete mattresses, using a conservatively shallow cover depth of 0.7 ft (0.2 m). The largest predicted induced electric field is 20 mV/m, but rapidly decreases with distance away from the cable centerline and into the water column. At a height of 3.3 ft (1 m) above the seafloor, induced electric field values decrease to less than 0.02 mV/m, which is 1,000 times lower than the value at the seafloor (**Error! Reference source not found.**). At distances beyond 12 ft (3.7 m) from the cable centerline, the induced electric fields drop below 4e-5 mV/m.

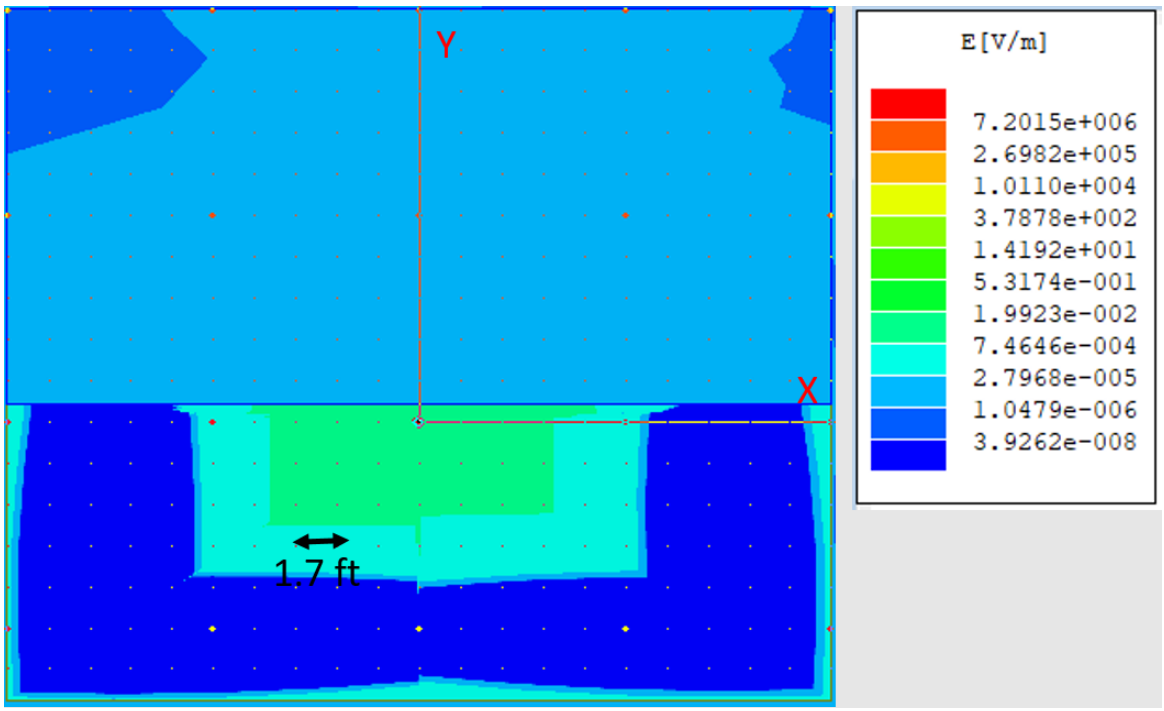

Figure 27. Induced Electric Field along the Interarray Cables. The Burial Depth is 0.7 ft (0.2 m).

Using a burial depth of 6.6 ft (2 m), at the assumed WNC rating for the HVAC interarray cables, the largest predicted induced electric fields were 0.2 mV/m or less at the seafloor and 7e-3 mV/m or less at 3.3 ft (1 m) above the seafloor, 29 times lower than the value at the seafloor (**Figure 28**). At distances beyond 12 ft (3.7 m) from the cable centerline, the induced electric fields decrease below 7e-6 mV/m.

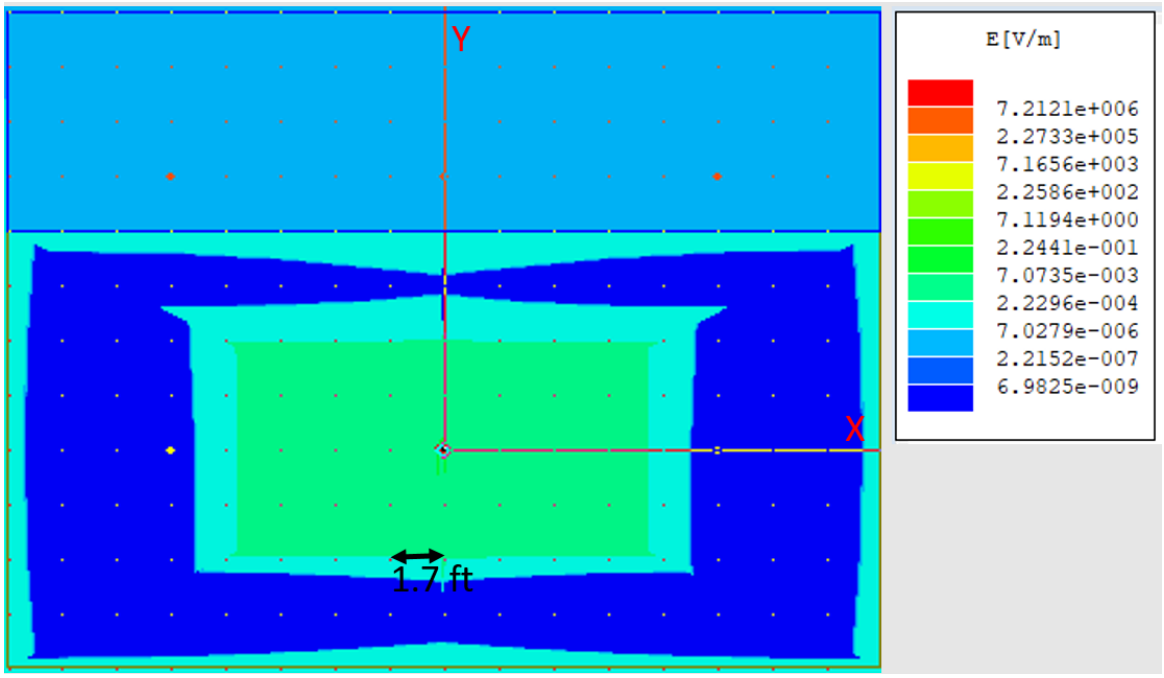

Figure 28. Induced Electric Field along the Interarray Cables. The Burial Depth is 6.6 ft (2 m).

Table 23. Maximum Induced AC Electric Field along the Interarray Cables.

Burial Depth (ft [m])	Maximum Induced Electric Field Strength (mV/m) at Seafloor	Maximum Induced Electric Field Strength (mV/m) at 3.3 ft (1 m) Above Seafloor
0.7 [0.2]	20	0.02
6.6 [2]	0.2	7e-3

4.3 WIND TURBINES

Model results for AC magnetic fields and induced electric fields for the HVAC interarray cables extending vertically within J-tubes along the lower portion of the wind turbine monopiles are presented below. It is assumed that the J-tube will exit the wind turbine monopile at 16 ft (5 m) above the seafloor and extend vertically on the exterior of the monopile to the seafloor where it will be covered by protective mattresses.

Per the Institute of Electrical and Electronics Engineers Standard 1127, in a substation, here used as a proxy for the wind turbines and offshore substation facilities, the strongest EMFs near the perimeter fence come from the transmission and distribution lines entering and leaving the substation. The strength of EMFs from equipment inside the substation fence decreases rapidly

with distance, reaching very low levels at relatively short distances beyond the perimeter (IEEE 2013).

4.3.1 AC Magnetic Fields

The strength of the magnetic field from the two HVAC interarray cables extending vertically within J-tubes along the lower portion of a single wind turbine monopile was evaluated at a single burial depth, 0.2 ft (5 cm), representative of the cables within steel J-tubes. In addition, the strength of the magnetic field was evaluated at the J-tube and at 3.3 ft (1 m) away from the J-tube, in the water column, directly in line with the cable and out to 100 ft (30 m) on either side of the cable centerline. At the assumed WNC rating, the largest predicted magnetic field strength was 18,200 mG or less at the J-tubes and 50 mG or less at 3.3 ft (1 m) away from the J-tube, 364 times lower as compared to the value at the J-tube **(Figure 29**). At distances beyond 25 ft (7.6 m) from the centerline of the cables, the predicted magnetic field strength decreases to below 0.9 mG.

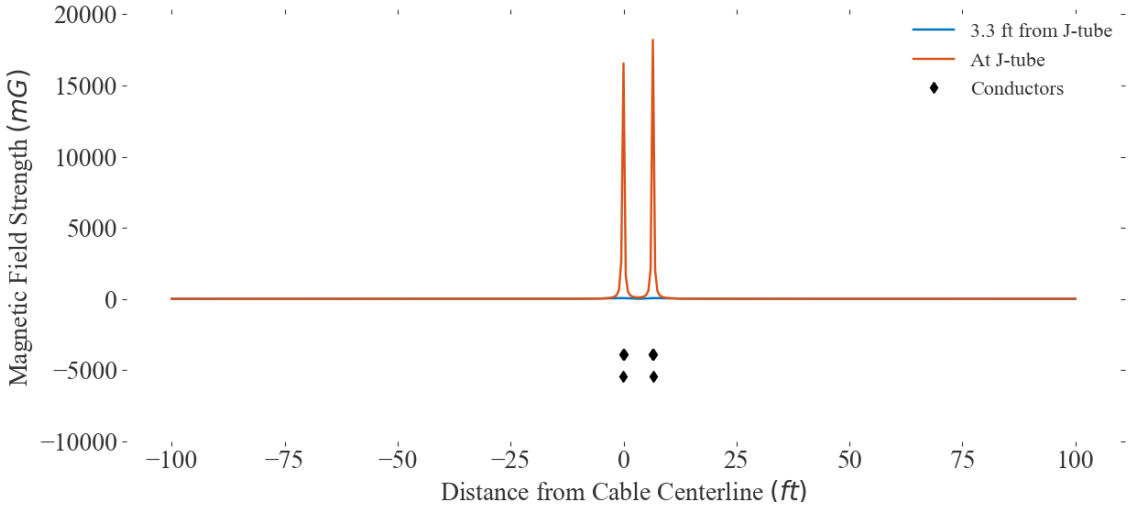

Figure 29. Magnetic Field Strength along the Interarray Cables Within J-tubes on a Wind Turbine Monopile.

4.3.2 Induced AC Electric Fields

The strength of the induced electric field from the two HVAC interarray cables on a single wind turbine was also evaluated at a single burial depth, 0.2 ft (5 cm), representative of the cables within steel J-tubes. At the assumed WNC rating the largest predicted induced electric field was 11 mV/m or less at the J-tubes and 0.013 mV/m or less at 3.3 ft (1 m) away from the J-tubes,

846 times below the value at the J-tube **(Figure 30**). For distances beyond 12 ft (3.7 m) from the centerline of the cables, the predicted induced electric fields drop below 0.3 mV/m.

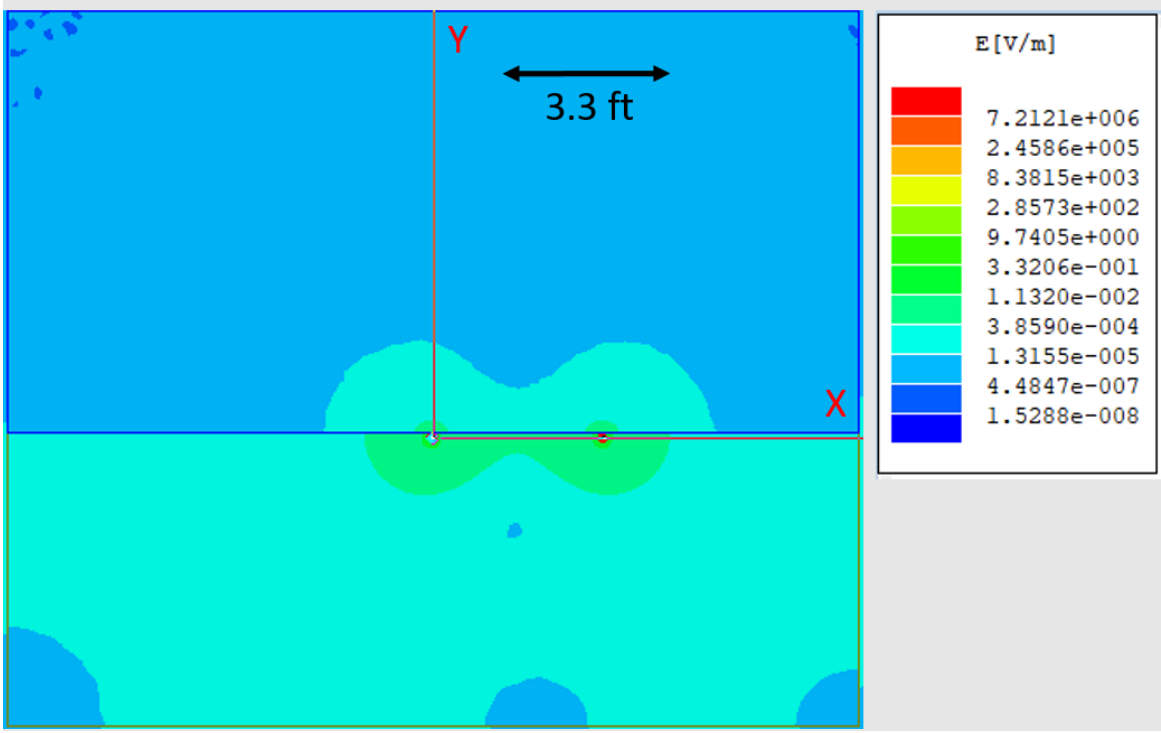

Figure 30. Induced AC Electric Field along the Interarray Cables Within J-tubes on a Wind Turbine Monopile.

4.4 OFFSHORE SUBSTATION FACILITIES

Model results for AC and DC magnetic fields, compass deflection (DC only), and induced electric fields for the BW1 and BW2 cables extending vertically along the offshore substation facility support structures are presented below. The offshore substation facilities are not differentiated between BW1 and BW2, though they are independent circuits and electrically isolated.

4.4.1 Offshore Substation Facility AC Cables

The offshore substation facilities will be supported by a jacketed structure and the HVAC interarray cables will travel vertically through the water column within J-tubes along the exterior of the support structure before contacting the seafloor and being buried. It is assumed that on the upper portion of the support structure, the J-tubes will be installed within the

jacketed support structure, and near the seafloor to where the cables will be buried, the J-tubes will be installed on the exterior of the support structure. A subset of the 18–22 HVAC interarray cables, separated by 8.2 ft (2.5 m) were modeled to determine the AC EMF generated by the cables on the offshore substation facilities. The subset consists of a group of six HVAC interarray cables, each of which is described in **Section 2.2.1** and shown in **Figure 3**.

4.4.1.1 AC Magnetic Fields

The strength of the magnetic field from the six HVAC interarray cables extending vertically along the offshore substation facility support structure was evaluated at a single burial depth, 0.2 ft (5 cm), representative of the cables within steel J-tubes. In addition, the strength of the magnetic field was evaluated at the J-tube and at 3.3 ft (1 m) away from the J-tube, suspended in the water column, directly in line with the cable and out to 100 ft (30 m) on either side of the cable centerline. At the assumed WNC rating, the largest predicted magnetic field strength was 17,500 mG or less at the J-tubes and 50 mG or less at 3.3 ft (1 m) away from the J-tubes, 350 times below the value at the J-tube **(Figure 31**). For distances beyond 25 ft (7.6 m) from the centerline of the cable group, the predicted magnetic field strength decreases below 0.9 mG.

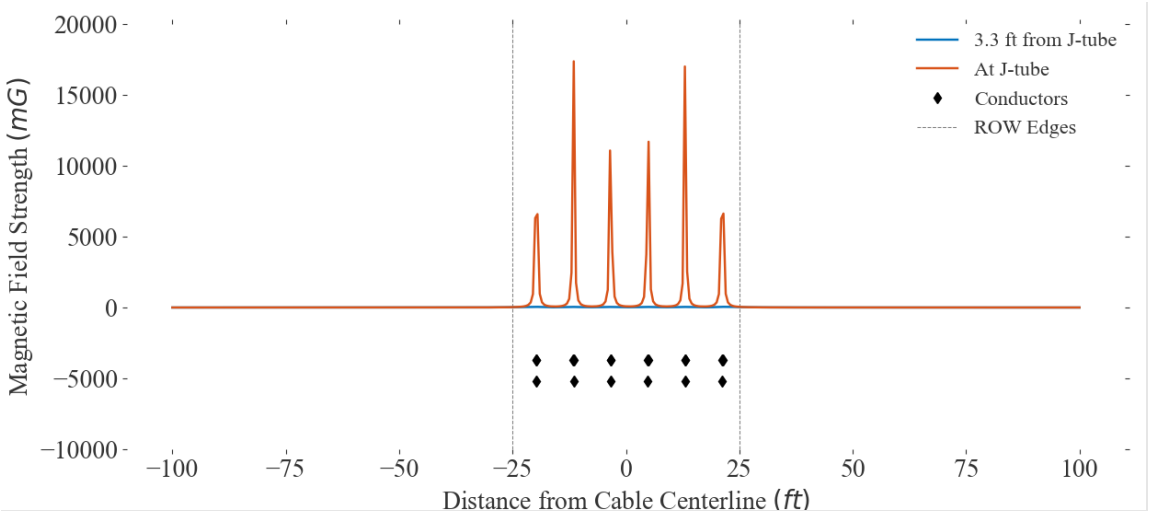

Figure 31. Magnetic Field Strength along the Interarray Cables Within J-tubes on the Offshore Substation Facility Support Structure.

4.4.1.2 Induced AC Electric Fields

The strength of the induced electric field from the six HVAC interarray cables extending vertically along the offshore substation facility support structure was evaluated at a single burial depth, 0.2 ft (5 cm), representative of the cables within steel J-tubes. At the assumed WNC rating, the largest predicted induced electric field was 10 mV/m or less at the J-tubes and

2e-5 mV/m or less at 3.3 ft (1 m) away from the J-tubes **(Figure 32**). For distances beyond 12 ft (3.7 m) from the centerline of the cables, the predicted induced electric fields decrease below 0.1 mV/m.

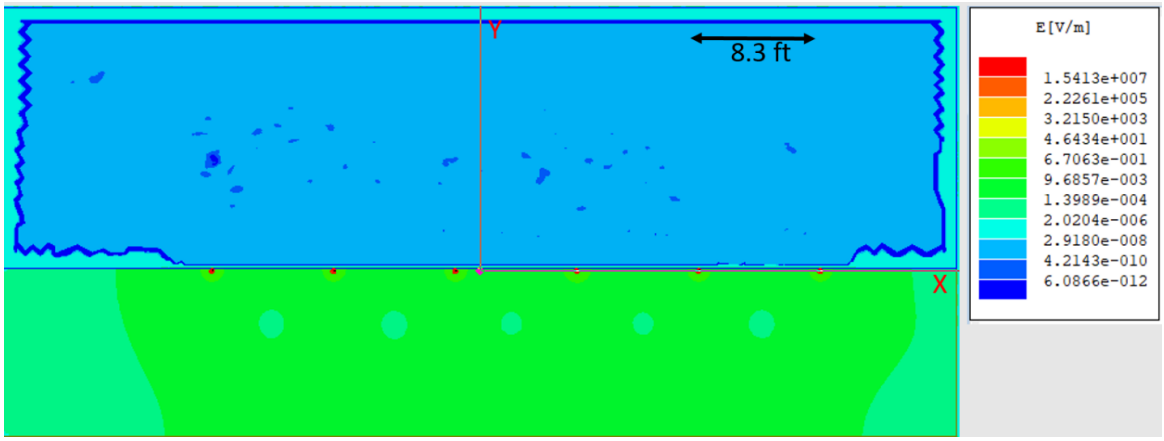

Figure 32. Induced AC Electric Field along the Interarray Cables Within J-tubes on the Offshore Substation Facility Support Structure.

4.4.2 Offshore Substation Facility DC Cables

The HVDC submarine export cables will travel vertically through the water column within J-tubes along the exterior of the support structures before contacting the seafloor and being buried. It is assumed that on the upper portion of the support structure, the J-tubes will be installed within the jacketed support structure, and near the seafloor to where the cables will be buried, the J-tubes will be installed on the exterior of the support structure. Two conductors for BW1 and two conductors for BW2 will comprise the HVDC transmission lines exiting the offshore substation facility in route to their respective landfalls. For the DC EMF modeling, the offshore substation facilities were modeled as a single offshore substation facility, representing a cross section of the HVDC submarine export cables exiting the structure, separated by 20 ft (6 m).

4.4.2.1 DC Magnetic Fields

The strength of the magnetic field from the HVDC submarine export cable extending vertically along the offshore substation facility was evaluated at a single burial depth, 1 ft (0.3 m), representing the cable within the J-tube along the support structure (**Figure 33**). In addition, the strength of the magnetic field was evaluated at the J-tube and at 3.3 ft (1 m) away from the J-tube, suspended in the water column, directly in line with the cable and out to 100 ft (30 m) on either side of the cable centerline. The largest predicted value for the magnetic field strength

was 11,689 mG directly on the J-tube and 2,988 mG at 3.3 ft (1 m) away from the J-tube, a 74% reduction. Within 6 ft (2 m) on either side of the J-tube, the magnetic field strength has decreased to 1,000 mG or less. The magnetic field strength for this cable configuration does decline rapidly moving farther away from the J-tube or cable centerline into the water column.

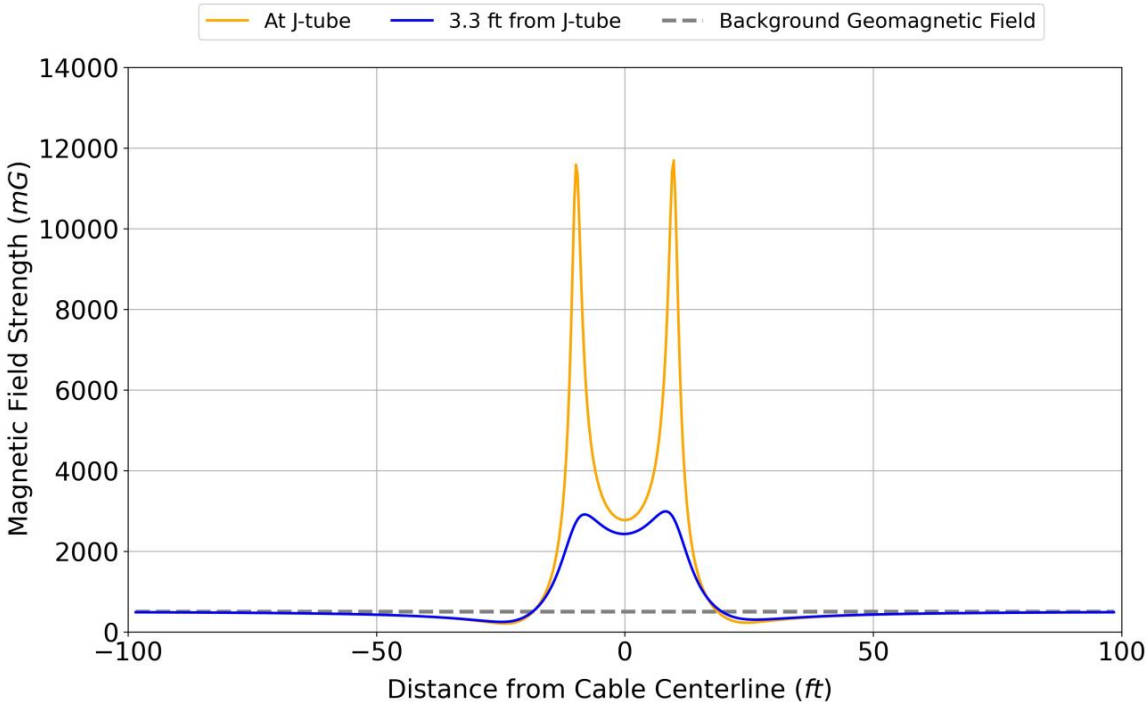

Figure 33. Magnetic Field Strength along the Submarine Export Cable Within J-tubes on the Offshore Substation Facility Support Structure. Earth's Background Magnetic Field is Shown as a Gray Dashed Line.

4.4.2.2 Compass Deflection

The altered DC magnetic fields due to the HVDC submarine export cables extending along the offshore substation facility support structure can create compass deflection, though it was not evaluated for this section of the cables. The cables will be extending vertically through the water column and not horizontally, and the area around the offshore substation facility will likely have a perimeter and not be accessible to the general public, thus the compass deflection can be expected to be at minimal levels outside the facility perimeters. It is important to note that modern navigational instruments (e.g., LORAN-C, GPS) will not be impacted by the altered magnetic field along the cable.

4.4.2.3 Induced DC Electric Fields

The strength of the motion-induced DC electric field was calculated for the cable on the offshore substation facility support structure, assuming an ocean current velocity of 2 ft/s (0.6 m/s). The largest predicted induced electric field was 0.41 mV/m directly on the J-tube, and decreased to 0.15 mV/m at 3.3 ft (1 m) away from the J-tube, a 63% reduction in strength. Similar to the magnetic field trends, the electric field is strongest closest to the J-tube and declines rapidly moving away from the cable into the water column.

5 RISK CHARACTERIZATION

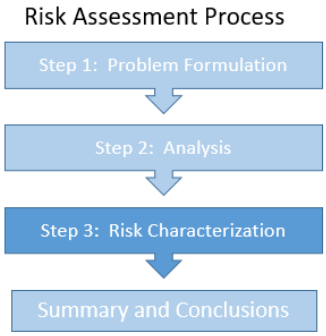

The characterization of potential risk is based upon a comparison of the modeled results for the Project electric transmission systems presented in **Section 4** to the EMF ERVs identified for marine life in **Section 2.5.5**.

Potential risks are characterized for both BW1 and BW2 electric transmission systems and exposure areas associated with the HVDC submarine export cables, HVAC interarray cables, the wind turbines, and offshore substation facilities. While the locations of the separate systems will differ between BW1 and BW2, many of the construction, design, and configurations are similar. As presented in **Section 4**, EMF levels predicted for BW1 and BW2 vary by 1% or less difference. Therefore, for the presentation below, the discussions and findings are applicable to both BW1 and BW2.

5.1 HVDC SUBMARINE EXPORT CABLES

Modeled EMF results are compared to the ERVs presented in **Table 4** to assess the potential for Project-related risk to marine life from EMF. For 90% of the HVDC submarine export cable routes, for BW1 and BW2, the cables will be buried beneath the seafloor, and the remaining 10% are assumed to require placement at the surface and will be covered with rock, rock bags, or concrete mattresses to protect the cables and reduce EMF exposure.

5.1.1 DC Magnetic Fields

The HVDC submarine export cables will be buried the majority of time beneath the seafloor at depths of 3 ft (0.9 m) and 6 ft (1.8 m), and up to 15 ft (4.6 m) below the U.S. Army Corps of Engineers authorized dredge depth within navigation channels. When the cables are buried to a depth of 3 ft (0.9 m), the maximum magnetic field strengths are approximately 4,155 mG (separated) and 917 mG (bundled), evaluated at the seafloor, directly over the cable centerline. When buried to a depth of 6 ft (1.8 m), the proposed target burial depth for the cables, the maximum magnetic field strengths are approximately 2,350 mG (separated) and approximately 615 mG (bundled) at the seafloor. These predicted magnetic field strengths at the seafloor, directly above the buried cable, are considered more representative of potential EMF exposure for sessile (e.g., mussels) and less mobile (e.g., crabs, lobsters) species.

For more mobile species, such as elasmobranchs and finfish, exposures above the seafloor in the lower water column are considered more representative of potential EMF exposure. At a height of 3.3 ft (1 m) above the seafloor, directly over the cable assuming a cable burial depth of 3 ft

(0.9 m), the magnetic field strength is reduced to approximately 2,240 mG (separated) and 600 mG (bundled). At the target burial depth of 6 ft (1.8 m), the magnetic field strength is 1,714 mG (separated) and for the bundled configuration is within 8% of earth's background geomagnetic field.

As shown in **Figure 11** and **Figure 12** (bundled) and **Figure 14** and **Figure 15** (separated), these levels decrease dramatically to within background levels within tens of feet on each side of the cable.

The highest DC magnetic fields calculated for the HVDC submarine export cables were associated with the separated cable configuration assuming cables were laid at the surface and covered to a depth of 1 ft (0.3 m) with rock, rock bags, or concrete mattresses. This burial depth is conservatively shallow as the proposed cover depth for the surface laid cables is 5 ft (1.5 m). As described above, this scenario is expected to occur in 10% or less of the total cable length, with the remaining 90% of the cable being buried below the seafloor resulting in far lower strengths (see above discussion). A maximum field strength of approximately 11,800 mG was predicted directly at the seafloor (representative of demersal invertebrate exposure). At 3.3 ft (1 m) above the seafloor (representative of demersal elasmobranch and finish exposures), a maximum field strength of approximately 3,050 mG was predicted. Alongside the separated cables, the magnetic field strengths return to background within approximately 50 ft (15.2 m) or less (see **Figure 14** and **Figure 15**).

The separated cable configuration resulting in the highest predicted magnetic field strength is proposed only for a short transect of the cables as they approach their proposed landfall points. Down the length of a majority of Long Island Sound and in offshore waters, a bundled cable configuration is proposed. For this same surface-laid cable scenario, but with the cables instead bundled, the maximum magnetic field strength was 4,240 mG at the seafloor directly above the cable. These levels decrease dramatically and return to background within 10 ft (3 m) of either side of the cable.

5.1.1.1 Potential Risk to Demersal Invertebrates

Based on the ERV for demersal invertebrates of 10,000 mG (see **Table 4**), the calculated magnetic field strengths indicate *de minimis* risk[21] for the majority of the HVDC submarine export cable route where the cable will be buried and either bundled or separated.

In the few areas (i.e., 10% or less) where it is assumed the cables will be placed at the surface and covered by rock, rock bags, or concrete mattresses, the maximum predicted strength of approximately 11,800 mG exceeds the ERV of 10,000 mG (a factor of 1.2 above) immediately at the seafloor. However, as described in **Section 2.5**, the ERV of 10,000 mG from Scott et al. (2021), based on behavioral changes, is considered a conservative estimate of potential

[21] In risk assessment, the term *de minimis* is used to refer to risks that are too minor to merit consideration.

population level effects. In addition, the modeled cover depth is conservatively shallow and the combined areas associated with the HVDC submarine export cables for both BW1 and BW2 is approximately 2,190 ac (9 km^2), or 2,810 ac (11 km^2) with the BW2 submarine export cable landing at the Astoria Power Complex. Assuming 10% of this total area (i.e., 219 ac [0.9 km^2] or 281 ac [1.1 km^2]) could hypothetically consist of cables laid at the surface, the area of maximum predicted magnetic field strength—above the ERV by a factor of 1.2—would constitute 0.001% or 0.002% of the southern New England ecoregion, and 0.0004% or 0.0005% of the NEUS Continental Shelf Ecosystem. This demonstrates that population level risks to demersal invertebrates are *de minimis*, even under the maximum magnetic field strengths predicted for the HVDC submarine export cables.

5.1.1.2 Potential Risk to Demersal Elasmobranchs

For demersal elasmobranchs, exposures are compared to the ERV of 653 mG above the seafloor in the lower water column. At a height of 3.3 ft (1 m) above the seafloor, directly over the cable at the burial depth of 3 ft (0.9 m), the magnetic field strength is 2,240 mG (separated) and 600 mG (bundled). At the deepest target burial depth of 6 ft (1.8 m), the magnetic field strengths are 1,714 mG (separated) and approximately 550 mG (bundled). On either side of the cables, magnetic field strengths reach background levels within tens of feet. While the maximum predicted value of 2,240 mG (separated) at 3.3 ft (1 m) immediately above the seafloor exceeds the ERV of 653 mG (by a factor of 3.4), because the ERV is based on changes in swimming behavior alone of skate (Hutchison et al. 2018, 2020a,b), and the field strength reduces so quickly on either side of the cable poles, the overall potential population level risks are considered *de minimis*.

In the few areas (i.e., 10% or less) where it is assumed the cables will be placed at the surface and covered by protective mattresses, the maximum predicted magnetic field strength of approximately 3,000 mG exceeds the ERV of 653 mG by a factor of 4.6. The maximum field strengths diminish rapidly away from the cables to background levels within approximately 25 ft (7.6 m) or less. As described above, the modeled cover depth is conservatively shallow and 10% of the area where cables will be laid at the surface constitutes 0.001% or 0.002% of the southern New England ecoregion and 0.0004% or 0.0005% of the NEUS Continental Shelf Ecosystem. For this reason, population level risks to demersal elasmobranchs are considered *de minimis*, even under the maximum magnetic field strengths predicted for the HVDC submarine export cables.

5.1.1.3 Potential Risk to Demersal Finfish

For demersal finfish, exposures are compared to the ERV of 20,000 mG above the seafloor in the lower water column. At a height of 3.3 ft (1 m) above the seafloor, directly over the cable at the burial depth of 3 ft (0.9 m), the magnetic field strength is 2,240 mG (separated) and 600 mG (bundled). In 10% of the area where the cables are placed at the seafloor and covered with

rocks, rock bags, or concrete mattresses, the maximum predicted magnetic field strength was approximately 3,000 mG. All predicted magnetic field strengths for the HVDC submarine export cables are below the ERV, demonstrating that risks to demersal finfish are *de minimis*.

5.1.2 Induced DC Electric Fields

The strength of the motion-induced DC electric field was calculated for the bundled and separated cable configurations assuming an ocean current velocity of 2 ft/s (0.6 m/s) (**Table 14** and **Table 15**). The maximum induced DC electric fields were 0.4 mV/m. Similar to the magnetic field trends, the induced electric fields are strongest at the seafloor, directly over the cable poles, and decline rapidly moving to either side of the cable pole and into the water column.

5.1.2.1 Potential Risk to Demersal Invertebrates

No demersal invertebrates located in the offshore waters of southern New England possess electroreceptive capabilities. Risks associated with potential exposures to induced DC electric field associated with the HVDC submarine export cables are *de minimis*.

5.1.2.2 Potential Risk to Demersal Elasmobranchs

Demersal elasmobranchs are capable of detecting static electric fields at levels as low as 5e-4 mV/m. However, as discussed in **Section 2.5**, no evidence exists to suggest that exposures at or above these levels result in effects to elasmobranchs. The ERV of 60 mV/m for DC electric fields for demersal finfish is used as a surrogate value for elasmobranchs. The maximum induced DC electric field of 0.4 mV/m is 150 times lower than the ERV, demonstrating that risks to demersal elasmobranchs from induced DC electric fields associated with the HVDC submarine export cables are *de minimis*.

5.1.2.3 Potential Risk to Demersal Finfish

The maximum induced DC electric field of 0.4 mV/m is 150 times lower than the ERV of 60 mV/m for demersal finish, demonstrating that risks to demersal finfish are *de minimis*.

5.2 HVAC INTERARRAY CABLES

Modeled EMF results are compared to the ERVs presented in **Table 4** to assess the potential for Project-related risk to EMF associated with the HVAC interarray cables for marine life. The HVAC interarray cables are not differentiated between BW1 and BW2, though they are independent circuits and electrically isolated.

5.2.1 AC Magnetic Fields

The strength of the AC magnetic field from the HVAC interarray cables was evaluated at two burial depths: 0.7 ft (0.2 m), representing a conservatively shallow cover depth by rock, rock bags, or concrete mattresses; and 6.6 ft (2 m), slightly below the maximum target burial depth of 6 ft (1.8 m) (**Figure 25** and **Figure 26**). The cover depth of 0.7 ft (0.2 m) is conservatively shallow as the proposed cover depth for the surface laid cables is 5 ft (1.5 m). The largest predicted magnetic field strength directly over the cable centerline was 600 mG, at the seafloor assuming the cables were laid at the surface (representative of exposures to demersal invertebrates). Using a burial depth of 6.6 ft (2 m), evaluated at the seafloor, the magnetic field strength decreases to less than 17 mG, a reduction of 97%.

For more mobile species, such as elasmobranchs and finfish, exposures above the seafloor in the lower water column are considered more representative of potential EMF exposure. At a height of 3.3 ft (1 m) above the seafloor, directly over the cable, the predicted magnetic field strength decreases to below 34 mG and 7 mG, for the 0.7 ft (0.2 m) and 6.6 ft (2 m) burial depths, respectively.

5.2.1.1 Potential Risk to Demersal Invertebrates

The maximum AC magnetic field of 600 mG is 17 times lower than the ERV of 10,000 mG for demersal invertebrates, demonstrating that risks to demersal invertebrates associated with the HVAC interarray cables are *de minimis*.

5.2.1.2 Potential Risk to Demersal Elasmobranchs

As discussed in **Section 2.5**, elasmobranchs are not capable of detecting frequencies above 20 Hz. As the HVAC interarray cables will be present at 60 Hz, outside the range detectable by this group, risks to elasmobranchs are *de minimis*.

5.2.1.3 Potential Risk to Demersal Finfish

The maximum AC magnetic field of 600 mG is 100 times lower than the ERV of 60,000 mG for demersal finfish, demonstrating that risks to demersal finfish associated with the HVAC interarray cables are *de minimis*.

5.2.2 Induced AC Electric Fields

The strength of the induced electric field from the HVAC interarray cables was evaluated at the same two burial depths as the AC magnetic fields (**Figure 27** and **Figure 28**). The largest predicted induced electric field is 20 mV/m, but rapidly decreases with distance away from the cable centerline and into the water column. At a height of 3.3 ft (1 m) above the seafloor, the induced AC electric field values decrease to less than 0.02 mV/m, which is 1,000 times lower

than the value at the seafloor. At distances beyond 12 ft (3.7 m) from the cable centerline, the induced electric fields drop below 4e-5 mV/m.

5.2.2.1 Potential Risk to Demersal Invertebrates

No demersal invertebrates located in the offshore waters of southern New England possess electroreceptive capabilities. Risks associated with potential exposures to induced AC electric fields associated with the HVAC interarray cables are *de minimis*.

5.2.2.2 Potential Risk to Demersal Elasmobranchs

Elasmobranchs are not capable of detecting frequencies above 20 Hz. As the HVAC interarray cables will be present at 60 Hz, outside the range detectable by this group, risks to elasmobranchs associated with AC induced electric fields are *de minimis*.

5.2.2.3 Potential Risk to Demersal Finfish

The maximum induced AC electric field of 20 mV/m is 3 times lower than the ERV of 60 mV/m for demersal finish, demonstrating that risks to demersal finfish are *de minimis*.

5.3 WIND TURBINES

AC magnetic fields and induced electric fields for the HVAC interarray cables extending vertically within J-tubes along the lower portion of the wind turbine monopiles were modeled. These vertical surfaces represent worst-case exposure conditions to EMF in the open water column. It is assumed that the J-tube will exit the wind turbine monopile at 16 ft (5 m) above the seafloor and extend vertically on the exterior of the monopile to the seafloor where it will be covered by secondary protection, typically consisting of rock, rock bags, or concrete mattresses. While the vertical surface of the J-tube may be subject to biofouling (e.g., growth of barnacles), it will not provide suitable habitat for larger crabs and lobsters. Accordingly, exposures are evaluated only for elasmobranch and finfish in the open water column, and not adhering invertebrates (e.g., filter feeding amphipods, barnacles, mussels, anemones) directly on the surface of the J-tubes.

5.3.1 AC Magnetic Fields

The strength of the magnetic field from the two HVAC interarray cables extending vertically along a single wind turbine monopile was modeled at 3.3 ft (1 m) away from the J-tube in the open water column (**Figure 29**). At 3.3 ft (1m) away and along the centerline of the J-tubes, the maximum AC magnetic field of 50 mG was predicted.

5.3.1.1 Potential Risk to Elasmobranchs

Elasmobranchs are not capable of detecting frequencies above 20 Hz. As the HVAC interarray cables within the J-tubes along the wind turbine monopiles will be present at 60 Hz, outside the range detectable by this group, risks to elasmobranchs associated with AC induced electric fields are *de minimis*.

5.3.1.2 Potential Risk to Finfish

The maximum AC magnetic field strength of 50 mG is 1,200 times lower than the ERV of 60,000 mG for demersal finish, demonstrating that risks to demersal finfish are *de minimis*.

5.3.2 Induced AC Electric Fields

The strength of the induced electric field from the two HVAC interarray cables along the exterior of the wind turbine monopile was modeled (**Figure 30**). A maximum induced electric field of 0.013 mV/m was predicted at 3.3 ft (1 m) away from the J-tubes.

5.3.2.1 Potential Risk to Elasmobranchs

Elasmobranchs are not capable of detecting frequencies above 20 Hz. As the HVAC interarray cables within the J-tubes at the wind turbines will be present at 60 Hz, outside the range detectable by this group, risks to elasmobranchs associated with induced AC electric fields are *de minimis*.

5.3.2.2 Potential Risk to Finfish

The maximum induced AC electric field of 0.013 mV/m is approximately 4,600 times lower than the ERV of 60 mV/m for demersal finish, demonstrating that risks to demersal finfish are *de minimis*.

5.4 OFFSHORE SUBSTATION FACILITIES

AC and DC magnetic fields and induced electric fields for HVAC interarray cables leading to, and the HVDC submarine export cables leading away from, the offshore substation facility support structures were modeled.

5.4.1 Offshore Substation Facility AC Cables

The offshore substation facilities will be supported by a jacketed structure and the HVAC interarray cables will travel vertically through the water column within J-tubes. It is assumed that on the upper portion of the support structure, the J-tubes will be installed within the

jacketed support structure, and near the seafloor to where the cables will be buried, the J-tubes will be installed on the exterior of the support structure. Upon the J-tubes reaching the seafloor, they will be covered by secondary protection, typically consisting of rock, rock bags, or concrete mattresses. AC magnetic fields and induced electric fields for the HVAC interarray cables extending vertically along the exterior of the offshore substation facility support structures were modeled. A subset of the 18–22 HVAC interarray cables, separated by 8.2 ft (2.5 m), were modeled to determine the AC EMF generated, specifically 6 HVAC interarray cables.

As in the case of the wind turbines, these vertical surfaces represent worst-case exposure conditions to EMF in the open water column. The vertical surfaces may be subject to biofouling (e.g., growth of barnacles), but they will not provide suitable habitat for larger crabs and lobsters. Accordingly, exposures are evaluated only for elasmobranch and finfish in the open water column.

5.4.1.1 AC Magnetic Fields

The strength of the magnetic field from the six HVAC interarray cables extending vertically along the exterior of the offshore substation facility support structure was evaluated at 3.3 ft (1 m) away from the J-tube in the open water column (**Figure 31**). At 3.3 ft (1 m) away and along the centerline of the J-tubes, a maximum AC magnetic field of 50 mG was predicted.

Potential Risk to Elasmobranchs

Elasmobranchs are not capable of detecting frequencies above 20 Hz. As the HVAC interarray cables within the J-tubes on the offshore substation facility support structures will be present at 60 Hz, outside the range detectable by this group, risks to elasmobranchs associated with AC induced electric fields are *de minimis*.

Potential Risk to Finfish

The maximum AC magnetic field strength of 50 mG is 1,200 times lower than the ERV of 60,000 mG for demersal finish, demonstrating that risks to demersal finfish are *de minimis*.

5.4.1.2 Induced AC Electric Fields

The strength of the induced electric field from the six HVAC interarray cables along the exterior of the offshore substation facility support structures was modeled (**Figure 32**). A maximum induced electric field of 2e-5 mV/m was predicted at 3.3 ft (1 m) away from the J-tubes.

Potential Risk to Elasmobranchs

Elasmobranchs are not capable of detecting frequencies above 20 Hz. As the HVAC interarray cables within the J-tubes on the offshore substation facility support structures will be present at 60 Hz, outside the range detectable by this group, risks to elasmobranchs associated with AC induced electric fields are *de minimis*.

Potential Risk to Finfish

The maximum induced AC electric field strength of 2e-5 mV/m is multiple orders of magnitude lower than the ERV of 60 mV/m for demersal finish, demonstrating that risks to demersal finfish are *de minimis*.

5.4.2 Offshore Substation Facility DC Cables

DC magnetic fields and induced electric fields for the HVDC submarine export cables extending vertically along the offshore substation facility support structures were modeled (**Figure 33**). It is assumed that on the upper portion of the support structure, the J-tubes will be installed within the jacketed support structure, and near the seafloor to where the cables will be buried, the J-tubes will be installed on the exterior of the support structure. Upon the J-tubes reaching the seafloor, they will be covered by secondary protection, typically consisting of rock, rock bags, or concrete mattresses. As in the case of the wind turbines, these vertical surfaces represent worst-case exposure conditions to EMF in the open water column. The cables will be contained in J-tubes. Because the J-tubes will not be subject to biofouling, exposures are evaluated only for elasmobranch and finfish in the open water column.

5.4.2.1 DC Magnetic Fields

The maximum predicted value for the magnetic field strength for the HVDC submarine export cables extending vertically along the offshore substation facility support structures was approximately 3,000 mG at 3.3 ft (1 m) away from the J-tube.

Potential Risk to Elasmobranchs

The maximum predicted DC magnetic field strength of 3,000 mG at 3 ft (1m) away from the J-tubes in the open water column exceeds the ERV of 653 mG (by a factor of 4.6).

The area housing the J-tubes, on the offshore substation facility support structures, represents an infinitely small area relative to the broader ecosystem. As described in **Sections 3 and 4**, the J-tubes will be separated by a distance of 20 ft (6 m). Assuming a water depth of 200 ft (61 m), and a J-tube of equivalent length, would represent an area of approximately 0.09 ac (364 m^2), or 0.18 ac (728 m^2) combined for both BW1 and BW2 offshore substation facilities. This area

represents less than 0.000001% of the southern New England ecoregion. Accordingly, potential population level risks to elasmobranchs associated with the DC magnetic fields from the HVDC submarine export cables in J-tubes on the offshore substation facility support structures are considered *de minimis*.

Potential Risk to Finfish

The maximum predicted DC magnetic field strength of 3,000 mG at 3.3 ft (1 m) away from the J-tubes in the open water column is 6.7 times below the ERV of 20,000 mG for finfish. Accordingly, risks to finfish are *de minimis*.

5.4.2.2 Induced DC Electric Fields

The strength of the motion-induced DC electric field was calculated for the cable on the offshore substation facility support structure, assuming an ocean current velocity of 2 ft/s (0.6 m/s). The largest predicted induced electric field was 0.15 mV/m at 3.3 ft (1 m) away from the J-tube.

Potential Risk to Elasmobranchs

The ERV of 60 mV/m for DC electric fields for demersal finfish is used as a surrogate value for elasmobranchs. The maximum induced DC electric field of 0.15 mV/m is 400 times lower than the ERV, demonstrating that risks to elasmobranchs associated with induced DC electric fields are *de minimis*.

Potential Risk to Finfish

The maximum induced DC electric field of 0.15 mV/m is 400 times lower than the ERV of 60 mV/m for demersal finish, demonstrating that risks to finfish are *de minimis*.

6 SUMMARY AND CONCLUSIONS

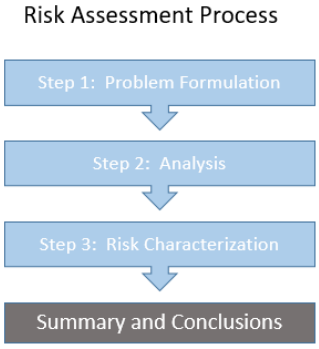

Integral performed the assessment for Project-related offshore EMF for BW1 and BW2 presented in support of the COP. The approach for assessing Project-related EMF impacts to the marine environment was guided by the internationally accepted environmental risk assessment approach, as well as other standard methods for EMF assessment accepted within the scientific, engineering, and health communities.

The BW1 proposed transmission system will connect the offshore wind farm to the POI at the Astoria Power Complex in Queens, New York. The BW1 transmission system components evaluated in this report include one 320-kV HVDC submarine export cable, multiple 66-kV HVAC interarray cables, and the cables installed on the wind turbines and offshore substation facilities.

The BW2 proposed transmission system will connect the offshore wind farm to the POI at the Millstone Power Complex in Waterford, Connecticut. The BW2 transmission system components evaluated in this report include one 320-kV HVDC submarine export cable circuit. The HVAC interarray cables, wind turbines, and offshore substation facilities are not differentiated between BW1 and BW2, though they are electrically isolated.

The EMF assessment included quantitative modeling of EMF for the BW1 and BW2 offshore components of the transmission system and was based on the maximum capacity limits of the cables corresponding to the WNC rating. ERVs were used for the risk assessment as representative field strength levels associated with EMF impacts to species within each of the demersal invertebrate, elasmobranch, and finfish groups. The ERVs were selected based on established ecological risk assessment procedures for selection of toxicity reference values and ecological screening benchmarks used in chemical risk assessment.

The modeled results were compared to the ERVs to assess the potential for Project-related risk to marine life from EMF. The predicted DC and AC EMF values are summarized below.

- The maximum magnetic field strengths calculated for the BW1 and BW2 HVDC submarine export cables have a *de minimis* risk to all demersal marine species for the majority of the cable route where the cable will be buried and either bundled or separated.
  - In areas where the cable is surface laid and covered with rock, rock bags, or concrete mattresses, the maximum magnetic field is a factor of 1.2 above the ERV at the seafloor, though the modeled cover depth is conservatively shallow and the ERV is based on behavioral changes, and is considered a conservative estimate of potential

population level effects. This demonstrates that population level risks to demersal invertebrates are *de minimis*, even under the maximum magnetic field strengths.

- The maximum compass deflection for the BW1 and BW2 HVDC submarine export cables is *de minimis* for a majority of the cable route. In the limited shallow areas where the cable may be surface laid and covered by secondary protection (i.e., rock, rock bags, concrete mattresses), resulting in the largest magnetic fields, there is a possibility of impacting surface vessel compasses, though the impact would be minimal and likely not be noticeable by mariners.
  - Modern navigational instruments (e.g., LORAN-C, GPS) will not be impacted by the altered magnetic field along the cable, or any other Project cables.
- The maximum induced DC electric fields calculated for the BW1 and BW2 HVDC submarine export cables are 150 times lower than the ERVs for demersal elasmobranchs and finfish, indicating a *de minimis* risk to all demersal marine species. No demersal invertebrates located in the offshore waters of southern New England possess electroreceptive capabilities.
- The maximum magnetic field strengths calculated for the BW1 and BW2 HVAC interarray cables are 170 to 1,000 times lower than the ERV for demersal invertebrates and finfish. Elasmobranchs are not capable of detecting frequencies above 20 Hz, which is applicable to all AC magnetic field and electric field conclusions provided below. Risks associated with potential exposures to AC magnetic fields associated with the HVAC interarray cables are *de minimis*.
- The maximum induced AC electric fields calculated for the BW1 and BW2 HVAC interarray cables are three times lower than the ERV for demersal finish. No demersal invertebrates located in the offshore waters of southern New England possess electroreceptive capabilities. Risks associated with potential exposures to induced AC electric fields associated with the HVAC interarray cables are *de minimis*.
- The maximum magnetic field strength calculated for the HVAC interarray cables installed along the lower portion of the wind turbine monopiles is 1,200 times lower and the maximum induced AC electric field is 4,600 times lower than the ERV for demersal finish. Risks associated with potential exposures to AC magnetic fields and induced electric fields associated with the wind turbine HVAC interarray cables are *de minimis*.
- The maximum magnetic field strength calculated for the HVAC interarray cables installed along the lower portion of the offshore substation facility support structure is 1,200 times lower and the maximum induced AC electric field is multiple orders of magnitude times lower than the ERV for demersal finish. Risks associated with potential exposures to AC magnetic fields associated with the offshore substation facility HVAC interarray cables are *de minimis*.

- The maximum magnetic field strength calculated for the HVDC submarine cables installed along the lower portion of the offshore substation facility support structure exceeds the elasmobranch ERV by a factor of 4.6 and is 6.7 times below the ERV for finfish. However, the area housing the J-tubes on the offshore substation facility support structures represent an infinitely small area relative to the broader ecosystem, thus concluding that the potential population level risks to elasmobranchs and finfish associated with the DC magnetic fields from the HVDC submarine export cables on the offshore substation facility support structures are *de minimis*.
- The maximum induced DC electric field calculated for the HVDC submarine cables installed along the lower portion of the offshore substation facility support structure is 400 times lower than the ERV for elasmobranchs and finfish. Risks associated with potential exposures to induced DC electric fields associated with the offshore substation facility HVDC submarine export cables are *de minimis*.

Background EMF levels will be dominant everywhere except within close proximity to the cable because of the proportional relationship between the strength of an induced electro-magnetic field and distance. Overall exposure of the study area to the EMF produced will be minimal (<1% of total habitat).

The EMF modeling suggests that small changes of less than 10% of the geomagnetic field within 10 ft (3 m) of the submerged cable are likely. When cables are not able to be at their proposed target burial depths, concrete mattresses or other materials will serve as a buffer, but the strength of the EMF near unburied cables will be higher than those that are buried to target depth. However, as suggested by the literature, at a distance of 10 ft (3 m), the effects of EMF are expected to be similarly negligible whether the submerged cable is buried or exposed.

The overall conclusions of this assessment demonstrating *de minimis* risk to marine life are generally consistent with the updated 2020 comprehensive review by the U.S. Pacific Northwest National Laboratory of the ecological impacts of marine renewable energy development (Copping and Hemery 2020). As part of that overall review, Gill and Desender (2020) concluded that while some field and laboratory studies of EMF have shown effects to a small number of individual species (behavioral, physiological, developmental, and genetic levels), the levels are not at the EMF intensities associated with marine renewable energy. Further, while some effects or responses have been identified, this "does not necessarily mean there are impacts."

As in any risk assessment, sources of uncertainty remain. An expansive knowledge base is available regarding the degree to which species may be able to "sense" EMF, while relatively fewer data are available related to the dose–response relationship between EMF and actual effects. Studies that focus on endpoints related to behavioral, biochemical, cellular, and genetic responses will continue to offer less insight, unless these endpoints can be explicitly linked to population level risks. The knowledge base would be significantly improved through

continued consideration of the risk assessment paradigm directly incorporating dose–response testing of laboratory-derived endpoints on growth, survival, and reproduction in order to continue to better inform the potential for population level significance.

In addition, there exists the very real need to balance uncertainty associated with risk from EMF with the compensatory benefits associated with the addition of structure and novel habitats creating a reef effect in the offshore environments. The introduction of rock, for example at the base of wind turbines and offshore substation facilities, affects seafloor habitat complexity, particularly in mobile sediments, expanding the habitats available to serve as refuges and to support food sources for biota (Degraer et al. 2020). While physically this new habitat closely resembles natural rocky reef habitats, it also results in biologically similar communities to those occupying natural reef (Coolen et al. 2020). Further opportunities may exist for the incorporation of additional nature-based solutions to not only provide physical protection to infrastructure, but also to additionally promote biological production and diversity.

7 REFERENCES

Anderson, J.M. 2018. Perception & Use of Magnetic Field Information in Navigation Behaviors in Elasmobranch Fishes (Doctoral dissertation, University of Hawai'i at Mānoa).

Andrianov, Y., G.R. Broun, O.B. Il'inskii, and V.M. Muraveiko. 1984. Frequency characteristics of skate electroreceptive central neurons responding to electrical and magnetic stimulation. *Neurophysiology* 16(4):364–369.

Armstrong, J.D., D.C. Hunter, R.J. Fryer, P. Rycroft, and J.E. Orpwood. 2015. Behavioural responses of Atlantic Salmon to mains frequency magnetic fields. *Scottish Marine and Freshwater Science*. 6:9.

Basov, B.M. 1999. Behavior of sterlet Acipenser ruthenus and Russian sturgeon A. gueldenstaedtii in low-frequency electric fields. *J Ichthyol*. 39:782–787.

Basov, B.M. 2007. On electric fields of power lines and on their perception by freshwater fish. *Journal of Ichthyology* 47(8):656–661.

Bedore, C., and S. Kajiura. 2013. Bioelectric Fields of Marine Organisms: Voltage and Frequency Contributions to Detectability by Electroreceptive Predators. *Physiological and Biochemical Zoology* 86:298–311.

Bedore, C.N., L.L. Harris, and S.M. Kajiura. 2014. Behavioral responses of batoid elasmobranchs to prey-simulating electric fields are correlated to peripheral sensory morphology and ecology. *Zoology* 117(2):95–103.

Benhamou, S., J. Sudre, J. Bourjea, S. Ciccione, A. De Santis, and P. Luschi. 2011. The Role of Geomagnetic Cues in Green Turtle Open Sea Navigation. *PLoS ONE* 6(10):e26672. https://doi.org/10.1371/journal.pone.0026672.

Bevelhimer, M.S., G.F. Cada, A.M. Fortner, P.E. Schweizer, and K. Riemer. 2013. Behavioral responses of representative freshwater fish species to electromagnetic fields. *Transactions of the American Fisheries Society* 142(3):802–813.

Bochert, R., and M.L. Zettler. 2004. Long-term exposure of several marine benthic animals to static magnetic fields. Bioelectromagnetics: Journal of the Bioelectromagnetics Society, The Society for Physical Regulation in Biology and Medicine, The European Bioelectromagnetics Association, 25(7):498-502.

Bochert, R. and M.L. Zettler. 2006. Effect of electromagnetic fields on marine organisms. In: Koller J., J. Koppel, W. Peters (eds.). Offshore Wind Energy. Research on Environmental Impacts. Springer-Verlag, Berlin. 223-234.

BRI. 2015. Offshore wind energy development and birds in New York: managing risks and identifying data gaps. Prepared for South Shore Audubon Society and New York City Audubon. Biodiversity Research Group. December. 34 pp.

Brothers, J.R., and K.J. Lohmann. 2018. Evidence that magnetic navigation and geomagnetic imprinting shape spatial genetic variation in sea turtles. *Current Biology*. 28(8):1325–1329.

Bull, A.S., and M.E. Helix. 2011. Highlights of renewable energy studies and research in the Bureau of Ocean Energy Management, regulation and enforcement. *OCEANS'11 MTS/IEEE KONA*, Waikoloa, HI. Available online at: https://www.infona.pl/resource/bwmeta1.element.ieee-art-000006107284.

Cada, G.F., M.S. Bevelhimer, A.M. Fortner, K.P. Riemer, and P.E. Schweizer. 2012. Laboratory Studies of the Effects of Static and Variable Magnetic Fields on Freshwater Fish. ORNL/TM-2012/119. Oak Ridge National Laboratory, TN.

Chulliat, A., W. Brown, P. Alken, C. Beggan, M. Nair, G. Cox, A. Woods, S. Macmillan, B. Meyer, and M. Paniccia. 2020. The US/UK World Magnetic Model for 2020-2025: Technical Report, National Centers for Environmental Information. NOAA. doi: 10.25923/ytk1-yx35

Claisse, J.T., D.J. Pondella, C.M. Williams, L.A. Zahn, and J.P. Williams. 2015. Final Technical Report, Current ability to assess impacts of electromagnetic fields associated with marine and hydrokinetic technologies on marine fishes in Hawaii. DE-EE0006390.0000, OCS Study BOEM 2015-042.

CMACS. 2003. A Baseline Assessment of Electromagnetic Fields Generated by Offshore Windfarm Cables. Final Report COWRIE-EMF-01-2002 prepared by University of Liverpool and ECONNECT Ltd. Available online at: https://tethys.pnnl.gov/sites/default/files/publications/COWRIE_EMF_Offshore_Cables.pdf.

Coolen, J.W.P., B. van der Weide, J. Cuperus, M. Blomberg, G.W.N.M. van Moorsel, M.A. Faasse, O.G. Bos, S. Degraer, and H.J. Lindeboom. 2020. Benthic biodiversity on old platforms, young wind farms and rocky reefs. *ICES Journal of Marine Science* 77(3):1250–1265.

Copping, A.E., and L.G. Hemery. 2020. OES-Environmental 2020 State of the Science Report: Environmental Effects of Marine Renewable Energy Development Around the World. Report for Ocean Energy Systems (OES). doi:10.2172/163287.

Dannheim, J., L. Bergström, S. Birchenough, R. Brzana, A.R. Boon, J. Coolen, and I. Dauvin. 2020. Benthic effects of offshore renewables: Identification of knowledge gaps and urgently needed research. *ICES Journal of Marine Science* 77(3):1092–1108.

Degraer, S., D. Carey, J. Coolen, Z. Hutchison, F. Kerckhof, and Rumes. 2020. Offshore Wind Farm Artificial Reefs Affect Ecosystem Structure and Functioning: A Synthesis. *Oceanography* 33:48–57. 10.5670/oceanog.2020.405.

Dunlop, E.S., S.M. Reid, and M. Murrant. 2016. Limited influence of a wind power project submarine cable on a Laurentian Great Lakes fish community. *Journal of Applied Ichthyology* 32:18031.

Dunne, J.A., R.J. Williams, and N.D. Martinez. 2002. Food-web structure and network theory: the role of connectance and size. *Proc Natl Acad Sci USA*. 99:12917–12922.

Durda, J.L., and D.V. Preziosi. 2000. Data quality evaluation of toxicological studies used to derive exotoxicological benchmarks. *Hum. Ecol. Risk Assess.* 6(5):747–765.

Ebenman B., and T. Jonsson. 2005. Using community viability analysis to identify fragile systems and keystone species. *Trends Ecol Evol (Amst)*. 20:568–575.

European Offshore Wind Deployment Centre. 2011. Environmental Statement, Chapter 13: Electromagnetic Fields. July.

Formicki, K., and T. Perkowski. 1998. The effect of a magnetic field on the gas exchange in rainbow trout Oncorhynchus mykiss embryos (Salmonidae). *Italian Journal of Zoology* 65(S1):475–477.

Gill, A., and M. Desender. 2020. State of the Science Report – Chapter 5: Risks to Animals from Electromagnetic Fields Emitted by Electric Cables and Marine Renewable Energy Devices. In. A. Copping and L. Hemery (eds.), OES-Environmental 2020 State of the Science Report: Environmental Effects of Marine Renewable Energy Development Around the World. Report for Ocean Energy Systems. Available online at: https://tethys.pnnl.gov/publications/state-of-the-science-2020-chapter-5-electromagnetic-fields.

Gill, A.B., and H. Taylor. 2001. The potential effects of electromagnetic fields generated by cabling between offshore wind turbines upon elasmobranch fishes. Countryside Council for Wales.

Gill, A.B., Y. Huang, I. Gloyne-Philips, J. Metcalfe, V. Quayle, J. Spencer, and V. Wearmouth. 2009. COWRIE 2.0 Electromagnetic Fields (EMF) Phase 2: EMF-sensitive fish response to EM emissions from sub-sea electricity cables of the type used by the offshore renewable energy industry. Commissioned by COWRIE Ltd. (project reference COWRIE-EMF-1-06).

Hanski, I. 1998. Metapopulation dynamics. *Nature* 396:41–49.

Hanson, M., and H. Westerberg. 1987. Occurrence of magnetic material in teleosts. Comparative Biochemistry and physiology. *A, Comparative Physiology* 86(1):169-172.

Harrison R.J., R.E. Dunin-Borkowski, and A. Putnis. 2002. Direct imaging of nanoscale magnetic interactions in minerals. *Proceed Nat Acad Sci.* 99:16556–16561.

Harsanyi, P., K. Scott, B.A. Easton, G. de la Cruz Ortiz, E.C. Chapman, A.J. Piper, C.M. Rochas, and A.R. Lyndon. 2022. The Effects of Anthropogenic Electromagnetic Fields (EMF) on the Early Development of Two Commercially Important Crustaceans, European Lobster, Homarus gammarus (L.) and Edible Crab, Cancer pagurus (L.). *Journal of Marine Science and Engineering* 9(7):16.

Hays, G., and R. Scott. 2013. Global patterns for upper ceilings on migration distance in sea turtles and comparisons with fish, birds and mammals. *Functional Ecology* (27):748–756.

Hui, C.A. 1994. Lack of association between magnetic patterns and the distribution of free-ranging dolphins. *Journal of Mammalogy* 75(2):399–405.

Hutchison Z., P. Sigray, H. He, A. Gill, J. King, and C. Gibson. 2018. Electromagnetic Field (EMF) Impacts on Elasmobranch (shark, rays, and skates) and American Lobster Movement and Migration from Direct Current Cables. Report by University of Rhode Island, Cranfield University, and FOI (Swedish Defence Research Agency).

Hutchison, Z., M. Bartley, S. Degraer, P. English, and A. Khan. 2020a. Offshore Wind Energy and Benthic Habitat Changes: Lessons from Block Island Wind Farm. *Oceanography* 33:58-69. 10.5670/oceanog.2020.406.

Hutchison, Z.L., A.B. Gill, P. Sigray, H. He, and J.W. King. 2020b. Anthropogenic electromagnetic fields (EMF) influence the behaviour of bottom-dwelling marine species. *Scientific Reports* 10(1):1–15.

IEEE. 2013. IEEE Guide for the Design, Construction, and Operation of Electric Power Substations for Community Acceptance and Environmental Compatibility (IEEE Std. 1127-2013). Institute of Electrical and Electronic Engineers, NY.

Ingram, E.C., R.M. Cerrato, K.J. Dunton, and M.G. Frisk. 2019. Endangered Atlantic Sturgeon in the New York Wind Energy Area: implications of future development in an offshore wind energy site. *Scientific Reports* 9(1):1–13.

Integral. 2022. DRAFT - Onshore Electric and Magnetic Field Assessment, Beacon Wind Project. Prepared for Beacon Wind LLC, Stamford, CT. Integral Consulting Inc., Berlin, MD. May.

Jakubowska, M., B. Urban-Malinga, Z. Otremba, and E. Andrulewicz. 2019. Effect of low frequency electromagnetic field on the behavior and bioenergetics of the polychaete *Hediste diversicolor*. *Marine Environmental Research* 150:104766.

Jordan, L.K., J.W. Mandelman, and S.M. Kajiura. 2011. Behavioral responses to weak electric fields and a lanthanide metal in two shark species. *Journal of Experimental Marine Biology and Ecology* 409(1-2):345–350.

Kajiura, S.M., and K.N. Holland. 2002. Electroreception in juvenile scalloped hammerhead and sandbar sharks. *Journal of Experimental Biology* 205(23):3609–3621.

Kavet, R., M.T. Wyman, A.P. Klimley, and X. Vergara. 2016. Assessment of potential impact of electromagnetic fields from undersea cable on migratory fish behavior. Report by Electric Power Research Institute (EPRI). Report for Bureau of Ocean Energy Management (BOEM). Report for US Department of Energy (DOE).

Kempster, R.M., N.S. Hart, and S.P. Collin. 2013. Survival of the stillest: predator avoidance in shark embryos. *Plos One* 8:e52551.

Klimley, A.P. 1993. Highly directional swimming by scalloped hammerhead sharks, Sphyrna Lewini, and subsurface irradiance, temperature, bathymetry, and geomagnetic field. *Marine Biol.* 117:22.

Klimley, A.P., M.T. Wyman, and R. Kavet. 2017. Chinook salmon and green sturgeon migrate through San Francisco Estuary despite large distortions in the local magnetic field produced by bridges. *PLoS One*. 12(6):30169031.

Kramer V.J., M.A. Etterson, M. Hecker, C.A. Murphy, G. Roesijadi, D.J. Spade, J.A. Spromberg, M. Wang, and G.T. Ankley. 2011. Adverse outcome pathways and ecological risk assessment: bridging to population-level effects. *Environ Toxicol Chem.* 30:64–76.

Kremers, D., J.L. Marulanda, M. Hausberger, and A. Lemasson. 2014. Behavioural evidence of magnetoreception in dolphins: detection of experimental magnetic fields. *Naturwissenschaften* 101(11):907–911.

Krone, R., G. Dederer, P. Kanstinger, P. Krämer, and C. Schneider. 2017. Mobile demersal megafauna at common offshore wind turbine foundations in the German Bight (North Sea) two years after deployment– Increased production rate of *Cancer pagurus*. *Marine Environmental Research* 123:53–61.

Kuhnz, L.A., J.P. Barry, K. Buck, C. Lovera, and P.J. Whaling. 2015. Potential impacts of the Monterey Accelerated Research System (MARS) cable on the seabed and benthic faunal assemblages. MARS Biological Survey Report, Monterey Bay Aquarium Research Institute.

Leggett, W.C. 1977. The ecology of fish migrations. *Annual Review of Ecology and Systematics* 285–308.

Link, J., C.A. Griswold, E. Methratta, and J. Gunnard. 2006. Documentation for the Energy Modeling and Analysis eXercise (EMAX). Northeast Fisheries Science Center Reference Document. 6.

Lohmann, K.J., P. Luschi, and G.C. Hays. 2008. Goal navigation and island-finding in sea turtles. *Journal of Experimental Marine Biology and Ecology* 356:83–95.

Love, M.S., M.M. Nishimoto, S. Clark, and A.S. Bull. 2015. Identical response of caged rock crabs (genera Metacarcinus and Cancer) to energized and unenergized undersea power cables in Southern California, USA. Bulletin, Southern California Academy of Sciences, 114(1):33-41.

Love, M.S., M.A. Nishimoto, S. Clark, and A.S. Bull. 2016. Renewable Energy in situ Power Cable Observation. OCS Study 2016-008. U.S. Department of the Interior, Bureau of Ocean Energy Management, Pacific OCS Region, Camarillo, CA.

Love, M.S., M.M. Nishimoto, S. Clark, M. McCrea, and A.S. Bull. 2017a. Assessing potential impacts of energized submarine power cables on crab harvests. *Continental Shelf Research* 151:23–29.

Love, M.S., M.M. Nishimoto, S. Clark, M. McCrea, and A.S. Bull. 2017b. The organisms living around energized submarine power cables, pipe, and natural sea floor in the inshore waters of southern California. Bulletin, Southern California Academy of Sciences, 116(2):61-87.

Luschi, P., S. Åkesson, A.C. Broderick, F. Glen, and B.J. Godley. 2001. Testing the navigational abilities of oceanic migrants: displacement experiments on green sea turtles (Chelonia mydas). *Behavioural Ecology and Sociobiology* 50:528–534.

Luschi, P., S. Benhamou, C. Girard, S. Ciccione, and D. Roos. 2007. Marine turtles use geomagnetic cues during open-sea homing. *Current Biology* 17:126–133.

Murray, R. 1960. Electrical Sensitivity of the Ampullae of Lorenzini. *Nature* 187:957.

McIntyre, A., T. Janeski, G. Garman, C. Deloglos, and A. Filippas 2016. Behavioral responses of sub-adult Atlantic Sturgeon (*Acipenser oxyrinchus oxyrinchus*) to electromagnetic and magnetic fields under laboratory conditions. Final Grant Report to the Virginia Coastal Zone Management Program. Virginia Commonwealth University.

NRC. 1983. Risk Assessment in the Federal Government: Managing the Process. National Research Council. The National Academies Press, Washington, DC. https://doi.org/10.17226/366.

Nestler, E., A. Pembroke, and W. Bailey. 2010. Effects of EMFs from undersea power lines on marine species. Energy. Ocean International, Ft. Lauderdale, FL.

Nordmann, G.C., T. Hochstoeger, and D.A. Keays, 2017. Magnetoreception—a sense without a receptor. *PLoS biology* 15(10):e2003234.

Normandeau Associates, Inc., Exponent, Inc., T. Tricas, and A. Gill. 2011. Effects of EMFs from Undersea Power Cables on Elasmobranchs and Other Marine Species. OCS Study BOEM 2011-09. Available online at: https://espis.boem.gov/final%20reports/5115.pdf. U.S. Department of the Interior, Bureau of Ocean Energy Management.

NYSERDA. 2010. Pre-development assessment of avian species for the proposed Long Island – New York City offshore wind project area. Final Report. NYSERDA Report No. 9998-03. Prepared by AWS Truepower LLC and GEO-Marine. New York State Energy Research and Development Authority, Albany, NY.

NYSERDA. 2017. New York State Offshore Wind Master Plan, Fish and Fisheries Study. Final Report. Report No. 17-25j. Prepared by Ecology and Environment Engineering, P.C., New York, NY. New York State Energy Research and Development Authority, New York, NY.

Orpwood, J., R.J. Fryer, P. Rycroft, and J.D. Armstrong. 2015. Effects of AC magnetic fields (MFs) on swimming activity in European eels *Anguilla anguilla*. *Scottish Marine and Freshwater Science* 6:8.

Pastorok, R.A., and D.V. Preziosi. 2011. Beyond qualitative assessment of ecosystem services. *IEAM* 7:693–695.

Patullo, B.W., and D.L. Macmillan. 2007. Crayfish respond to electrical fields. *Current Biology* 17(3):R83–R84.

Petersen, J.K., and T. Malm. 2006. Offshore windmill farms: threats to or possibilities for the marine environment. *AMBIO: A Journal of the Human Environment* 35(2):75–80.

Preziosi, D.V., and J.L. Durda. 1999. Where is the population in your risk assessment? Society of Environmental Toxicology and Chemistry (SETAC) News. 19(6):19–20.

Quigel, J.C., and W.L. Thornton. 1989. Rigs to reefs—a case history. Bulletin of Marine Science. 44:799–806.

Reubens, J.T., S. Degraer, and M. Vincx. 2014. The ecology of benthopelagic fishes at offshore wind farms: A synthesis of 4 years of research. *Hydrobiologia* 727:121–136.

Sadowski, M., A. Winnicki, K. Formicki, A. Sobocinski, and A. Tanski. 2007. The effect of magnetic field on permeability of egg shells of salmonid fishes. *Acta Ichthyologica et Piscatoria* 2(37):129–135.

Sample, B., D. Opresko and G. Suter. 1996. Toxicological benchmarks for wildlife – 1996 revision. Health Science Research Division, Oak Ridge. ES/ER/TM-86/R3.

Scott, K., P. Harsanyi, and A.R. Lyndon. 2018. Understanding the effects of electromagnetic field emissions from Marine Renewable Energy Devices (MREDs) on the commercially important edible crab, Cancer pagurus (L.). *Marine Pollution Bulletin* 131:580–588.

Scott, K., P. Harsanyi, B. Easton, A. Piper, C. Rochas, A. Lyndon. 2021. Exposure to Electromagnetic Fields (EMF) from Submarine Power Cables Can Trigger Strength-Dependent Behavioural and Physiological Responses in Edible Crab, Cancer pagurus (L.) *Journal of Marine Science and Engineering* 9(7):16.

Sherwood, J., S. Chidgey, P. Crockett, D. Gwyther, P. Ho, S. Stewart, D. Strong, B. Whitely, and A. Williams. 2016. Installation and operational effects of a HVDC submarine cable in a continental shelf setting: Bass Strait, Australia. *Journal of Ocean Engineering and Science* 1(4):337–353.

Snyder, D.B., W.H. Bailey, K. Palmquist, B.R.T. Cotts, and K.R. Olsen. 2019. Evaluation of Potential EMF Effects on Fish Species of Commercial or Recreational Fishing Importance in Southern New England. OCS Study BOEM 2019-049. U.S. Dept. of the Interior, Bureau of Ocean Energy Management, Headquarters, Sterling, VA.

Spromberg, J.A., B.M. John, and W.G. Landis. 1998. Metapopulation dynamics indirect effects and multiple distinct outcomes in ecological risk assessment. *Environ Toxicol Chem.* 17:1640–1649.

Steullet, P., D.H. Edwards, and C.D. Derby. 2007. An electric sense in crayfish?. *The Biological Bulletin* 213(1):16–20.

Suter, G.W., S.B. Norton, and A. Fairbrother. 2005. Individuals versus organisms versus populations in the definition of ecological assessment endpoint. *Integr Environ Assess Manage.* 1:397–400.

Suter, G.W. 2007. *Ecological Risk Assessment*. 2cd ed. CRC Press, Boca Raton, FL.

Suter, G.W. 2008. Ecological risk assessment in the United States Environmental Protection Agency: a historical overview. *Integr Environ Assess Manage.* 4:285–289.

Tański, A., A. Korzelecka-Orkisz, L. Grubišić, V. Tičina, J. Szulc, and K. Formicki. 2011. Directional responses of sea bass (*Dicentrarchus labrax*) and sea bream (*Sparus aurata*) fry under static magnetic field. *Electron. J. Pol. Agric. Univ*. 14:1–8.

Taormina, B., C. Di Poi, A.L. Agnalt, A. Carlier, N. Desroy, R.H. Escobar-Lux, J.F. D'eu, F. Freytet, and C.M. Durif. 2020. Impact of magnetic fields generated by AC/DC submarine power cables on the behavior of juvenile European lobster (*Homarus gammarus*). *Aquatic Toxicology* 220:105401.

Taormina, B., J. Bald, A. Want, G. Thouzeau, M. Lejart, N. Desroy, and A. Carlier. 2018. A review of potential impacts of submarine power cables on the marine environment: knowledge gaps, recommendations and future directions. *Renewable and Sustainable Energy Reviews* 96:380–391. Available online at: https://doi.org/10.1016/j.rser.2018.07.026.

Teeter, J.H., R.B. Szamier, and M.V.L. Bennett. 1980. Ampullary electroreceptors in the sturgeon *Scaphirhynchus platorynchus* (rafinesque). *Journal of Comparative Physiology* 138(3):213–223.

Tetra Tech. 2021. Offshore Wind Submarine Cabling Overview – Fisheries Technical Working Group, Final Report. Prepared for New York State Energy Research and Development Authority. NYSERDA Report 21-14. April.

USEPA. 1992. Framework for ecological risk assessment. EPA 630/R-92/001. Available at: http://rais.ornl.gov/documents/FRMWRK_ERA.PDF. U.S. Environmental Protection Agency, Risk Assessment Forum, Washington, DC. 57 pp. February.

USEPA. 1998. Guidelines for Ecological Risk Assessment. EPA/630/R-95/002F. Available at: https://www.epa.gov/sites/production/files/2014-11/documents/eco_risk_assessment1998.pdf. U.S. Environmental Protection Agency, Washington, DC. May 14.

USEPA. 2005. Guidance for Developing Ecological Soil Screening Levels. U.S. Environmental Protection Agency, Office of Solid Waste and Emergency Response, Washington, DC. OSWER Directive 9285.7-55.

Walker, M.M., J.L. Kirschvink, G. Ahmed, and A.E. Dizon. 1992. Evidence that fin whales respond to the geomagnetic field during migration. *Journal of Experimental Biology* 171(1):67–78.

Walker, M.M., T.P. Quinn, J.L. Kirschvink, and C. Groot. 1988. Production of single-domain magnetite throughout life by sockeye salmon, Oncorhynchus nerka. *Journal of Experimental Biology* 140(1):51–63.

Westerberg, H., and M.L. Begout-Anras. 1999. Orientation of silver eel (*Aguilla anguilla*) in a disturbed geomagnetic field. Advances in fish telemetry. In Proceedings of the Third Conference on Fish Telemetry in Europe, Norwich, England. June.

Wilber, D.L., R. Griffin, and D. Carey. 2020. Block Island Wind Farm Demersal Fish Trawl Survey Synthesis Report—Years 1 to 6, October 2012 through September 2018. Technical report prepared for Deepwater Wind, INSPIRE Environmental, Newport, RI. 182 pp.

Wilkens, L.A., and M.H. Hofmann. 2005. Behavior of animals with passive, low-frequency electrosensory systems. pp. 229–263 in T.H. Bullock, C.D. Hopkins, A.N. Popper, and R.R. Fay, eds. Electroreception. Springer, New York.

Woodruff, D.L., I.R. Schultz, K.E. Marshall, J.A. Ward, and V.I. Cullinan. 2012. Effects of Electromagnetic Fields on Fish and Invertebrates: Task 2.1. 3: Effects on Aquatic Organisms-Fiscal Year 2011 Progress Report-Environmental Effects of Marine and Hydrokinetic Energy (No. PNNL-20813 Final). Pacific Northwest National Laboratory (PNNL), Richland, WA.

Wueringer, B.E., L. Squire Jr., S.M. Kajiura, I.R. Tibbetts, N.S. Hart, and S.P. Collin. 2012. Electric field detection in sawfish and shovelnose rays. *PLoS One* 7(7):340605.

Zhang, X., J. Song, C. Fan, H. Guo, X. Wang, and H. Bleckmann. 2012. Use of electrosense in the feeding behavior of sturgeons. *Integrative Zoology* 7(1):74–82.

Photo credit: Matt Goldsmith, Equinor